Infection Dynamics and Cell Type Specific Responses to Vesicular Stomatitis Virus Infection in the Mouse Brain

HARVARD
Kenneth C. Griffin

GRADUATE SCHOOL
OF ARTS AND SCIENCES

DISSERTATION ACCEPTANCE CERTIFICATE

The undersigned, appointed by the

Division of Medical Sciences

Committee on Virology

have examined a dissertation entitled

Infection Dynamics and Cell Type Specific Responses to Vesicular Stomatitis Virus Infection in the Mouse Brain

presented by Tyler Bennette Krause

candidate for the degree of Doctor of Philosophy and hereby certify that it is worthy of acceptance.

Signature: Jonathan Kagan
Jonathan Kagan (Oct 24, 2023 17:54 EDT)

Typed Name: Dr. Jonathan Kagan

Signature: Benjamin Gewurz
Benjamin Gewurz (Oct 24, 2023 17:13 EDT)

Typed Name: Dr. Benjamin Gewurz

Signature: Isaac Chiu
Isaac Chiu (Oct 24, 2023 16:46 EDT)

Typed Name: Dr. Isaac Chiu

Signature: Dorothy P Schafer

Typed Name: Dr. Dorothy Schafer

Date: October 24, 2023

Infection Dynamics and Cell Type Specific Responses to Vesicular Stomatitis Virus Infection in the Mouse Brain

A dissertation presented

by

Tyler Bennette Krause

to

The Division of Medical Sciences

In partial fulfillment of the requirement for the degree of

Doctor of Philosophy

in the subject of

Virology

Harvard University

October 2023

Dissertation Advisor: Constance Cepko Tyler Bennette Krause

Infection Dynamics and Cell Type Specific Responses to Vesicular Stomatitis Virus Infection in the Mouse Brain

Abstract

Viruses are excellent cell biologists. They can be harnessed to interrogate biological systems and co-opted as tools for therapeutic or research purposes. For a tool to operate best, it's crucial to know how it functions in the environment in which it is utilized. The neuroscience field has adopted neurotropic viruses as transsynaptic tracers to label and modify neural circuits. Although these viruses are used as practical tools in the brain, our understanding of their specific cellular interactions and the brain tissue's response to them are still limited. We aimed to address these knowledge gaps by developing a viral system to track differential states of infection, better defining tropism in a cell type specific manner, and investigating factors that influence viral infection outcomes. Additionally, we profiled the brain's response to viral infection and monitored how various cell types contribute to this response over time. Our findings better inform viral tool design for neuroscience and broaden our understanding of the early immune response to viral infections in the brain parenchyma.

Table of Contents

Title page i

Copyright ii

Abstract iii

Table of contents iv

Acknowledgments vii

Chapter I. Introduction 1

1.1 Neurotropic viruses 2

Vesicular stomatitis virus (VSV) 2

Rabies Virus (RV) 7

1.2 Viral neuronal tracing 8

Directionality 9

Targeting and spread 9

1.3 Innate immunity 10

Sensing 11

Interferon (IFN) responses 12

1.4 Intrinsic Immunity 13

1.5 Cell types of the brain: an immunological perspective 14

Neurons 14

Astrocytes 15

Microglia 15

Oligodendrocyte lineage 16

Ependymal cells 17

1.6 References 19

Chapter II. Dual Reporting Virus Identifies Differential States of Infection *in vivo* 34

2.1 Abstract 35

2.2 Introduction 36

2.3 Results 40

Dual labeling VSV design and *in vitro* control experiments 40

Infection readouts *in vivo* and visualizing correlates of infection readouts with viral genomes/transcripts 48

Characterization of infection dynamics on a cell type specific basis *in vivo* 55

Assaying the role of interferon stimulated genes in the differential readouts of infection 63

2.4 Discussion 67

2.5 Material and Methods 76

2.6 References 84

2.7 Acknowledgements 91

Chapter III. IFN Signaling Heterogeneity in the Brain and Influence of IFN Signaling on Primary Infection Outcome 92

3.1 Abstract 93

3.2 Introduction 94

3.3 Results 97
IFN types detected in the brain post infection with dual labeling VSV 97
IFNb time course: shifting contributions by glial cells 100
Microglia observations: number and morphology changes 111
IFN signaling influence on primary infection outcomes 114
3.4 Discussion 121
3.5 Materials and Methods 129
3.6 References 136
3.7 Acknowledgments 140
Chapter IV. Discussion and Future Directions 141
4.1 Dual labeling viruses to track viral/host dynamics 142
Cell type primary infection outcomes 142
Applicability to other viruses 144
4.2 IFN production upon viral infection of CNS 145
Oligodendrocytes expressing IFNb 145
Temporal progression of IFNb production 147
Regional heterogeneous IFN response 149
4.3 Mechanisms dictating primary infection outcome 150
Innate immunity 151
Intrinsic immunity 152
4.4 References 154

Acknowledgments

Dr. Connie Cepko – I will never be able to express how grateful I am for having been able to conduct research in your lab. One of the main reasons for choosing your lab was because of our engaging weekly meetings. Even if I thought I did not have much to talk about from the previous week of experiments, somehow an hour (or more) would fly by with our conversations about science. You are patient, encouraging and insightful. Your support throughout this journey has been unwavering and I will always look back on our time together fondly.

Dr. Jon Kagan, Dr. Beth Stevens, Dr. David Knipe – Contrary to the script I was told by elder graduate students at the time, I always looked forward to my DAC meetings. Being able to converse about the intricacies of my project with you all was a joy. Through all the ups and downs of my projects you all were always supportive.

Dr. Kartik Chandran – You took a chance on a recent midwestern college graduate and provided the framework for my scientific pursuit in the field of virology. Without my time in your lab, I wouldn't be the scientist I am today. You showed me that science can rewarding and fun.

Dr. Josh Benoit – You were the one who first got me interested in scientific research. By letting me be part of your projects you gave me my first glimpse of what it takes to be a

scientist. My journey as a scientist began with you and I am so grateful to have begun this journey under your supervision.

Cepko/Tabin labs - Research is so much easier when you have a great environment. I am happy to say that I got to work with friends every single day in the lab. Thank you for creating such an inviting and engaging atmosphere.

Eric Krause, Dr. Joan Langholz, and Kristina Krause – I could not have asked for better parents or a sister. You instilled strong values, a sense for adventure, and my innate curiosity. Your love and support throughout the years has shaped the person I am today more than anyone else.

Dr. Anna Wec – We have been together since the start of my graduate career, and you have been cheering me on throughout the entire process. During this time, I have also had the pleasure to see you develop into one the most incredible scientists and leaders I have encountered. You are an inspiration. I can't wait to see what new adventures await us next.

Chapter I.

Introduction

1.1 Neurotropic viruses

Viruses have often been exploited for the understanding of their pathogenesis to improve human health and as tools to better elucidate underlying biology. Neurotropic viruses are viruses that can infect and cause disease within the central nervous system (CNS). A number of neurotropic viruses exist, including but not limited to retroviruses (e.g., MMLV, HIV), parvoviruses (e.g., AAV), adenoviruses (e.g., Ad5), herpes viruses (e.g., HSV, PRV, HCMV), rhabdoviruses (e.g., RABV, VSV), and alphaviruses (e.g., SIN, SFV) [1]. All these viruses share the capability to be neuroinvasive and neurovirulent. We will focus on two that are popular in the field of neuroscience and virology to better understand how they can be used as tools and how manipulations to these viruses can change their properties to inform us about novel biological processes.

Vesicular stomatitis virus (VSV)

VSV is a prototypical non-segmented, single-stranded, negative-sense RNA virus in the rhabdovirus family. The genome is approximately 11kb and encodes five proteins: the nucleocapsid (N), the phosphoprotein (P), the matrix protein (M), the glycoprotein (G) and the polymerase (L) [2]. These genes contain conserved transcriptional start and end sites with intergenic regions separating them. The five proteins together produce a bullet-shaped virion [3]; where the N protein coats the viral genome [4, 5], the P protein links the L to the N-coated viral genome to form a ribonucleoprotein complex [5-9], the M protein condenses the complex into a helical structure [10, 11], and it is enveloped in the host derived cell membrane that is decorated with trimeric G proteins (Figure 1.1) [12, 13].

VSV infection/replication cycle begins with the G protein mediating attachment to the low-density lipoprotein receptor (LDLR) on the host cell [14, 15]. It is thought that one of the reasons for VSV's broad tropism is due to the ubiquity and conservation of LDLR across cells, along with evidence that VSV-G might be able to mediate attachment/entry via other lipid components, albeit less efficiently [14, 16-19]. Post attachment the virion is endocytosed via both clathrin and actin mediate pathways [20]. While in the endocytic pathway, acidification of the endosome induces a conformational change in the G protein that exposes hydrophobic loops. These loops then mediate fusion of the viral envelope with the host endosomal membrane [21-23]. This fusion event releases the nucleocapsid core of the virion into the host cytoplasm where transcription and replication begin [24].

VSV transcription and genome replication are driven by the RNA polymerase complex, L and P [25]. The initial step after nucleocapsid core release and uncoating in the cytoplasm is primary transcription of the parental viral genome. This primary transcription event generates mRNAs from all the viral genes [26]. The polymerase begins transcription at the 3' end of the genome and sequentially moves towards the 5' end. Importantly, the polymerase may dissociate from the template genome when at the intergenic regions, in which case it must re-engage back at the 3' end [27]. This creates a transcriptional gradient where genes most proximal to the 3' end are transcribed more (N > P > M > G > L) [28, 29]. The viral mRNAs will then be subsequently translated by the host cell machinery, and the accumulation of viral proteins, namely N and P, will trigger the polymerase's switch from transcription to genome replication due to the encapsidation of nascent RNA [30]. Genome replication

initiating at a promoter in the 3' end produces a complementary, positive-sense anti-genome which serves as the template for progeny genomes [26]. The new, encapsidated progeny genomes can serve in viral transcription and genome replication representing an increased amplification process. The amplification of transcription is labeled "secondary transcription", and leads to the largest accumulation of translated viral proteins [31].

The encapsidated progeny genomes will associate with the other viral proteins to create nucleocapsids and then full-fledged virions. The nucleocapsids are condensed at the plasma membrane by interactions with the M protein [32, 33]. The sites where this condensation and budding occur are also enriched with the G protein which was embedded in the plasma membrane while transiting via the secretory pathway [34, 35]. The final budding of the enveloped virion is mediated by the M protein's interaction with host proteins involved in multivesicular body formation [36, 37]. This entire VSV replication process is rapid and results in high propagation of viral titers.

VSV was first described as causing an acute disease (vesicular stomatitis) in hoofed animals, characterized by the vesicular lesions on the oral mucosa [38]. The virus is thought to be transmitted through arthropod vectors in the wild [39, 40]. Importantly, VSV is generally considered to be non-pathogenic to humans, where most individuals will have subclinical or mild symptoms. This makes VSV a safe and attractive tool to use for molecular biology [41, 42].

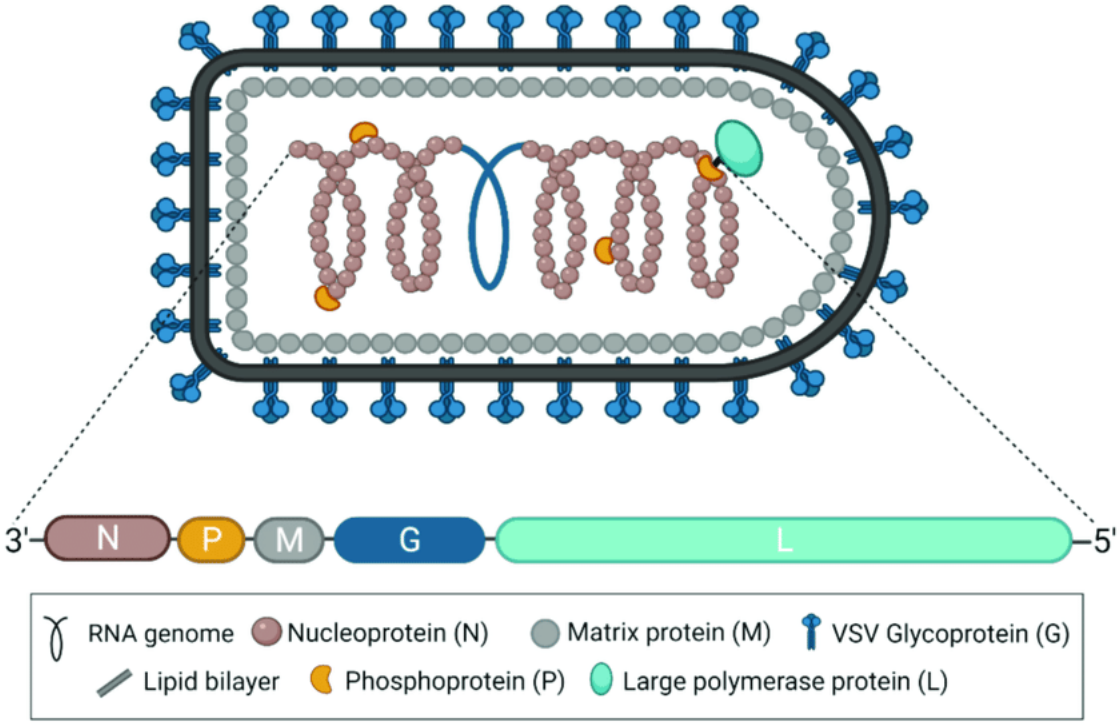

Figure 1.1 | Schematic of VSV virion with associated proteins [43]

VSV is a prototypical rhabdovirus and has therefore been widely used as a model system to study the replication and assembly of single-stranded, negative-sense RNA viruses. The utilization of VSV to investigate these phenomena was greatly advanced with the development of a reverse genetics approach generating VSV from a cDNA clone [41, 44, 45]. The successful rescue of VSV from cDNA required the combination of an RNA polymerase (T7) with plasmids encoding the anti-genome and helper plasmids N, P and L to form the replication complex [44]. The ability to make and rescue recombinant VSV allowed for it to be utilized as a molecular tool.

There are several aspects that make VSV such a valuable tool to study cell entry, virus/host interactions and viral replication. VSV has a relatively small genome yet can accommodate additional, large gene insertions [46]. Due to the rapid replication of VSV, genes that are inserted are highly expressed. The glycoprotein (G) of VSV is fairly promiscuous and facilitates broad tropism in a variety of cells and animals [14, 16] Lastly, VSV is able to incorporate unrelated glycoproteins into its envelope, allowing for greater control of tropism and for better use to study entry of various viruses [47].

All these aspects are exploited for the use of VSV to understand virus/host dynamics in the CNS, and as a neuronal tracing virus. Infection reporters can be inserted into the genome to track viral infection [1, 48, 49]. The G protein can be left in the genome to create a "replication competent" virus which can keep on spreading, or it can be deleted (VSVΔG) creating a "replication incompetent" virus. Using the VSVΔG virus, one can transiently express VSV-G or a heterologous glycoprotein to make a pseudotyped virus which exhibits entry dynamics associated with the viral glycoprotein on the envelope and does not spread after primary infection.

Rabies Virus (RV)

RABV is another virus in the Rhabdoviridae family that shares many commonalities with that of the related VSV. However, as opposed to VSV, RABV is highly pathogenic and extremely lethal [50]. Much of this increased pathogenicity is due to the differing properties of the viral proteins that RABV encodes [51]. These differences account for RABV tropism and immune evasion abilities, which are the basis for RABV being used heavily for the study of neuropathogenesis and neuronal tracing.

Natural infection with RV typically occurs when saliva containing RABV from a rabid animal enters a wound [52]. At the site of exposure, it is thought that some initial viral replication occurs before infecting peripheral motor neurons where the virus travels via retrograde transport from the periphery to the CNS. Within the CNS, RABV replication will continue, and infection will progress via centrifugal spread along nerves to infect salivary glands and other organ systems [53, 54]. Field isolates ("street" strains) differ in their pathogenesis as compared to laboratory-adapted ("fixed" strains) due to their differing effects on innate immunity. Comparison between strains has provided valuable insight into RABV propagation and evasion properties [55, 56].

RABV's neurotropism is heavily influenced by that of the RABV glycoprotein (RV-G). RABV-G mediates cell entry via attachment with several receptors that are implicated in the nervous system. Namely, RABV-G can bind to nicotinic acetylcholine receptor (nAChR), neuronal cell adhesion molecule (NCAM), and the p75 neurotrophin receptor (p75NTR) [52, 57, 58]. The differential interaction of RABV-G with these receptors allows for the propagation of RABV within the nervous system. Following attachment, RABV will undergo similar entry and replication mechanisms shared with

VSV, including lower pH triggering conformational changes in RABV-G resulting in fusion to the endosomal membrane, virion core release into the cytoplasm, primary transcription followed by genome replication and subsequent secondary transcription [59-61].

Another distinguishing attribute of RABV compared to that of VSV is the mechanism of immune evasion. VSV matrix protein shuts down host gene expression via several mechanisms: inhibition of host mRNA transcription, inhibition of host mRNA transport out of the nucleus, and inhibition of translation of host mRNA [62-64]. This can disrupt the antiviral properties of the host cell; however, these mechanisms can also induce a cytotoxic effect. Meanwhile, RABV takes a more nuanced approach with its phosphoprotein (RABV-P). Namely, RABV-P has emerged as a multifunctional IFN antagonist due to its ability to disrupt IFN-induced STAT signaling by binding to activated/phosphorylated STAT1 and STAT2, and by counteracting IFN gene expression by disrupting TBK-1 and IKKε activation/phosphorylation [65-69]. These attributes differ between street and fixed strains of RABV and have been shown to affect the tropism and neuropathogenesis of RABV in the CNS [70, 71].

1.2 Viral neuronal tracing

The inherent neurotropic abilities of some viruses have been leveraged as tools for neuroscientists. Specifically, viruses that can spread transsynaptically present a useful tool for studying neural anatomy and in some cases can manipulate these pathways [1].

To implement viruses as neurosynaptic tools, they must be tunable to the needs of the neuroscientist and their system.

Directionality

Depending on the cells and which circuits are intended to be labeled, one of the first considerations is the direction of viral spread. Virus can transit in an anterograde direction (cell body / soma to the synapse) or a retrograde direction (synapse to soma). Many viruses exhibit an intrinsic ability to transit in a specific direction [1]. In the case of the rhabdoviruses mentioned previously, VSV can transsynaptically spread in the anterograde direction, while RABV can transsynaptically spread in the retrograde direction. The direction of spread for these viruses has been shown to be tethered to the glycoprotein of the respective viruses [48, 49, 72, 73]. This was demonstrated elegantly by creating a pseudotyped VSV where RABV-G was transiently expressed and present on the VSV particle. This pseudotyped virus was then able to transsynaptically spread in the retrograde direction rather than the inherent anterograde direction exhibited by VSV with its own glycoprotein [72, 73].

Targeting and spread

Viruses used for labeling synaptic connections have proven to be invaluable to the field of neuroscience. However, indiscriminate infection of neurons at the site of injection and continual spread by replication competent viruses makes distinguishing specific synaptic partners difficult. To improve upon neurosynaptic tracing viral systems, additional modifications to the virus can be made. To control the amount of spread, replication incompetent viruses can be designed. These viruses are often lacking the

glycoprotein in the viral genome and therefore cannot mediate attachment and fusion to synaptic partners [74, 75]. In some iterations, other viral components can be removed, which stunts viral replication and propagation [76]. However, by removing the glycoprotein the virus will only be able to mediate primary infection and cannot spread at all. This obstacle can be overcome by expressing a glycoprotein in a specific starter cell and can be combined with a viral targeting system to direct infection to a specific cell type; for example, utilizing the avian tumor receptor A (TVA) along with the cognate glycoprotein (EnvA). In this system, a pseudotyped RABV or VSV with EnvA can be used to infect cells expressing TVA and RABV-G or VSV-G; this dual expression could be introduced from a previous viral infection with conditional promoters [77-79]. The final output is a monosynaptic tracing system where a specific cell is infected, and the replication incompetent virus can spread transsynaptically once.

1.3 Innate immunity

Whether during natural infection with a neurotropic virus or upon introduction of a neurosynaptic tracing virus as a tool, the brain responds to the infection rapidly [80, 81]. This first line of defense is the innate immune response, which functions to detect the pathogen, limit spread, and activate/modulate the adaptive immune response. Given the time frame of the acute primary viral infection that we are investigating, the innate immune response is the main antiviral system contributing to infection outcome.

Sensing

For the host to respond to infection it might first recognize that it is being infected. The recognition strategy of the host cell is to identify molecular motifs unique to pathogens, called pathogen-associated molecular patterns (PAMPs) [82]. PAMPs can span a diverse set of molecular structures and can be detected by germline encoded pattern recognition receptors (PRRs). The PRRs are classified by their location and ligand. Membrane bound PRRs include Toll-like receptors (TLRs) and C-type lectin receptors (CLRs); while cytoplasmic localized receptors include retinoic acid inducible gene-I (RIG-I)-like receptors (RLRs), nucleotide-binding oligomerization domain (NOD)-like receptors (NLRs) and cytosolic DNA sensors (CDS). Once a PRR engages with its cognate PAMP, it will initiate a signal transduction cascade that leads to the production of proinflammatory cytokines and chemokines [83-86].

VSV and RABV, being single-stranded RNA viruses, can be detected by several PRRs. The main PRR that detects rhabdovirus infections is RIG-I, which specifically recognizes 5’ ppp RNAs generated from replication intermediates as well as the genome and anti-genomes themselves [87-89]. Binding of RIG-I to VSV PAMPs is limited by the VSV nucleocapsid, which protects the genome [90, 91], therefore 5’ ppp RNAs detected by RIG-I are thought to be exposed byproducts [92]. The endosomal TLR7, which recognizes ssRNA, has also been shown to detect VSV infections, and induce an antiviral response in some cases, yet in others cases the response is insufficient [93-95]; indicating that RIG-I likely contributes more to the antiviral response. Lastly, VSV’s glycoprotein is also able to be recognized by TLR4 in myeloid dendritic cells and macrophages [96].

Interferon (IFN) responses

Viral PAMPs recognized by the host PRRs lead to the production of the cytokine interferon (IFN). IFN signals in an autocrine and paracrine fashion to trigger the expression of protective, antiviral proteins called interferon-stimulated genes (ISGs) in the host cells and to activate/recruit other immune cells [97, 98]. There are three major groups of IFN, classified by their receptor, including type I, type II, and type III IFNs [99, 100]. Type I and type III interferons are further comprised of multiple subtypes of IFN. The combination of receptor expression and IFN subtype production dictates which cells (type and location) are going to respond to the IFN signaling and express ISGs [101].

Type I IFNs are one of the most extensively studied and most potent antiviral pathways of the innate immune system. They are comprised of subtypes such as IFNα, IFNβ, IFNω, IFNκ, and IFNε [99, 102, 103]. All of these IFNs signal through the IFN-α/β receptor (IFNAR), which is expressed to varying degrees in all nucleated cells, leading to a signal transduction cascade and the expression of ISGs. There are hundreds of known ISGs, and they can inhibit many stages of the viral replication cycle [81, 104, 105]. By using IFNAR KO mice/cells or by inhibiting the downstream signaling, one can interrogate the role of type I IFN signaling in viral pathogenesis. VSV is known to be highly sensitive to type I IFNs both *in vitro* and *in vivo* [80, 106-108]. This sensitivity has been shown to both reduce the initial amount of productively infected cells and to prevent spread from secondary infection in the brain. Recently, it has also been observed that type I IFN signaling can influence tropism, where susceptibility of specific cell types changed depending on the presence or absence of IFNAR signaling [109-111].

Type II IFN is so solely comprised of IFNγ and signals through IFNGR. The expression of IFNγ is more restricted, where activated T cells and NK cells are the main producers [112, 113]. Despite this restriction, IFNγ has been shown to elicit antiviral activity [113-115]. Additionally, IFNγ provides a significant support role type I IFNs by aiding in the priming and activation of macrophages/microglia and other immune cells [116]. This in turn can lead to a feedback loop where ISGs from type I IFN signaling can potentiate and recruit the involvement of type II IFNs [117, 118].

The more recently discovered type III IFNs are comprised of IFNλ subtypes and signal through the IFNLR and an IL10Rβ subunit [119]. Although type III and type I IFNs share similar downstream signaling mechanisms, type III IFNs are primarily restricted to tissue barriers and have been demonstrated in coordinating nonredundant antiviral functions in epithelial cells, especially in the context of gastrointestinal infections [120, 121]. Similarly, type III IFNs have also been implicated in epithelial maintenance and viral restriction at the blood-brain barrier. Specifically, IFNλ signaling has been shown to enhance tight junction integrity of the BBB and prevent neuroinvasion from peripheral infection [122].

1.4 Intrinsic Immunity

"Intrinsic" and "innate" immunity are often used interchangeably in virology; however, they are mechanistically distinct. Intrinsic immunity consists of preexisting restriction factors present in a cell, while innate immunity consists of antiviral factors that

are induced upon infection [123, 124]. Confusingly, these antiviral factors can be shared between these two arms of immunity, but importantly intrinsic immunity refers to the basal levels rather than any upregulation or activation event (as characteristic in innate immunity). In some contexts, these intrinsic antiviral factors are called "restriction factors" and have been extensively studied in the context of HIV infections [125]. Some of these factors include APOBEC3G, TRIM5α, and tetherin [126]. Intrinsic factors that have been shown to inhibit VSV include IFITMs, IFITs, and PKR [127-130]. These antiviral factors can be upregulated upon IFN stimulation but are able to confer viral infection resistance even at basal, homeostatic levels.

1.5 Cell types of the brain: an immunological perspective

The CNS is an immunologically active organ, comprised of several different types of cells. Evidence indicates that region- and cell type- specific responses are induced upon viral infection. These cell type specific responses are thought, in part, to contribute to viral tropism and infection outcome. However, which cells are contributing to the response is dependent on the virus, route of infection, and experimental system.

Neurons

Neurons, or nerve cells, are the fundamental cell type of the CNS that transmits information in the form of electrical and chemical signals. As such, it is a central focus of neuroscientists and the main target for neurosynaptic tracing viruses. Several studies have observed that neurons both respond to and produce a type I IFN response [131-133].

However, this response does not apply to all neuronal cell types equally; granule cell neurons from the cerebellum exhibited increased resistance to viral infection compared to cortical neurons [134]. This difference among neuronal types also extends to the developmental stage where neural progenitor cells display more viral resistance than committed neurons [135, 136]. Many of these differences are thought to be related to ISG expression and differing responsiveness to IFN. Moreover, due to the successful pathogenesis of neurotropic viruses, IFN-responsive neurons are typically not sufficient in preventing productive infection as compared to their glial cell counterparts.

Astrocytes

Astrocytes are the most abundant glial cell in the adult CNS. Some of their main functions include ion homeostasis, roles in the preservation of tripartite synapses, and BBB maintenance [137, 138]. More recently, astrocytes have been recognized as one of the main IFNβ producing cells upon several neurotropic viral infections including RABV, TMEV, and VSV [139-141]. This is partially attributable to the fact that they have higher expression of PRRs as compared to neurons [142]. Curiously, the infectability and responsiveness of astrocytes in the context of RABV depends on the strain. Lab-attenuated RABV abortively infects astrocytes while street strains can sustain more productive infection [143]. This indicates that the virus and its ability to manipulate the innate immune response can change the contribution of specific cell types.

Microglia

Microglia are considered the main immunocompetent, phagocytic cell type of the CNS. Although they make up part of the glia population in the CNS, they originate from

yolk sac progenitors that populate the brain during development rather than the ectodermal tissue like the other glial cells [144, 145]. The immune and phagocytic properties of microglia contribute greatly to their function in synaptic pruning during development and controlling the local immune environment (upon viral infection or other injury) [146, 147]. As such, in several studies, microglia are identified as the main IFNβ producing cells in viral infections including La Crosse virus, RABV, murine coronavirus (MHV), and even VSV [80, 148-151]. This shows that depending on the strain and experimental conditions, different CNS cell types can function as type I IFN producers for the same virus. The capacity of microglia to coordinate this innate immune response is also because of the immune repertoire and responsiveness of microglia as compared to neurons and other cells (e.g., higher expression of ISG and PRRs). Similarly, this higher ISG expression contributes to microglia being more resistant to viral infection compared to its contemporaries [142]. Although much of the focus is on microglia producing type I IFNs, they are also highly responsive to type II IFNs, where they are further activated by simulating effect of IFNγ [116].

Oligodendrocyte lineage

Oligodendrocyte lineage cells constitute another glia population in the brain consisting of oligodendrocyte progenitor cells (OPCs) and mature oligodendrocytes. The main function of oligodendrocytes is to generate and support the myelin sheaths that surround neuronal axons [152]. Compared to astrocytes and microglia, oligodendrocytes are significantly understudied in terms of their role in viral infections. The few studies that do exist indicate that OPCs and mature oligodendrocytes are able to survive infection

and can contribute to neuroinflammation upon infection with TMEV or MHV [153, 154]. Other studies also indicate the role of viral infection in disrupting oligodendrocyte homeostasis contributing to myelin toxicity [155-157]. Myelin toxicity and developmental defects of oligodendrocytes are also recognized in the field of neurodegeneration where it has been demonstrated that oligodendrocytes can respond to IFNγ, and at high doses, this can contribute to toxicity in multiple sclerosis (MS) and experimental autoimmune encephalomyelitis (EAE) models [158, 159]. This pathway has been extended to viral infection where it has been suggested that reduced infection of oligodendrocyte by JHMV is due to their responsiveness to IFNγ [160]. From single-cell RNA sequencing data, oligodendrocyte lineage cells in some circumstances have basal ISG and PRR expression comparable to the more recognized immunocompetent astrocytes and microglia [142, 161]. This suggests oligodendrocyte lineage cells have the potential to be involved in coordinating an innate immune response, but further investigation is required.

Ependymal cells

Ependymal cells are a type of multiciliated, neuroepithelial glial cell lining the cerebral ventricles. Their main functions include controlling the production and flow of cerebrospinal fluid, brain metabolism, and waste clearance [162]. Although ependymal cells express many receptors that facilitate viral attachment, viral infection of ependymal cells is also understudied [163]. A few studies that do exist indicate that ependymal cells can be productively infected by polyomaviruses (MuPyV) and coronaviruses (JHMV); and this leads to Stat1-dependent expression of chemokines in the CNS [164, 165].

Similar to the oligodendrocytes, single-cell RNA sequencing suggests that ependymal cells also express ISG and PRR at levels comparable to those of astrocytes and microglia [142]. Considering the ependyma's function as a barrier between the cerebrospinal fluid (CSF) and brain parenchyma, along with the diverse immune capabilities these cells possess, they may have a substantial role in the pathogenesis and spread of viruses. These cells also warrant more significant attention in the field of neurovirology.

1.6 References

1. Nassi, J.J., et al., *Neuroanatomy goes viral!* Front Neuroanat, 2015. **9**: p. 80.

2. Rodriguez, L.L., et al., *Full-length genome analysis of natural isolates of vesicular stomatitis virus (Indiana 1 serotype) from North, Central and South America.* J Gen Virol, 2002. **83**(Pt 10): p. 2475-2483.

3. Ge, P., et al., *Cryo-EM model of the bullet-shaped vesicular stomatitis virus.* Science, 2010. **327**(5966): p. 689-93.

4. Thomas, D., et al., *Mass and molecular composition of vesicular stomatitis virus: a scanning transmission electron microscopy analysis.* J Virol, 1985. **54**(2): p. 598-607.

5. Green, T.J., et al., *Structure of the vesicular stomatitis virus nucleoprotein-RNA complex.* Science, 2006. **313**(5785): p. 357-60.

6. Ding, H., et al., *Crystal structure of the oligomerization domain of the phosphoprotein of vesicular stomatitis virus.* J Virol, 2006. **80**(6): p. 2808-14.

7. Leyrat, C., et al., *Structure of the vesicular stomatitis virus N(0)-P complex.* PLoS Pathog, 2011. **7**(9): p. e1002248.

8. Liang, B., et al., *Structure of the L Protein of Vesicular Stomatitis Virus from Electron Cryomicroscopy.* Cell, 2015. **162**(2): p. 314-327.

9. Gould, J.R., et al., *The Connector Domain of Vesicular Stomatitis Virus Large Protein Interacts with the Viral Phosphoprotein.* J Virol, 2020. **94**(6).

10. Gaudier, M., Y. Gaudin, and M. Knossow, *Crystal structure of vesicular stomatitis virus matrix protein.* EMBO J, 2002. **21**(12): p. 2886-92.

11. Newcomb, W.W. and J.C. Brown, *Role of the vesicular stomatitis virus matrix protein in maintaining the viral nucleocapsid in the condensed form found in native virions.* J Virol, 1981. **39**(1): p. 295-9.

12. Roche, S., et al., *Structure of the prefusion form of the vesicular stomatitis virus glycoprotein G.* Science, 2007. **315**(5813): p. 843-8.

13. Roche, S., et al., *Crystal structure of the low-pH form of the vesicular stomatitis virus glycoprotein G.* Science, 2006. **313**(5784): p. 187-91.

14. Finkelshtein, D., et al., *LDL receptor and its family members serve as the cellular receptors for vesicular stomatitis virus.* Proc Natl Acad Sci U S A, 2013. **110**(18): p. 7306-11.

15. Nikolic, J., et al., *Structural basis for the recognition of LDL-receptor family members by VSV glycoprotein.* Nat Commun, 2018. **9**(1): p. 1029.

16. Mundell, N.A., et al., *Vesicular stomatitis virus enables gene transfer and transsynaptic tracing in a wide range of organisms.* J Comp Neurol, 2015. **523**(11): p. 1639-63.

17. Mastromarino, P., et al., *Characterization of membrane components of the erythrocyte involved in vesicular stomatitis virus attachment and fusion at acidic pH.* J Gen Virol, 1987. **68 (Pt 9)**: p. 2359-69.

18. Superti, F., et al., *Role of sialic acid in cell receptors for vesicular stomatitis virus.* Acta Virol, 1986. **30**(1): p. 10-8.

19. Wilsie, L.C., A.M. Gonzales, and R.A. Orlando, *Syndecan-1 mediates internalization of apoE-VLDL through a low density lipoprotein receptor-related protein (LRP)-independent, non-clathrin-mediated pathway.* Lipids Health Dis, 2006. **5**: p. 23.

20. Belot, L., A. Albertini, and Y. Gaudin, *Structural and cellular biology of rhabdovirus entry.* Adv Virus Res, 2019. **104**: p. 147-183.

21. Cabot, M., et al., *Endosomes supporting fusion mediated by vesicular stomatitis virus glycoprotein have distinctive motion and acidification.* Traffic, 2022. **23**(4): p. 221-234.

22. Eidelman, O., et al., *pH-dependent fusion induced by vesicular stomatitis virus glycoprotein reconstituted into phospholipid vesicles.* J Biol Chem, 1984. **259**(7): p. 4622-8.

23. Kim, I.S., et al., *Mechanism of membrane fusion induced by vesicular stomatitis virus G protein.* Proc Natl Acad Sci U S A, 2017. **114**(1): p. E28-E36.

24. Mire, C.E., J.M. White, and M.A. Whitt, *A spatio-temporal analysis of matrix protein and nucleocapsid trafficking during vesicular stomatitis virus uncoating.* PLoS Pathog, 2010. **6**(7): p. e1000994.

25. Banerjee, A.K. and S. Barik, *Gene expression of vesicular stomatitis virus genome RNA.* Virology, 1992. **188**(2): p. 417-28.

26. Barr, J.N., S.P. Whelan, and G.W. Wertz, *Transcriptional control of the RNA-dependent RNA polymerase of vesicular stomatitis virus.* Biochim Biophys Acta, 2002. **1577**(2): p. 337-53.

27. Barr, J.N. and G.W. Wertz, *Polymerase slippage at vesicular stomatitis virus gene junctions to generate poly(A) is regulated by the upstream 3'-AUAC-5' tetranucleotide: implications for the mechanism of transcription termination.* J Virol, 2001. **75**(15): p. 6901-13.

28. Barr, J.N., et al., *The VSV polymerase can initiate at mRNA start sites located either up or downstream of a transcription termination signal but size of the intervening intergenic region affects efficiency of initiation.* Virology, 2008. **374**(2): p. 361-70.

29. Hwang, L.N., N. Englund, and A.K. Pattnaik, *Polyadenylation of vesicular stomatitis virus mRNA dictates efficient transcription termination at the intercistronic gene junctions.* J Virol, 1998. **72**(3): p. 1805-13.

30. Arnheiter, H., et al., *Role of the nucleocapsid protein in regulating vesicular stomatitis virus RNA synthesis.* Cell, 1985. **41**(1): p. 259-67.

31. Morin, B., A.A. Rahmeh, and S.P. Whelan, *Mechanism of RNA synthesis initiation by the vesicular stomatitis virus polymerase.* EMBO J, 2012. **31**(5): p. 1320-9.

32. Lyles, D.S., *Assembly and budding of negative-strand RNA viruses.* Adv Virus Res, 2013. **85**: p. 57-90.

33. Schmitt, A.P. and R.A. Lamb, *Escaping from the cell: assembly and budding of negative-strand RNA viruses.* Curr Top Microbiol Immunol, 2004. **283**: p. 145-96.

34. Balch, W.E., et al., *Vesicular stomatitis virus glycoprotein is sorted and concentrated during export from the endoplasmic reticulum.* Cell, 1994. **76**(5): p. 841-52.

35. Sevier, C.S., et al., *Efficient export of the vesicular stomatitis virus G protein from the endoplasmic reticulum requires a signal in the cytoplasmic tail that includes both tyrosine-based and di-acidic motifs.* Mol Biol Cell, 2000. **11**(1): p. 13-22.

36. Jenni, S., et al., *Visualizing molecular interactions that determine assembly of a bullet-shaped vesicular stomatitis virus particle.* Nat Commun, 2022. **13**(1): p. 4802.

37. Zhou, K., et al., *Atomic model of vesicular stomatitis virus and mechanism of assembly.* Nat Commun, 2022. **13**(1): p. 5980.

38. Hanson, R.P., *Discussion of the natural history of vesicular stomatitis.* Am J Epidemiol, 1968. **87**(2): p. 264-6.

39. Rozo-Lopez, P., B.S. Drolet, and B. Londono-Renteria, *Vesicular Stomatitis Virus Transmission: A Comparison of Incriminated Vectors.* Insects, 2018. **9**(4).

40. Corn, J.L., et al., *Isolation of vesicular stomatitis virus New Jersey serotype from phlebotomine sand flies in Georgia.* Am J Trop Med Hyg, 1990. **42**(5): p. 476-82.

41. Munis, A.M., E.M. Bentley, and Y. Takeuchi, *A tool with many applications: vesicular stomatitis virus in research and medicine.* Expert Opin Biol Ther, 2020. **20**(10): p. 1187-1201.

42. Fields, B.N. and K. Hawkins, *Human infection with the virus of vesicular stomatitis during an epizootic.* N Engl J Med, 1967. **277**(19): p. 989-94.

43. Liu, G., et al., *Vesicular Stomatitis Virus: From Agricultural Pathogen to Vaccine Vector.* Pathogens, 2021. **10**(9).

44. Whelan, S.P., et al., *Efficient recovery of infectious vesicular stomatitis virus entirely from cDNA clones.* Proc Natl Acad Sci U S A, 1995. **92**(18): p. 8388-92.

45. Harty, R.N., et al., *Vaccinia virus-free recovery of vesicular stomatitis virus.* J Mol Microbiol Biotechnol, 2001. **3**(4): p. 513-7.

46. Haglund, K., et al., *Expression of human immunodeficiency virus type 1 Gag protein precursor and envelope proteins from a vesicular stomatitis virus recombinant: high-level production of virus-like particles containing HIV envelope.* Virology, 2000. **268**(1): p. 112-21.

47. Whitt, M.A., *Generation of VSV pseudotypes using recombinant DeltaG-VSV for studies on virus entry, identification of entry inhibitors, and immune responses to vaccines.* J Virol Methods, 2010. **169**(2): p. 365-74.

48. Beier, K. and C. Cepko, *Viral tracing of genetically defined neural circuitry.* J Vis Exp, 2012(68).

49. Beier, K.T., et al., *Transsynaptic tracing with vesicular stomatitis virus reveals novel retinal circuitry.* J Neurosci, 2013. **33**(1): p. 35-51.

50. Maurya, I., et al., *State of globe: rabies: the lethality since antiquity!* J Glob Infect Dis, 2015. **7**(1): p. 1-2.

51. Zhang, H., et al., *Regulation of innate immune responses by rabies virus.* Animal Model Exp Med, 2022. **5**(5): p. 418-429.

52. Lafon, M., *Rabies virus receptors.* J Neurovirol, 2005. **11**(1): p. 82-7.

53. Jackson, A.C., et al., *Extraneural organ involvement in human rabies.* Lab Invest, 1999. **79**(8): p. 945-51.

54. Jogai, S., B.D. Radotra, and A.K. Banerjee, *Rabies viral antigen in extracranial organs: a post-mortem study.* Neuropathol Appl Neurobiol, 2002. **28**(4): p. 334-8.

55. Liu, S.Q., et al., *Rabies viruses of different virulence regulates inflammatory responses both in vivo and in vitro via MAPK and NF-kappaB pathway.* Mol Immunol, 2020. **125**: p. 70-82.

56. Yin, J., et al., *Research Advances on the Interactions between Rabies Virus Structural Proteins and Host Target Cells: Accrued Knowledge from the Application of Reverse Genetics Systems.* Viruses, 2021. **13**(11).

57. Thoulouze, M.I., et al., *The neural cell adhesion molecule is a receptor for rabies virus.* J Virol, 1998. **72**(9): p. 7181-90.

58. Tuffereau, C., et al., *Low-affinity nerve-growth factor receptor (P75NTR) can serve as a receptor for rabies virus.* EMBO J, 1998. **17**(24): p. 7250-9.

59. Etessami, R., et al., *Spread and pathogenic characteristics of a G-deficient rabies virus recombinant: an in vitro and in vivo study.* J Gen Virol, 2000. **81**(Pt 9): p. 2147-2153.

60. Le Blanc, I., et al., *Endosome-to-cytosol transport of viral nucleocapsids.* Nat Cell Biol, 2005. **7**(7): p. 653-64.

61. Ivanov, I., et al., *Structural insights into the rhabdovirus transcription/replication complex.* Virus Res, 2011. **162**(1-2): p. 126-37.

62. Ahmed, M., et al., *Ability of the matrix protein of vesicular stomatitis virus to suppress beta interferon gene expression is genetically correlated with the inhibition of host RNA and protein synthesis.* J Virol, 2003. **77**(8): p. 4646-57.

63. Petersen, J.M., et al., *The matrix protein of vesicular stomatitis virus inhibits nucleocytoplasmic transport when it is in the nucleus and associated with nuclear pore complexes.* Mol Cell Biol, 2000. **20**(22): p. 8590-601.

64. von Kobbe, C., et al., *Vesicular stomatitis virus matrix protein inhibits host cell gene expression by targeting the nucleoporin Nup98.* Mol Cell, 2000. **6**(5): p. 1243-52.

65. Rieder, M. and K.K. Conzelmann, *Interferon in rabies virus infection.* Adv Virus Res, 2011. **79**: p. 91-114.

66. Brzozka, K., S. Finke, and K.K. Conzelmann, *Identification of the rabies virus alpha/beta interferon antagonist: phosphoprotein P interferes with phosphorylation of interferon regulatory factor 3.* J Virol, 2005. **79**(12): p. 7673-81.

67. Rieder, M., et al., *Genetic dissection of interferon-antagonistic functions of rabies virus phosphoprotein: inhibition of interferon regulatory factor 3 activation is important for pathogenicity.* J Virol, 2011. **85**(2): p. 842-52.

68. Vidy, A., M. Chelbi-Alix, and D. Blondel, *Rabies virus P protein interacts with STAT1 and inhibits interferon signal transduction pathways.* J Virol, 2005. **79**(22): p. 14411-20.

69. Vidy, A., et al., *The nucleocytoplasmic rabies virus P protein counteracts interferon signaling by inhibiting both nuclear accumulation and DNA binding of STAT1.* J Virol, 2007. **81**(8): p. 4255-63.

70. Ito, N., et al., *Role of interferon antagonist activity of rabies virus phosphoprotein in viral pathogenicity.* J Virol, 2010. **84**(13): p. 6699-710.

71. Yamaoka, S., et al., *Involvement of the rabies virus phosphoprotein gene in neuroinvasiveness.* J Virol, 2013. **87**(22): p. 12327-38.

72. Beier, K.T., et al., *Anterograde or retrograde transsynaptic labeling of CNS neurons with vesicular stomatitis virus vectors.* Proc Natl Acad Sci U S A, 2011. **108**(37): p. 15414-9.

73. Beier, K.T., et al., *Vesicular stomatitis virus with the rabies virus glycoprotein directs retrograde transsynaptic transport among neurons in vivo.* Front Neural Circuits, 2013. **7**: p. 11.

74. Callaway, E.M. and L. Luo, *Monosynaptic Circuit Tracing with Glycoprotein-Deleted Rabies Viruses.* J Neurosci, 2015. **35**(24): p. 8979-85.

75. Wickersham, I.R., H.A. Sullivan, and H.S. Seung, *Production of glycoprotein-deleted rabies viruses for monosynaptic tracing and high-level gene expression in neurons.* Nat Protoc, 2010. **5**(3): p. 595-606.

76. Chatterjee, S., et al., *Nontoxic, double-deletion-mutant rabies viral vectors for retrograde targeting of projection neurons.* Nat Neurosci, 2018. **21**(4): p. 638-646.

77. Masaki, Y., et al., *Monosynaptic rabies virus tracing from projection-targeted single neurons.* Neurosci Res, 2022. **178**: p. 20-32.

78. Wall, N.R., et al., *Monosynaptic circuit tracing in vivo through Cre-dependent targeting and complementation of modified rabies virus.* Proc Natl Acad Sci U S A, 2010. **107**(50): p. 21848-53.

79. Miyamichi, K., et al., *Cortical representations of olfactory input by trans-synaptic tracing.* Nature, 2011. **472**(7342): p. 191-6.

80. Drokhlyansky, E., et al., *The brain parenchyma has a type I interferon response that can limit virus spread.* Proc Natl Acad Sci U S A, 2017. **114**(1): p. E95-E104.

81. Singh, H., J. Koury, and M. Kaul, *Innate Immune Sensing of Viruses and Its Consequences for the Central Nervous System.* Viruses, 2021. **13**(2).

82. Mogensen, T.H., *Pathogen recognition and inflammatory signaling in innate immune defenses.* Clin Microbiol Rev, 2009. **22**(2): p. 240-73, Table of Contents.

83. Goubau, D., S. Deddouche, and C. Reis e Sousa, *Cytosolic sensing of viruses.* Immunity, 2013. **38**(5): p. 855-69.

84. Kawai, T. and S. Akira, *Innate immune recognition of viral infection.* Nat Immunol, 2006. **7**(2): p. 131-7.

85. Thompson, M.R., et al., *Pattern recognition receptors and the innate immune response to viral infection.* Viruses, 2011. **3**(6): p. 920-40.

86. Iwasaki, A. and R. Medzhitov, *Toll-like receptor control of the adaptive immune responses.* Nat Immunol, 2004. **5**(10): p. 987-95.

87. Takahasi, K., et al., *Solution structures of cytosolic RNA sensor MDA5 and LGP2 C-terminal domains: identification of the RNA recognition loop in RIG-I-like receptors.* J Biol Chem, 2009. **284**(26): p. 17465-74.

88. Panda, D., et al., *Induction of interferon and interferon signaling pathways by replication of defective interfering particle RNA in cells constitutively expressing vesicular stomatitis virus replication proteins.* J Virol, 2010. **84**(9): p. 4826-31.

89. Gaccione, C. and P.I. Marcus, *Interferon induction by viruses. XVIII. Vesicular stomatitis virus-New Jersey: a single infectious particle can both induce and suppress interferon production.* J Interferon Res, 1989. **9**(5): p. 603-14.

90. Weber, M., et al., *Incoming RNA virus nucleocapsids containing a 5'-triphosphorylated genome activate RIG-I and antiviral signaling.* Cell Host Microbe, 2013. **13**(3): p. 336-46.

91. Marcus, P.I. and M.J. Sekellick, *Defective interfering particles with covalently linked [+/-]RNA induce interferon.* Nature, 1977. **266**(5605): p. 815-9.

92. Kagan, J.C., *Infection infidelities drive innate immunity.* Science, 2023. **379**(6630): p. 333-335.

93. Shi, Z., et al., *A novel Toll-like receptor that recognizes vesicular stomatitis virus.* J Biol Chem, 2011. **286**(6): p. 4517-24.

94. Zhou, S., et al., *Role of MyD88 in route-dependent susceptibility to vesicular stomatitis virus infection.* J Immunol, 2007. **178**(8): p. 5173-81.

95. Sun, Q., et al., *The specific and essential role of MAVS in antiviral innate immune responses.* Immunity, 2006. **24**(5): p. 633-42.

96. Georgel, P., et al., *Vesicular stomatitis virus glycoprotein G activates a specific antiviral Toll-like receptor 4-dependent pathway.* Virology, 2007. **362**(2): p. 304-13.

97. Isaacs, A. and J. Lindenmann, *Virus interference. I. The interferon. By A. Isaacs and J. Lindenmann, 1957.* J Interferon Res, 1987. **7**(5): p. 429-38.

98. Parkin, J. and B. Cohen, *An overview of the immune system.* Lancet, 2001. **357**(9270): p. 1777-89.

99. Thaney, V.E. and M. Kaul, *Type I Interferons in NeuroHIV.* Viral Immunol, 2019. **32**(1): p. 7-14.

100. Chelbi-Alix, M.K. and J. Wietzerbin, *Interferon, a growing cytokine family: 50 years of interferon research.* Biochimie, 2007. **89**(6-7): p. 713-8.

101. Kalie, E., et al., *The stability of the ternary interferon-receptor complex rather than the affinity to the individual subunits dictates differential biological activities.* J Biol Chem, 2008. **283**(47): p. 32925-36.

102. Kalliolias, G.D. and L.B. Ivashkiv, *Overview of the biology of type I interferons.* Arthritis Res Ther, 2010. **12 Suppl 1**(Suppl 1): p. S1.

103. McNab, F., et al., *Type I interferons in infectious disease.* Nat Rev Immunol, 2015. **15**(2): p. 87-103.

104. Schneider, W.M., M.D. Chevillotte, and C.M. Rice, *Interferon-stimulated genes: a complex web of host defenses.* Annu Rev Immunol, 2014. **32**: p. 513-45.

105. Schoggins, J.W. and C.M. Rice, *Interferon-stimulated genes and their antiviral effector functions.* Curr Opin Virol, 2011. **1**(6): p. 519-25.

106. Trottier, M.D., Jr., B.M. Palian, and C.S. Reiss, *VSV replication in neurons is inhibited by type I IFN at multiple stages of infection.* Virology, 2005. **333**(2): p. 215-25.

107. Whitaker-Dowling, P.A., et al., *Interferon-mediated inhibition of virus penetration.* Proc Natl Acad Sci U S A, 1983. **80**(4): p. 1083-6.

108. Detje, C.N., et al., *Local type I IFN receptor signaling protects against virus spread within the central nervous system.* J Immunol, 2009. **182**(4): p. 2297-304.

109. Welsch, J.C., et al., *Type I Interferon Receptor Signaling Drives Selective Permissiveness of Astrocytes and Microglia to Measles Virus during Brain Infection.* J Virol, 2019. **93**(13).

110. Fares, M., et al., *Pathological modeling of TBEV infection reveals differential innate immune responses in human neurons and astrocytes that correlate with their susceptibility to infection.* J Neuroinflammation, 2020. **17**(1): p. 76.

111. Feige, L., et al., *Susceptibilities of CNS Cells towards Rabies Virus Infection Is Linked to Cellular Innate Immune Responses.* Viruses, 2022. **15**(1).

112. Chesler, D.A. and C.S. Reiss, *The role of IFN-gamma in immune responses to viral infections of the central nervous system.* Cytokine Growth Factor Rev, 2002. **13**(6): p. 441-54.

113. Kang, S., H.M. Brown, and S. Hwang, *Direct Antiviral Mechanisms of Interferon-Gamma.* Immune Netw, 2018. **18**(5): p. e33.

114. Cantin, E., B. Tanamachi, and H. Openshaw, *Role for gamma interferon in control of herpes simplex virus type 1 reactivation.* J Virol, 1999. **73**(4): p. 3418-23.

115. Chesler, D.A., et al., *Interferon-gamma-induced inhibition of neuronal vesicular stomatitis virus infection is STAT1 dependent.* J Neurovirol, 2004. **10**(1): p. 57-63.

116. Kann, O., F. Almouhanna, and B. Chausse, *Interferon gamma: a master cytokine in microglia-mediated neural network dysfunction and neurodegeneration.* Trends Neurosci, 2022. **45**(12): p. 913-927.

117. Lee, A.J. and A.A. Ashkar, *The Dual Nature of Type I and Type II Interferons.* Front Immunol, 2018. **9**: p. 2061.

118. Hwang, M. and C.C. Bergmann, *Alpha/Beta Interferon (IFN-alpha/beta) Signaling in Astrocytes Mediates Protection against Viral Encephalomyelitis and Regulates IFN-gamma-Dependent Responses.* J Virol, 2018. **92**(10).

119. Wack, A., E. Terczynska-Dyla, and R. Hartmann, *Guarding the frontiers: the biology of type III interferons.* Nat Immunol, 2015. **16**(8): p. 802-9.

120. Lazear, H.M., J.W. Schoggins, and M.S. Diamond, *Shared and Distinct Functions of Type I and Type III Interferons.* Immunity, 2019. **50**(4): p. 907-923.

121. Zhou, J.H., et al., *Type III Interferons in Viral Infection and Antiviral Immunity.* Cell Physiol Biochem, 2018. **51**(1): p. 173-185.

122. Lazear, H.M., et al., *Interferon-lambda restricts West Nile virus neuroinvasion by tightening the blood-brain barrier.* Sci Transl Med, 2015. **7**(284): p. 284ra59.

123. Alandijany, T., *Host Intrinsic and Innate Intracellular Immunity During Herpes Simplex Virus Type 1 (HSV-1) Infection.* Front Microbiol, 2019. **10**: p. 2611.

124. Majdoul, S. and A.A. Compton, *Lessons in self-defence: inhibition of virus entry by intrinsic immunity.* Nat Rev Immunol, 2022. **22**(6): p. 339-352.

125. Bergantz, L., et al., *Interplay between Intrinsic and Innate Immunity during HIV Infection.* Cells, 2019. **8**(8).

126. Yan, N. and Z.J. Chen, *Intrinsic antiviral immunity.* Nat Immunol, 2012. **13**(3): p. 214-22.

127. Diamond, M.S. and M. Farzan, *The broad-spectrum antiviral functions of IFIT and IFITM proteins.* Nat Rev Immunol, 2013. **13**(1): p. 46-57.

128. Li, K., et al., *IFITM proteins restrict viral membrane hemifusion.* PLoS Pathog, 2013. **9**(1): p. e1003124.

129. Durbin, R.K., et al., *PKR protection against intranasal vesicular stomatitis virus infection is mouse strain dependent.* Viral Immunol, 2002. **15**(1): p. 41-51.

130. Fensterl, V., et al., *Interferon-induced Ifit2/ISG54 protects mice from lethal VSV neuropathogenesis.* PLoS Pathog, 2012. **8**(5): p. e1002712.

131. Prehaud, C., et al., *Virus infection switches TLR-3-positive human neurons to become strong producers of beta interferon.* J Virol, 2005. **79**(20): p. 12893-904.

132. Hwang, M. and C.C. Bergmann, *Neuronal Ablation of Alpha/Beta Interferon (IFN-alpha/beta) Signaling Exacerbates Central Nervous System Viral Dissemination and Impairs IFN-gamma Responsiveness in Microglia/Macrophages.* J Virol, 2020. **94**(20).

133. Delhaye, S., et al., *Neurons produce type I interferon during viral encephalitis.* Proc Natl Acad Sci U S A, 2006. **103**(20): p. 7835-40.

134. Cho, H., et al., *Differential innate immune response programs in neuronal subtypes determine susceptibility to infection in the brain by positive-stranded RNA viruses.* Nat Med, 2013. **19**(4): p. 458-64.

135. Winkler, C.W., et al., *Neuronal maturation reduces the type I IFN response to orthobunyavirus infection and leads to increased apoptosis of human neurons.* J Neuroinflammation, 2019. **16**(1): p. 229.

136. Farmer, J.R., et al., *Activation of the type I interferon pathway is enhanced in response to human neuronal differentiation.* PLoS One, 2013. **8**(3): p. e58813.

137. Kimelberg, H.K., *Functions of mature mammalian astrocytes: a current view.* Neuroscientist, 2010. **16**(1): p. 79-106.

138. Verkhratsky, A., et al., *The Concept of Neuroglia.* Adv Exp Med Biol, 2019. **1175**: p. 1-13.

139. Pfefferkorn, C., et al., *Abortively Infected Astrocytes Appear To Represent the Main Source of Interferon Beta in the Virus-Infected Brain.* J Virol, 2016. **90**(4): p. 2031-8.

140. Detje, C.N., et al., *Upon intranasal vesicular stomatitis virus infection, astrocytes in the olfactory bulb are important interferon Beta producers that protect from lethal encephalitis.* J Virol, 2015. **89**(5): p. 2731-8.

141. So, E.Y., M.H. Kang, and B.S. Kim, *Induction of chemokine and cytokine genes in astrocytes following infection with Theiler's murine encephalomyelitis virus is mediated by the Toll-like receptor 3.* Glia, 2006. **53**(8): p. 858-67.

142. Saunders, A., et al., *Molecular Diversity and Specializations among the Cells of the Adult Mouse Brain.* Cell, 2018. **174**(4): p. 1015-1030 e16.

143. Potratz, M., et al., *Astrocyte Infection during Rabies Encephalitis Depends on the Virus Strain and Infection Route as Demonstrated by Novel Quantitative 3D Analysis of Cell Tropism.* Cells, 2020. **9**(2).

144. Ginhoux, F., et al., *Fate mapping analysis reveals that adult microglia derive from primitive macrophages.* Science, 2010. **330**(6005): p. 841-5.

145. Gomez Perdiguero, E., et al., *Tissue-resident macrophages originate from yolk-sac-derived erythro-myeloid progenitors.* Nature, 2015. **518**(7540): p. 547-51.

146. Paolicelli, R.C., et al., *Synaptic pruning by microglia is necessary for normal brain development.* Science, 2011. **333**(6048): p. 1456-8.

147. Li, Q. and B.A. Barres, *Microglia and macrophages in brain homeostasis and disease.* Nat Rev Immunol, 2018. **18**(4): p. 225-242.

148. Huang, K.W. and B.L. Sabatini, *Single-Cell Analysis of Neuroinflammatory Responses Following Intracranial Injection of G-Deleted Rabies Viruses.* Front Cell Neurosci, 2020. **14**: p. 65.

149. Kallfass, C., et al., *Visualizing production of beta interferon by astrocytes and microglia in brain of La Crosse virus-infected mice.* J Virol, 2012. **86**(20): p. 11223-30.

150. Roth-Cross, J.K., S.J. Bender, and S.R. Weiss, *Murine coronavirus mouse hepatitis virus is recognized by MDA5 and induces type I interferon in brain macrophages/microglia.* J Virol, 2008. **82**(20): p. 9829-38.

151. Hatton, C.F. and C.J.A. Duncan, *Microglia Are Essential to Protective Antiviral Immunity: Lessons From Mouse Models of Viral Encephalitis.* Front Immunol, 2019. **10**: p. 2656.

152. Wang, J.Q., et al., *Oligodendrocyte lineage cells: Advances in development, disease, and heterogeneity.* J Neurochem, 2023. **164**(4): p. 468-480.

153. Rodriguez, M., J.L. Leibowitz, and P.W. Lampert, *Persistent infection of oligodendrocytes in Theiler's virus-induced encephalomyelitis.* Ann Neurol, 1983. **13**(4): p. 426-33.

154. Pan, R., et al., *Oligodendrocytes that survive acute coronavirus infection induce prolonged inflammatory responses in the CNS.* Proc Natl Acad Sci U S A, 2020. **117**(27): p. 15902-15910.

155. Evans, C.F., et al., *Viral infection of transgenic mice expressing a viral protein in oligodendrocytes leads to chronic central nervous system autoimmune disease.* J Exp Med, 1996. **184**(6): p. 2371-84.

156. Schultz, V., et al., *Oligodendrocytes are susceptible to Zika virus infection in a mouse model of perinatal exposure: Implications for CNS complications.* Glia, 2021. **69**(8): p. 2023-2036.

157. Louie, A.Y., et al., *Influenza A virus infection disrupts oligodendrocyte homeostasis and alters the myelin lipidome in the adult mouse.* J Neuroinflammation, 2023. **20**(1): p. 190.

158. Popko, B. and K.D. Baerwald, *Oligodendroglial response to the immune cytokine interferon gamma.* Neurochem Res, 1999. **24**(2): p. 331-8.

159. Ottum, P.A., et al., *Opposing Roles of Interferon-Gamma on Cells of the Central Nervous System in Autoimmune Neuroinflammation.* Front Immunol, 2015. **6**: p. 539.

160. Parra, G.I., et al., *Gamma interferon signaling in oligodendrocytes is critical for protection from neurotropic coronavirus infection.* J Virol, 2010. **84**(6): p. 3111-5.

161. Kirby, L. and G. Castelo-Branco, *Crossing boundaries: Interplay between the immune system and oligodendrocyte lineage cells.* Semin Cell Dev Biol, 2021. **116**: p. 45-52.

162. Deng, S., et al., *Roles of Ependymal Cells in the Physiology and Pathology of the Central Nervous System.* Aging Dis, 2023. **14**(2): p. 468-483.

163. Tardieu, M. and H.L. Weiner, *Viral receptors on isolated murine and human ependymal cells.* Science, 1982. **215**(4531): p. 419-21.

164. Spencer, S.A. and A. Lukacher, *Polyomavirus ependyma infection induces region-specific and Stat1-dependent expression of chemokines in the CNS.* The Journal of Immunology, 2023. **210**(1_Supplement): p. 235.10-235.10.

165. Wang, F.I., et al., *Sequential infection of glial cells by the murine hepatitis virus JHM strain (MHV-4) leads to a characteristic distribution of demyelination.* Lab Invest, 1992. **66**(6): p. 744-54.

Chapter II.

Dual Reporting Virus Identifies Differential States of Infection *in vivo*

2.1 Abstract

Viral infection is often determined by markers of ongoing viral gene expression. However, this strategy fails to identify cells that were exposed to virus but do not host ongoing viral replication. By using a dual labeling Vesicular Stomatitis Virus (VSV) system, we can overcome these limitations. The virus encodes Cre, expressed from a transcriptional unit active early on during infection, leading to the stable marking of cells with at least low-level viral gene expression. Additionally, it encodes GFP, marking cells with higher levels of viral replication upon accumulation. This dual reporting virus provides a host readout (Cre recombination-induced) and viral readout (GFP expression) of infection. Comparing these two readouts enables us to better able to delineate the dynamics of viral infection. We have characterized this virus to confirm that the Cre recombination is induced from an early transcriptional unit and that GFP accumulation only occurs in cells with productive viral replication. Subsequently, we performed stereotactic injections with this dual reporting VSV into the CNS parenchyma of a floxed reporter mouse model and found that neurons are productively infected and that glia cells exhibit higher resistance to viral replication. These glial cells showed higher interferon stimulated gene expression, which correlated with reduced viral replication (GFP expression).

2.2 Introduction

In our lab we develop tools for neurosynaptic tracing. Previous iterations of the VSV development have shown that it can spread transsynaptically, but for it to be adopted by the neuroscience field, additional modifications to the system will be necessary [1-4]. Specifically, we have been working towards the implementation of VSV as a monosynaptic neuronal tracing virus by removing the glycoprotein from the viral genome and selectively supplying it back in trans. By controlling the location and amount of spread VSV undergoes upon infection, we can more accurately delineate synaptic connections and modify these connections for further study if necessary. Throughout this development process, we have encountered issues where our monosynaptic VSV does not spread to the downstream, anterograde projections (data not shown). Since we know that replication competent VSV, which contains the VSV glycoprotein, can spread to these connections it begs the question: why does it not spread under these monosynaptic tracing conditions?

The most likely explanation for this block of VSV monosynaptic spread is that there may be some type of host response inhibiting VSV infection/replication. One aspect of VSV is that the VSV glycoprotein (VSV-G) is quite promiscuous in terms of initiating infection of target cells. This is attributed to the proposed cognate receptor for VSV-G being the low-density lipoprotein receptor (LDLR) [5, 6]. LDLR is ubiquitously conserved and expressed, allowing VSV-G to mediate infection in a broad range of cells and organisms [7-10]. Since VSV should be able to infect most cells, the lack of viral spread to monosynaptic connections is puzzling. An intriguing possibility is that the

virus can infect a susceptible cell but is unable to productively replicate due to inhibition of downstream viral replication events. If this is the case, designing a system to identify which cells undergo these intermediate or abortive events of VSV replication would be ideal. Such a system would track the responses correlating with differentiated states of viral infection and pinpoint the specific cells contributing to the response that instigates viral replication inhibition.

Tracking viral infection on a cellular level can be performed several ways. The most common methods include performing immunohistochemistry (IHC) and/or immunofluorescence (IF) to detect viral proteins, or monitoring a fluorescent protein introduced into the viral genome backbone. In both scenarios, productive viral infection results in the expression of this virally-derived maker [2, 11, 12]. More recently, single-cell RNA sequencing has been used to track the state of viral infection through the detection of viral genomes and/or transcripts, while also providing information about the host cell that is infected [13-15]. However, both established techniques are limited in their ability to capture abortive infection events. The detection of virally-derived proteins requires productive infection and accumulation of the marker. Single-cell RNA, although potentially more capable of detecting intermediate/abortive infections than protein accumulation, is still limited in sensitivity and may not capture cells below a certain replication threshold.

Conversely, the viral replication of acute infections is dynamic, and having a stable marker of infection in the form of a protein can also have its own benefits. Some of these limitations can be addressed by recent advances in fluorescence in situ hybridization (FISH), which enables subcellular detection of single molecules of viral

genomes to investigate viral genome and transcript dynamics. FISH has greater sensitivity than RNA sequencing and can lower the detection threshold, enabling the detection of early viral infection events [16]. Despite this increased sensitivity, even FISH also has its limitations. Technical difficulties currently limit the throughput of such analyses, and genome detection alone cannot distinguish cells which have internalized viruses that have not escaped endosomes versus viruses that have undergone the beginning stages of replication. To overcome these challenges posed by other techniques, we have developed a new dual reporting system for tracking viral infections, providing a host and viral readout of infection.

This new dual reporting VSV system was inspired by the implementation of a host readout of viral infection previously used with rabies virus (RABV) [17]. In that study, the authors engineered the RABV genome to include Cre recombinase. When they infected a floxed fluorescent reporter mouse, the Cre recombinase triggered recombination in the host genome, leading to stable and observable expression of a host marker for viral infection. Consequently, the accumulation of the infection marker is dependent on the host, not on the virus, allowing us to discern cells that have been infected but do not support productive viral replication. We employ this method alongside FISH for VSV genome detection to validate various stages of infection. Together, these techniques enable us to more effectively identify abortively infected cells compared to the other methods mentioned previously.

We sought to investigate these infection dynamics *in vivo* for several reasons. Historically, many of these experiments have been performed *in vitro.* However, these primary cultures of CNS derived cells have shown conflicting results [18, 19]. One

reason for these results might be tied to the fact that the primary cultures are typically composed of a single cell type. Recently, there have been a number of studies indicating that the combination of two or more different types of CNS cells are required to work in conjunction with each other to elicit the proper antiviral response [20-23]. If this is the case, rather than recapitulating the *in vivo* microenvironment in culture, we decided to perform these studies in the murine brain itself. Additionally, by focusing our observations on the striatum, our findings can better inform our direct neuronal tracing studies, which we routinely utilize the well-characterized synaptic connection emanating from the striatum [1, 3, 24].

The data presented in this chapter describes the development and characterization of a novel dual-reporting VSV to explore infection dynamics *in vivo.* We identified cell populations by their infection status and looked at correlates of these different types of infections. The results of these findings better categorize VSV's tropism in the CNS and inform neuronal tracing studies as well as viral infection dynamics of the CNS at large.

2.3 Results

Dual labeling VSV design and *in vitro* control experiments

To generate a dual-reporting VSV we made several modifications to our rVSV neurosynaptic tracing viral backbone [2, 7]. In our traditional rVSV, we would encode for eGFP along with the other viral gene constituents. In some iterations, we would remove the glycoprotein for monosynaptic tracing studies to ensure that the virus does not keep spreading [1-3]. In our dual labeling viral approach, we made three modifications (Figure 2.1, A). 1) Most importantly, we added a Cre recombinase, which will induce recombination in a floxed reporter cell and allow us to visualize a host readout of infection [17, 25]. This readout is initiated early in the viral replication cycle and is induced independently of efficient viral replication, thus allowing us to capture abortive infection events where a cell is infected by a virus but is not able to replicate further and accumulate viral readouts of infection [17]. 2) We removed the glycoprotein (G) and replaced it with a nuclear-localized eGFP (H2B-eGFP) [26]. With the glycoprotein absent, this allows for the specific interrogation of primary infection events because the virus can replicate in the infected host cell but is unable to spread without the glycoprotein mediating attachment and fusion upon viral release [27]. Additionally, the glycoprotein can induce cytotoxicity [28, 29]. By removing the glycoprotein, we can better preserve cellular health and identity. The nuclear-localized H2B-eGFP, as compared to cytosolic eGFP, enables us to better delineate cells due to the more localized fluorescent signal. 3) We introduced a double mutation modification (M51R and M33A) in the matrix protein (M), which renders this virus less cytopathic, thus maintaining cellular health and identity. It has previously been shown that VSV M proteins contribute

significantly to the cytopathic effect due to the inhibition of cellular transcription and blocking mRNA transport from the nucleus [29-33]. These (M51R and M33A) mutations not only prevent the expression of two other polypeptides associated with cytotoxicity but also ensure that the Cre recombination readout from the host cell is not inhibited. Therefore, we are able to obtain both a host (Cre recombination) readout of infection and a viral (H2B-eGFP) readout of infection.

The benefit of using this dual reporting virus is that, since the infection readouts are separated (virus vs host), the differential readout of infection indicates the type of infection that occurs (Figure 2.1, B). The VSV infection cycle post-fusion, initially consists of the uncoating of the virion, followed by an initial round of primary transcription from the parental viral template, which produces a small amount of viral proteins. These proteins will then aid in the replication of the viral genome and anti-genome, which leads to genome replication and a secondary transcription step where the majority of the viral transcripts and viral protein products are produced due to the increased abundance of template viral genomes [34-36]. In cases where a cell was infected and the virus was able to replicate fully, as delineated above, we observe the expression of viral protein products. We can stain for one of the products or we can use eGFP as the viral readout of infection. Conversely, if a virus was able to infect a cell but the later stages of the viral replication were inhibited, then we wouldn't see an accumulation of the viral proteins and we might conclude that the cells were not "infected". Therefore, having a separate host readout of infection to track these cells with abortive infection events is paramount.

Figure 2.1| Design of dual labeling VSV and *in vitro* testing of early induction of Cre recombination

A) Design of traditional rVSV construct compared with our dual labeling rVSV. **B)** Productive VSV replication depicted if viral replication is able to occur. Abortive VSV replication phenotype if viral replication is stunted early on the in the replication cycle. **C)** Testing if Cre recombination is induced early on during viral replication. VSV needs the nucleocapsid (N), phosphoprotein (P) and polymerase (L) to productively replicate. Therefore, we used a modified VSV lacking the N and P but expressing GFP and Cre recombinase to test if primary transcription alone can induce Cre recombination (which can occur independently even if N and P is not present). In the first two vertical panels, plasmids encoding VSV N, P, L, and a Cre reporter were expressed in trans in 293Ts. In the second two vertical panels only VSV N and P were expressed in trans. In the last panels only the Cre reporter plasmid was expressed. All three conditions infected for 24hrs with the VSV lacking N and P. Images are split, showing GFP and tdTomato (Cre recombination readout) independently.

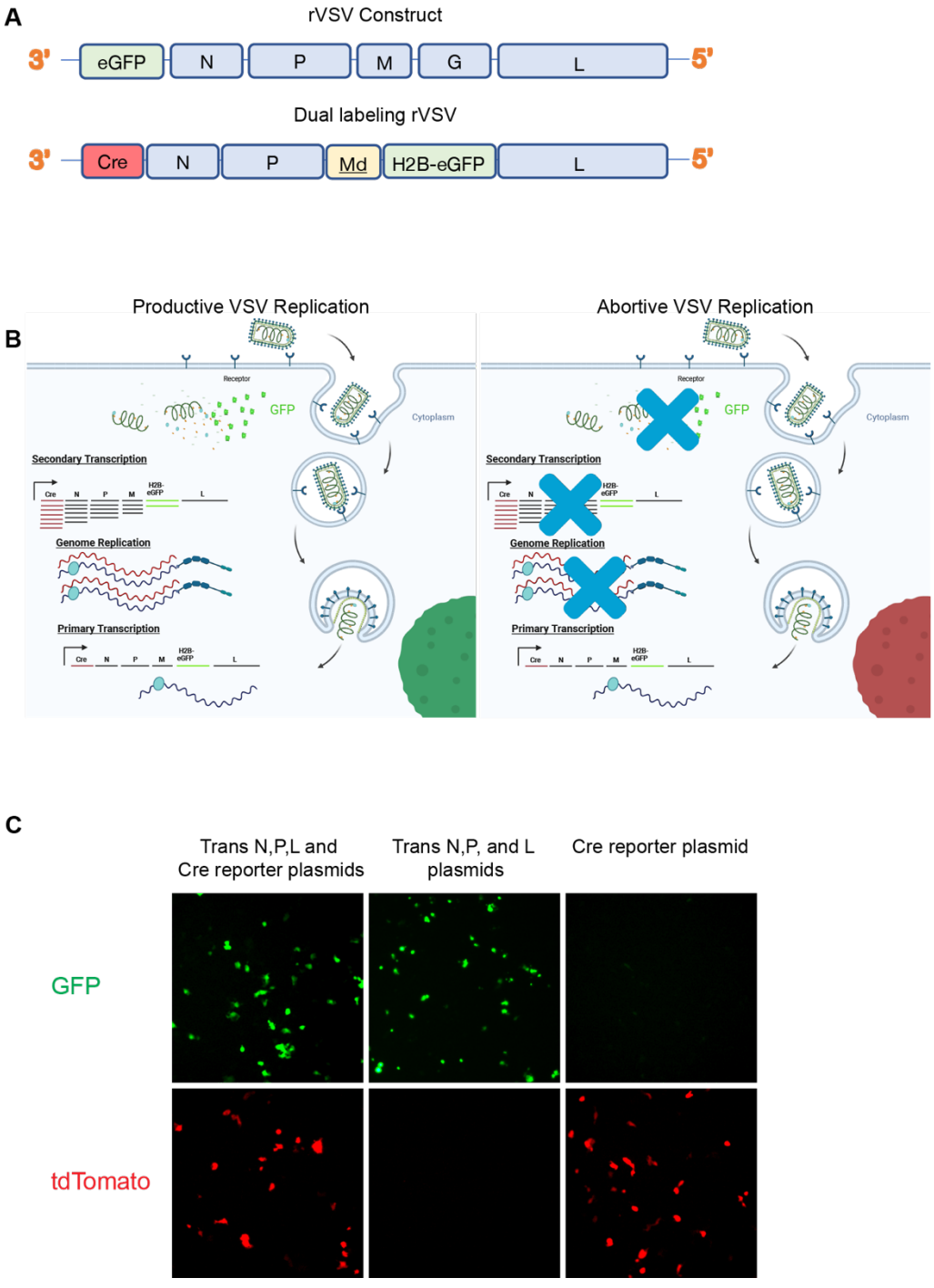

Figure 2.1 (continued)

For the dual labeling approach to effectively utilize the host readout of infection in the absence of productive viral replication, the readout must occur both early and sensitive. Cre recombination is naturally robust and able to mediate recombination in a highly sensitive manner [37, 38]. We aimed to demonstrate that in our system, the viral protein products made initially from viral primary transcription are sufficient to drive Cre recombination, thereby labeling cells in situations where the virus has entered the cell but not extensively replicated.

VSV genome replication requires the following viral proteins: nucleocapsid (N), phosphoprotein (P), and the polymerase (L) [39]. If these proteins are absent from infection, then the virus will infect a cell and primary transcription will occur, but there won't be a significant accumulation of viral genomes or subsequent expansion of the viral transcripts, as evident in the later stages of the replication process during secondary transcription. To test whether Cre recombination could be induced from primary transcription alone, we created a mutant dual labeling VSV lacking the nucleocapsid and the phosphoprotein. We infected 293Ts with this virus under three conditions: 1) where the N, P, L and Cre reporter were expressed in trans; 2) with only N, P, and L expressed in trans; 3) where only the Cre reporter was expressed [Figure 2.2, C]. When N, P, L, and the Cre reporter are expressed, we observe both the viral readout of infection (GFP) and the host readout of infection (tdTomato), indicating that viral replication was able to occur and these cells were productively infected. When only N, P, and L were expressed, and the Cre reporter was absent, there was subsequently no tdTomato, indicating that there is no background Cre recombination fluorescence occurring. Lastly, when only the Cre reporter is present, there was still Cre recombination still occurs despite the lack of

viral replication. This demonstrates that primary transcription alone is sufficient in driving Cre recombination and that the Cre recombination readout can capture cells containing viruses which have not undergone significant replication.

Utilizing Cre recombination as a host readout of infection is depends on whether the cell that exhibited Cre-mediated recombination was actually infected by a virus. Recent reports have suggested that Cre recombinase mRNA might be transferred between cells via extracellular vesicles and mediate recombination in bystander cells (cells that were not infected/transduced) both in immortalized cells lines and *in vivo* [40, 41]. To test whether this bystander effect exists within our *in vitro* experiments, we conducted a cell transfer and cell lysate experiment. In this experiment we transfected floxed reporter plasmids into four cellular conditions; 1) an infected control with our dual labeling VSV, 2) a no-infection control to ensure that we were not observing aberrant recombination readouts, 3) an infected cell transfer condition where we infected another set of cells with our dual labeling virus and then transferred these cells onto a monolayer of cells transfected with the floxed reporter, 4) an infected cell lysate condition that where we took the lysate of previously infected cells and overlaid it onto cells that were transfected with the floxed reporter (Figure 2.2, A). In the infected control condition, we observed successful viral replication, indicated by GFP and the host readout of infection (tdTomato) from Cre recombination. In the no-infection condition, we detected no readout of infection, viral or host, indicating that without infection, these markers do not appear. In the cell transfer of infected cells condition, we saw the previously infected cells (GFP-positive that were not transfected with the floxed reporter) but there is no Cre recombination in the floxed reporter transfected cell indicating that the infected cells did

Figure 2.2| *in vitro* testing of Cre recombination in bystander cells

A) Diagram of the *in vitro* experiment testing whether Cre recombination can be induced in bystander cells that were not infected by virus. 293Ts in all four conditions were transfected with a floxed reporter plasmid and left to incubate for 36hrs. Afterwards, cells were either infected with dual reporting virus, not infected, overlayed with cells previously infected (but not transfected with recombination reporter), or overlayed with cell lysate from previously infected cells. **B)** Panels of the four conditions showing GFP, tdTomato (floxed reporter), and DAPI images with a merged imaged of all the fluorescent channels.

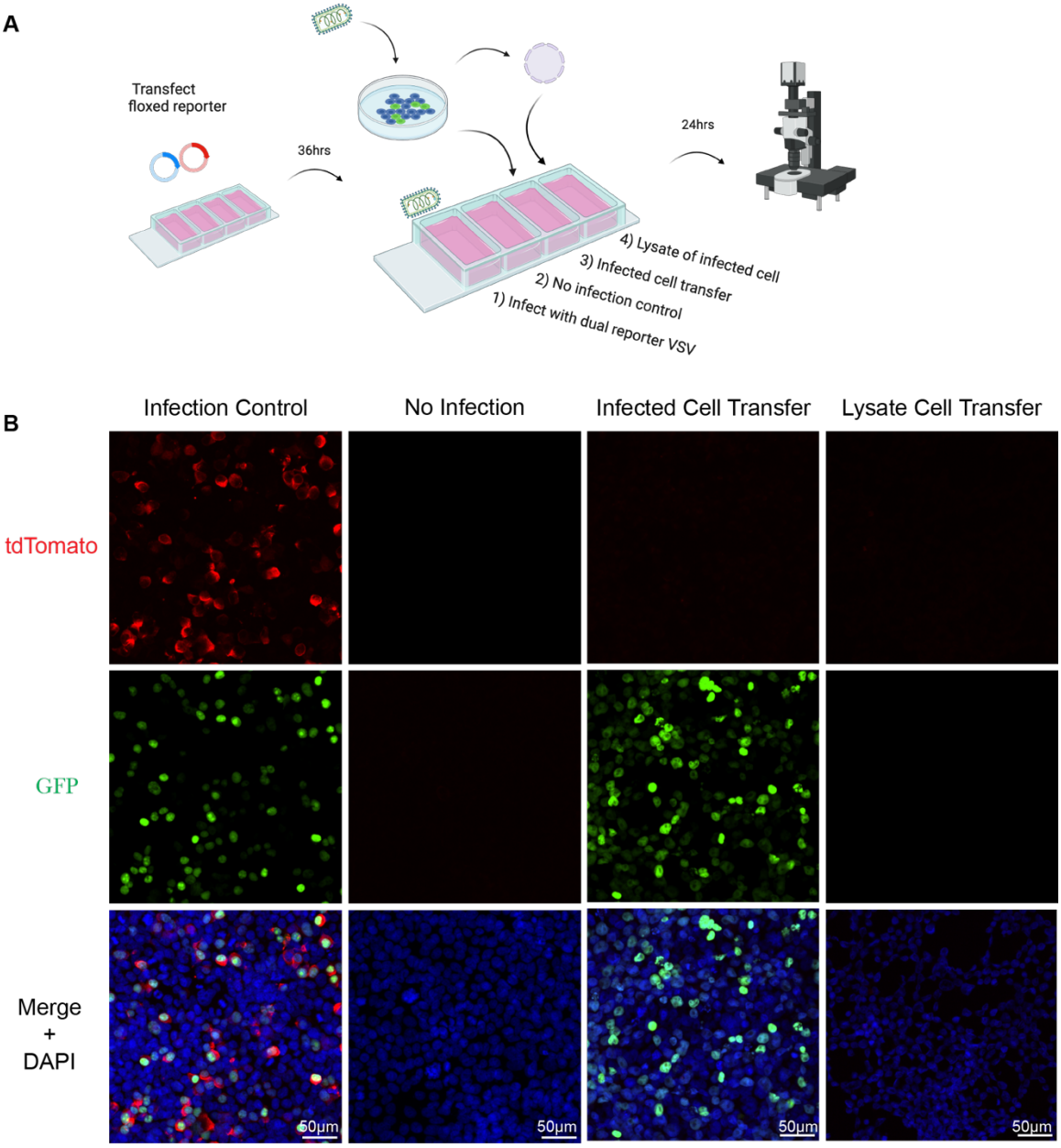

Figure 2.2 (continued)

not excrete anything that could induce Cre recombination in the bystander cells. Lastly, in the infected cell lysate condition, we do not observe any GFP or tdTomato, suggesting even artificially released (cell lysate) Cre mRNA or protein cannot penetrate and induce recombination in bystander cells (Figure 2.2, B). Altogether, this data suggests our Cre mediated infection readout is specific to virally infected cells within 24hrspi *in vitro*.

Infection readouts *in vivo* and visualizing correlates of infection readouts with viral genomes/transcripts

From the *in vitro* experiments we learned that our dual labeling VSV can induce Cre recombination early in the viral replication cycle and if the virus is able to replicate productively, H2B-eGFP will also be expressed and accumulate. Next, we aimed to determine infection dynamics of VSV *in vivo.* In line with our transsynaptic tracing experiments we performed stereotactic injections of the dual labeling VSV into the striatum of Ai75d mice; these mice contain a loxP-flanked STOP cassette that prevents the transcription of a CAG promoter-driven, nuclear-localized tdTomato. Upon Cre-mediated recombination resulting from viral infection, a cell will express tdTomato, which will accumulate in the nucleus.

When we inject our dual-labeling VSV into Ai75d mice, then harvest, section, and image the tissue we are able to identify differential infection patterns across the brain (Figure 2.3, A). In the infected zones, four distinct categories of injection types are observed (Figure 2.3, B). The majority of cells (~55%) express both GFP (from the H2B-eGFP) and tdTomato (Cre recombination reporter), which we consider “double positive” cells due to both the viral and host infection markers being present.

Figure 2.3| Infectious status outcome from *in vivo* injections with dual labeling VSV

A) Fluorescent infection markers in brain tissue sections from dual labeling VSV injections into the striatum 16hrs post infection. GFP from viral replication and tdTomato from Cre recombination. **B)** Single cell representation of differential infectious status outcomes based on infections markers. **C)** Percentage of cells classified by infection outcome. Average taken from ten brain sections.

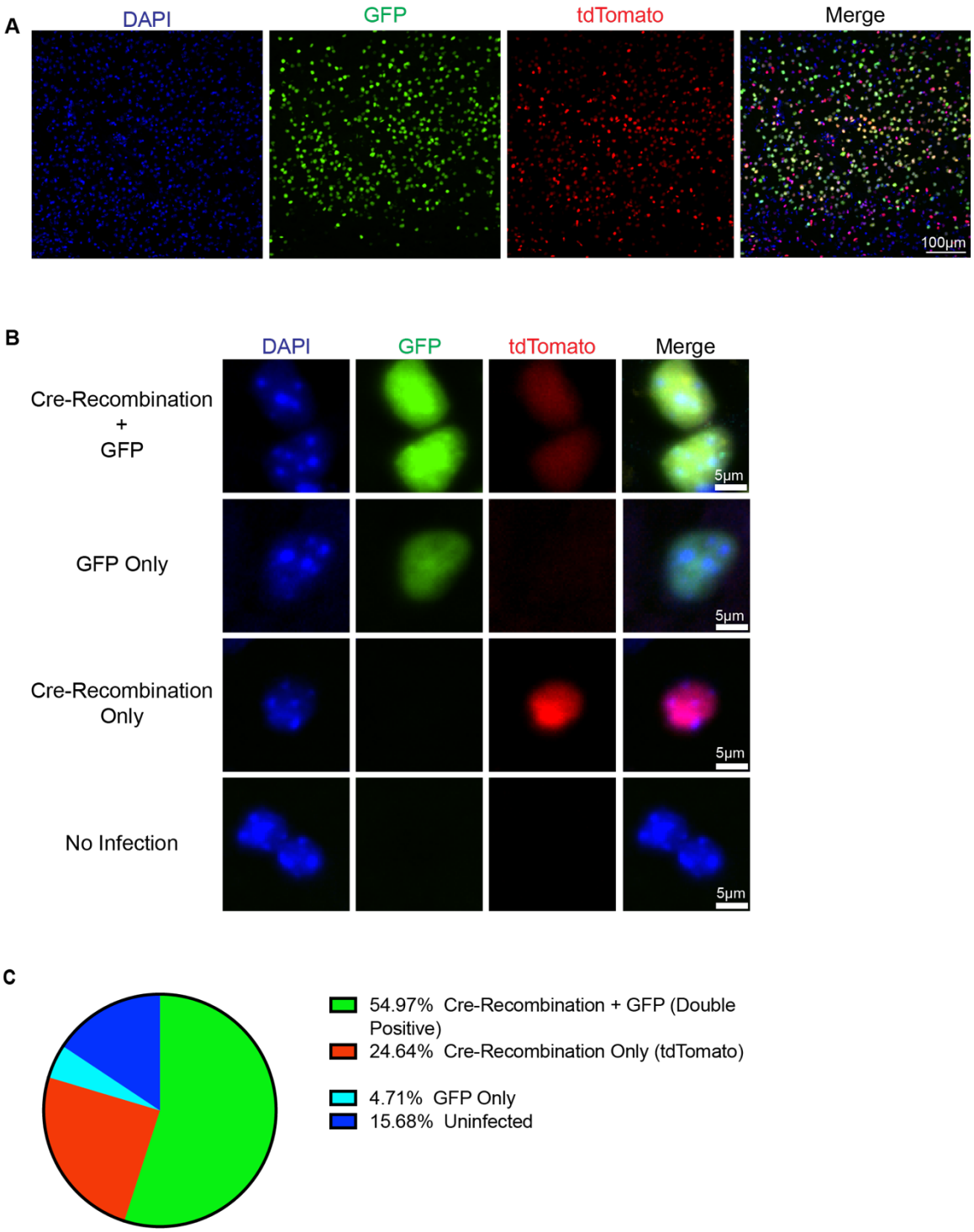

Figure 2.3 (Continued)

Approximately 5% of the cells are GFP-positive only, which do not express any tdTomato. Most interestingly, about 25% of the time we observe cells that express the tdTomato but not GFP. Since there was not sufficient GFP expression, it suggests that the viral infection was aborted or severely stunted. Lastly, ~15% of cells were in the infected region (surrounded by other infected cells) but did not exhibit expression of any of the infection markers. These uninfected cells were likely exposed to virus but the virus never initiated primary transcription either because primary transcription or an upstream step of viral infection (e.g. attachment, fusion) was inhibited (Figure 2.3, B,C).

The differential presence or absence of infection markers can be used as a proxy for determining infection status. If GFP is present, then viral infection and replication were successful. If only tdTomato is observable in the absence of GFP, then it suggests that viral replication did not proceed to the later stages and therefore the infection could be considered abortive. In this scenario the cell is susceptible to viral infection but resistant to viral replication. To confirm these infection markers, and to interpret infection status, we assayed the viral genomes and transcripts directly. VSV is a negative sense single-stranded RNA virus while the transcripts and antigenome are positive-sense [39]. This means we are able to differentiate between the genome and transcripts via fluorescence in situ hybridization (FISH). Specifically, we used single amplification by exchange reaction (SABER) and hybridization chain reaction (HCR-FISH) to detect the polymerase (L) section of the negative-sense genome or the positive-sense transcripts encoding for Cre, nucleocapsid (N), phosphoprotein (P), and matrix proteins.

Figure 2.4| *in vivo* VSV genome and transcript detection of infected region

A) 20x image of dual labeling VSV infected region depicting infection markers, VSV transcripts (cyan), and VSV genomes (magenta). Infected region spans white matter (left half of image) and grey matter (right half of image) sections. **B)** 60x image of infected region and VSV genomes (white). **C)** Magnified insets from panel B depicting single cells with infection markers and VSV genomes. All images were taken 16hrs post infection.

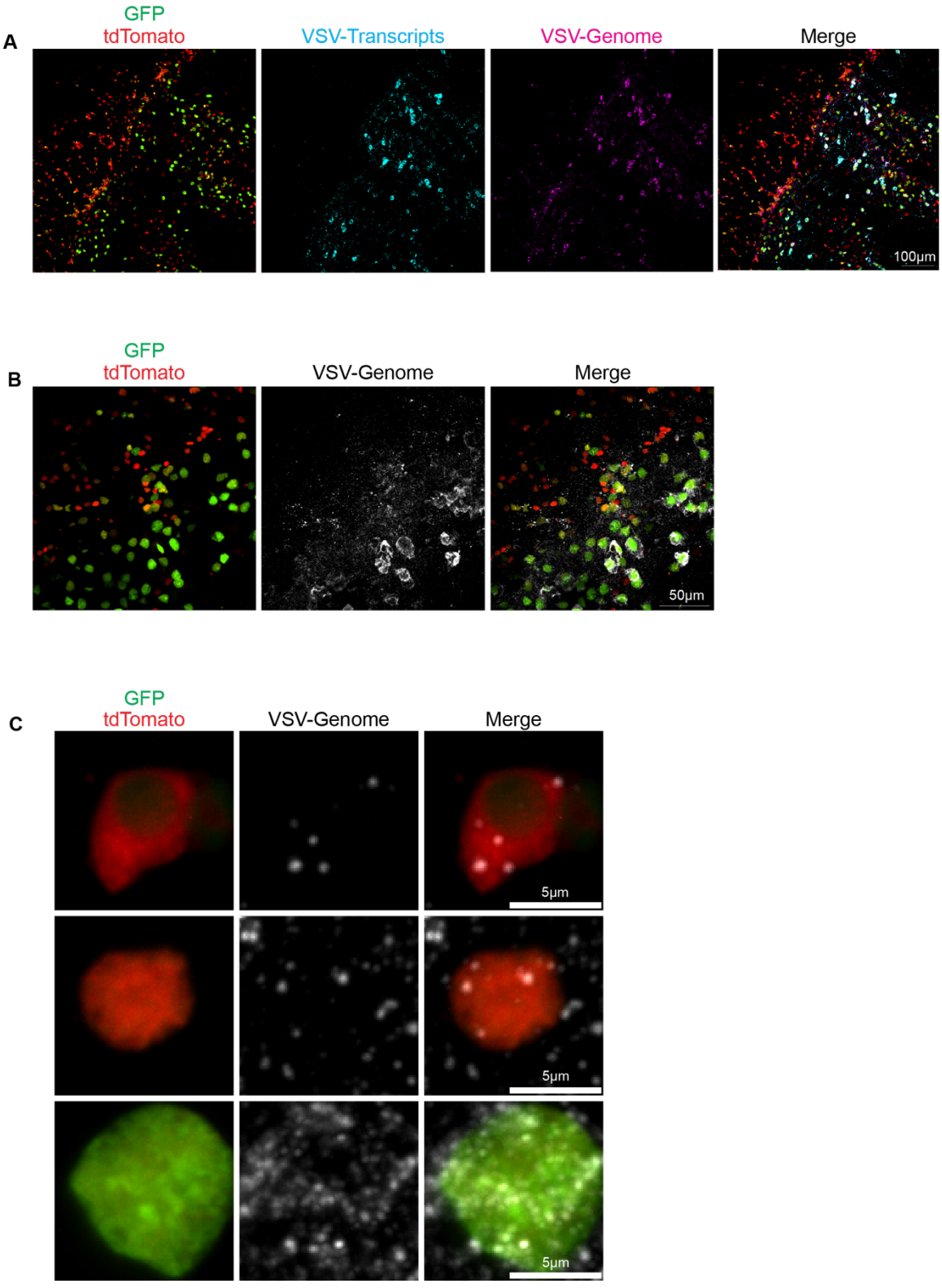

Figure 2.4 (continued)

Areas with observable GFP indicate that productive viral replication was occurring in these regions. If this is the case, we expect to see a significant number of viral transcripts in this region as well, given that the transcripts would accumulate in cells where viral replication persisted. Conversely, in regions that did not have a significant amount of GFP-positive cells but did contain a number of tdTomato-only cells, we would expect there to be significantly fewer VSV transcripts. When looking at an infected region that borders both white and grey matter (left vs right side of image respectively) we indeed observe a significant number of viral transcripts in regions with productive viral replication and a lack of viral transcripts in regions populated mostly with tdTomato-only cells (Figure 2.4, A). Additionally, even though regions with tdTomato-only cells exhibit reduced number of detectable viral transcripts, we still expect viral genomes to be present due to the assumption that the viral infection initiates the Cre recombination. VSV genomes are indeed present and detectable in these regions populated by tdTomato-only cells. When comparing the regions with tdTomato-only cells to the GFP-positive cells, we observe that both regions contain viral genomes, but there is greater accumulation of genomes in the GFP-positive cell region. This is due to productive viral replication occurring with subsequent expansion of the viral genome reservoir in the cell (Figure 2.4, A, B).

Although on a broad, qualitative scale we see an association of VSV genomes in tdTomato-only regions, we also want to be able to detect viral genomes in single cells to confirm that tdTomato-only cells are generated from Cre recombination events due to an abortive viral infection. At higher magnification, we can detect VSV genomes in tdTomato-only cells (Figure 2.4, C). Moreover, at this higher magnification, we once

again observe a large number of viral genomes in GFP-positive cells. This indicates that significant viral replication is occurring (Figure 2.4, C).

Characterization of infection dynamics on a cell type specific basis *in vivo*

From the first *in vivo* injections of the dual labeling VSV into floxed reporter mice, we observed differential presence of infection markers across the brain tissue. The question is whether these infection outcomes are present across all cell types and if certain cell types are more predisposed to a specific type of infection. To investigate this, we performed immunofluorescence (IF) for specific cell types (e.g., neurons, astrocytes, oligodendrocytes, and microglia) within the brain followed by semi-automated image analysis quantifying the association of cell type specific IF with infection markers at a population level. The outcome of this analysis allows us to identify the propensity for certain cells to be infected by VSV and the type of infection.

We first quantified the infection status of neurons using the nuclear localized marker, NeuN. NeuN stains nearly all postmitotic neurons in the brain, and most importantly, it is not present within glial cells [42]. In the striatum, approximately 80% of the neurons were GFP-positive, indicating that they were productively infected (Figure 2.5 A, B). The remainder of the cells were split between those positive only for Cre recombination (~10%), abortively infected, and uninfected (~10%). This indicates that neurons are susceptible to infection and capable of hosting viral replication. Many of the abortively infected neurons were on the perimeter of the infected area indicating local multiplicity of infection might also be a factor.

Figure 2.5| Infection status on a cell type specific basis *in vivo*

A) Neurons labeled with NeuN (magenta) and with infection markers GFP and tdTomato (Cre recombination). 20x image of infected region analyzed, top panels. Magnified inset of image on bottom panel. **B)** Quantification of NeuN labeled neurons depicted by infection status based on infection markers. The rest of the images and graphs pairing are for each individual cell type. **C)** and **D)** are images and graph for Sox9 (magenta) labeled astrocytes. **E)** and **F)** are images and graph for Sox10 (magenta) labeled oligodendrocytes. **G)** and **H)** are images and graph for Iba1 (magenta) labeled microglia. **I)** is a compiled summary of the cell types and proportion of each type of infection. Representative images from sagittal sections were taken 16hrs post injection of dual labeling VSV. Graph display means for each metric. Each point is a separate animal (4 males, 4 females) with an average of 2-4 images per animal. One-way ANOVA was performed with Tukey's multiple comparison test for statistical analysis. $* \leq 0.0332$, $** \leq 0.0021$, $*** \leq 0.0002$, $**** \leq 0.0001$

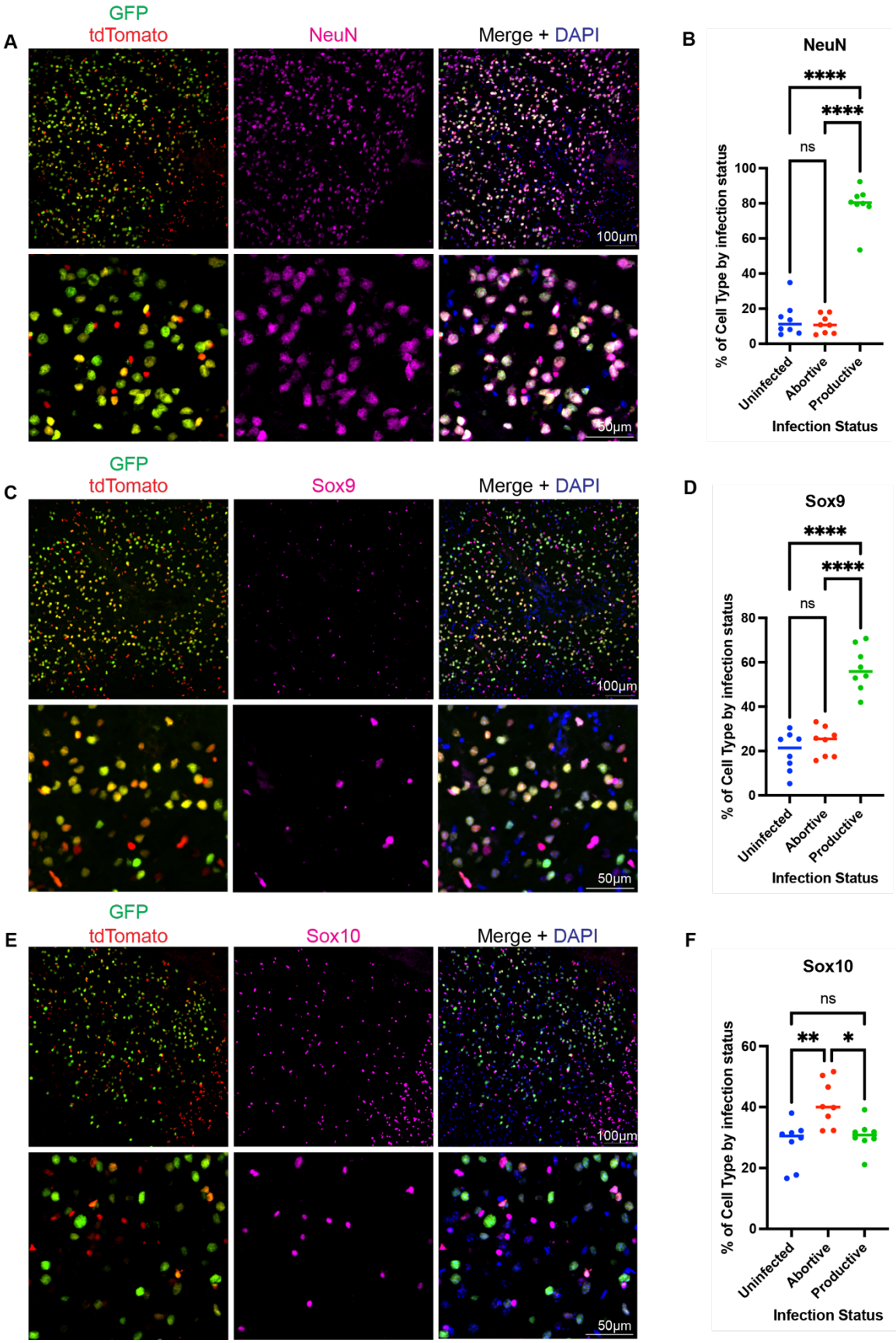

Figure 2.5 (continued)

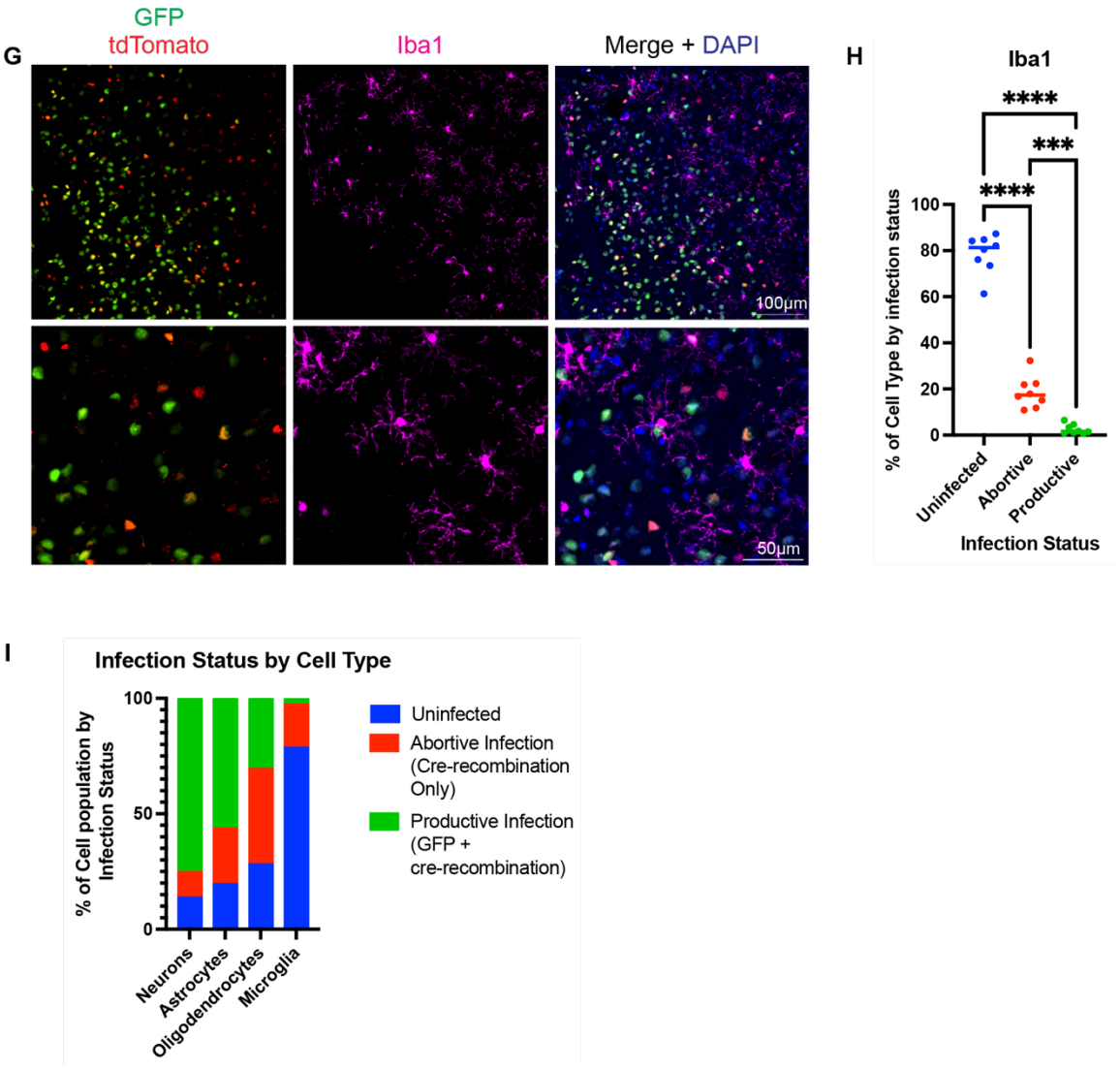

Figure 2.5 (continued)

Next, we began focusing on different types of glia cells where we first looked at astrocyte's infection status by staining for nuclear-localized SRY-Box transcription factor, Sox9. Apart from being present in ependymal cells and neural progenitor cells, Sox9 is primarily expressed in astrocytes [43]. By infecting the striatum, we avoid neurogenic regions or ventricles, thereby ensuring that the only Sox9-expressing cells in our infected region are astrocytes. When performing the infection marker colocalization studies, we observe that astrocytes are also mostly productively infected (~55%). The rest of the astrocytes are nearly evenly split, with ~20-25% either uninfected or abortively infected, respectively (Figure 2.5. C, D). Although, both neurons and astrocytes are mostly productively infected the ratios shift such that fewer astrocytes are productively infected, while there are more uninfected and abortively infected astrocytes as compared to neurons (Figure 2.5, I). This suggests that astrocytes are less susceptible to VSV infection compared to neurons.

The next cell type we investigated were oligodendrocytes. We used the nuclear-localized SRY-Box transcription factor 10, Sox10. Sox10 is involved in oligodendrocyte differentiation and maturation; therefore, it is expressed in both oligodendrocyte precursor cells (OPCs) and mature oligodendrocytes [44-46]. For our analysis, we did not differentiate between the two and instead labeled all oligodendrocyte lineage cells with the Sox10 marker and will refer to this lineage as 'oligodendrocytes' for the remainder of the results and discussions. Compared to the other cells, oligodendrocytes are the only cell type where the greatest population of infection is predominantly abortively infected (~40%). The remaining oligodendrocytes similarly are evenly split between uninfected and productively infected (~30% each) (Figure 2.5, E, F).

Lastly, we examined the infection status of the prototypic resident immune cell of the brain, the microglia. We labeled microglia using the ionized-binding adaptor molecule 1 (Iba1) marker, which detects both microglia and macrophages and can be used to detect morphological changes of the microglia depending on activation [47, 48]. At 16hrs post-infection with our dual labeling VSV, we mostly observed uninfected microglia (approximately 80% of cell microglia population). If the microglia were infected, then they were abortively infected, making up for nearly 20% of the microglia population. Less than 5% of the microglia cells were productively infected at this time point (Figure 2.5, G, H).

In comparison, we see a trend of neurons being the most susceptible to infection and conducive for viral replication, followed by varying degrees of distinct glial cells. Astrocytes were the next most susceptible, while oligodendrocytes were unique in terms of being susceptible to infection but more resistant in viral replication, given the greater proportion of abortively infected cells. Microglia were the most uninfected, with very few productively infected microglia present while abortively infected microglia make up the largest proportion of infected microglia. This indicates that microglia are both less susceptible and less conducive for viral replication (Figure 2.6, I).

While we characterized various cell types by their infection status through the binary indication of the presence or absence of infection markers, there is more information that can be gleaned from these images. We were using GFP as a readout of viral replication. Therefore, the more GFP expression there is, the more viral replication has occurred in an infected cell. By measuring and comparing the relative integrated intensity of GFP in infected cells, we can further classify productive infection.

Figure 2.6| Infection marker fluorescent intensity comparisons

A) Magnified images of representative infected cells with infection markers (GFP and tdTomato – Cre recombination) and their respective cell markers (magenta) Integrated intensity of **B)** GFP, or **C)** tdTomato, in productively infected neurons (NeuN), astrocytes (Sox9), and oligodendrocytes (Sox10) containing GFP and tdTomato. Integrated intensity represented in arbitrary units generated by CellProfiler. Images taken 16hrs post infection. Graph display means for each metric. Each point is a separate animal (4 males, 4 females) with an average of 2-4 images per animal. One-way ANOVA was performed with Tukey's multiple comparison test for statistical analysis. $* \leq 0.0332$, $** \leq 0.0021$, $*** \leq 0.0002$, $**** \leq 0.0001$

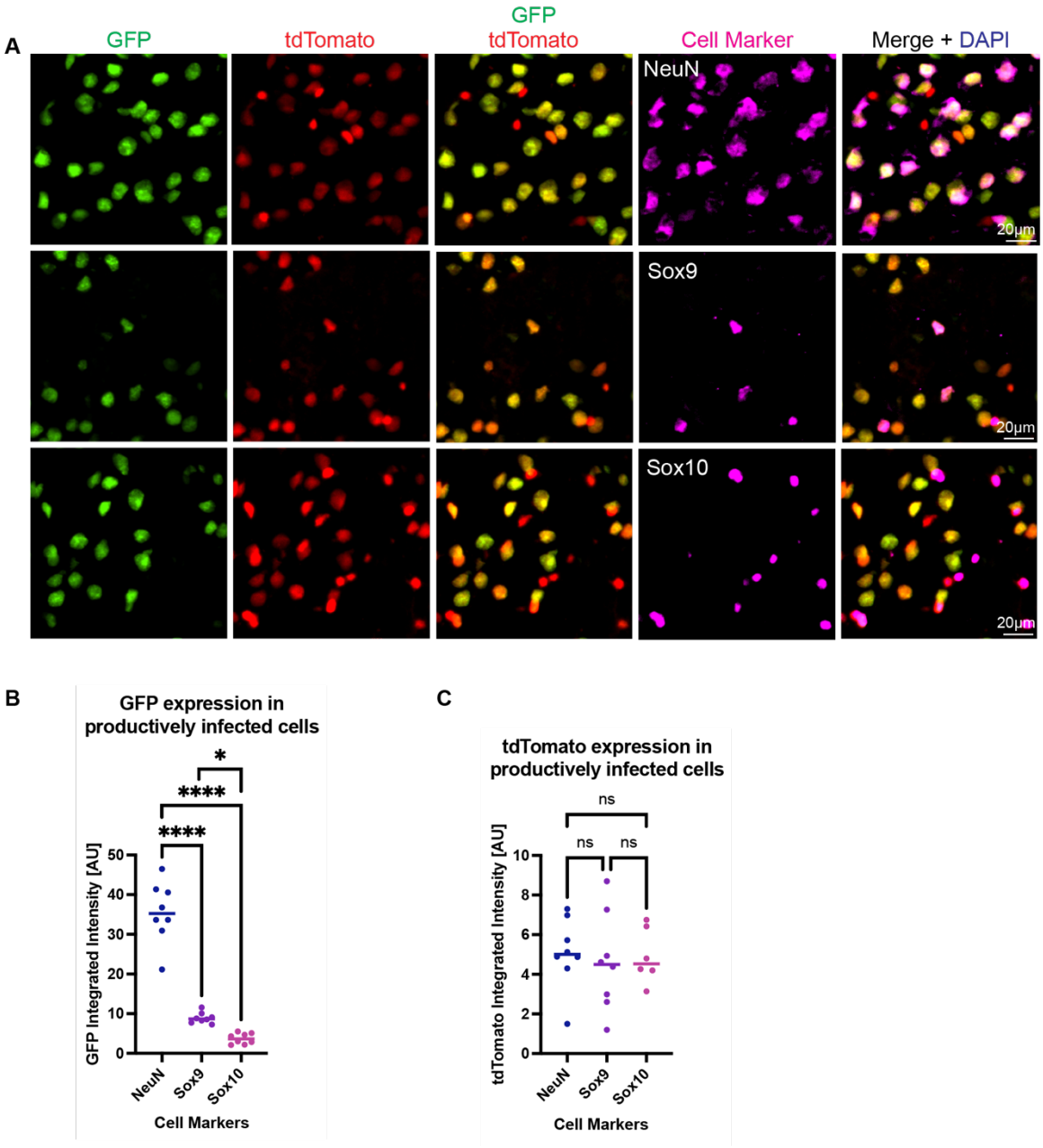

Figure 2.6 (continued)

In neurons, there was the most amount of GFP expression and subsequently, the most amount of viral replication as compared to astrocytes or oligodendrocytes in productively infected cells (Figure 2.7, A, B). The increased amount of GFP expression in neurons is not simply due to the size difference between neurons and glial cells. When comparing tdTomato expression across the cell types, they all exhibited equivalent levels of tdTomato fluorescent integrated intensity despite the size difference, suggesting that the difference in GFP expression is more associated with viral replication itself. Amongst the glial cells, oligodendrocytes harbored even less GFP expression than astrocytes. Microglia were not assessed given the low amount of GFP-positive cells. Even though approximately 30% of oligodendrocytes were productively infected, they harbored significantly less viral replication than astrocytes and especially neurons. The lower GFP integrated intensity in the productively infected oligodendrocytes indicates that, despite some viral replication occurring, the replication is not occurring as efficiently and might be due to some means of host pressure on the virus.

Assaying the role of interferon stimulated genes in the differential readouts of infection

One-way viral infections are controlled by the presence or absence of interferon-stimulated genes (ISGs). There are hundreds of ISGs that are associated with inhibiting viral infections are many different stages of the viral replication cycle [49, 50]. VSV itself is known to be sensitive to these antiviral ISG products, and this relationship has been shown before *in vivo* and in the brain [24, 51, 52]. We investigated the association of ISGs among the distinct cell types and whether there was a correlation with viral infection or replication. To do so, we performed HCR-FISH for a pooled number of prototypic ISGs (*ISG15, RSAD2,* and *IFIT3),* which have been known to be highly

upregulated in the context of viral brain infection [14, 24, 53]. We observed that less than 20% of neurons contained a detectable amount of ISGs. Conversely, both oligodendrocytes and astrocytes exhibited significant expression and correlation with ISGs (~80%). Surprisingly, only about 50% of microglia contained detectable levels of ISGs that were comparable to the other glial cells (Figure 2.7, A, B). This might reflect the ISGs that were utilized, the threshold level of detection we employed when determining association, or a reflection of timing, where microglia could have been expressing ISGs earlier post infection. Since ISGs are known to block viral replication, we looked at how the presence or absence of ISGs was associated with GFP expression. We would expect that if ISGs were present, then there would be lower viral replication and subsequently lower GFP expression. In both neurons and astrocytes, we saw lower GFP expression in ISG positive cells and conversely more GFP expression in cells in which we did not detect significant level of ISGs (Figure 2.7, C, D). Curiously, we did not see the same effect in oligodendrocytes and instead witnessed comparable levels of GFP intensity regardless of the presence or absence of ISGs (Figure 2.7, E). This could be for several reasons, including the possibility that dynamic range of GFP expression was not significant enough to detect differences in the oligodendrocytes, or that ISGs are not associated with lower viral replication in our assay, and/or the threshold level of ISG presence is not sufficient, and oligodendrocytes that were considered ISG negative from the automated image analysis contained enough ISG to still inhibit viral replication. Due to the limited number of productively infected microglia their GFP intensity was not quantified and was not considered.

Figure 2.7| Interferon Stimulated Gene (ISG) association with cell types and GFP intensity

Pooled HCR-FISH probes detecting *ISG15, RSAD2,* and *IFIT3* used to determine ISG expression and association with cell types in infected brains. **A)** Panels representative images of ISGs transcripts (yellow) and cell markers (magenta). **B)** Automated quantification of ISG associate with the various cell types. Graphs depicting GFP intensity across **C)** neurons (NeuN), **D)** astrocytes (Sox9), **E)** oligodendrocytes (Sox10). Images taken 16hrs post infection. Graph display means for each metric. Each point is a separate animal (2 males, 2 females) with an average of 2-4 images per animal. One-way ANOVA was performed with Tukey's multiple comparison test for statistical analysis. $* \leq 0.0332$, $** \leq 0.0021$, $*** \leq 0.0002$, $**** \leq 0.0001$

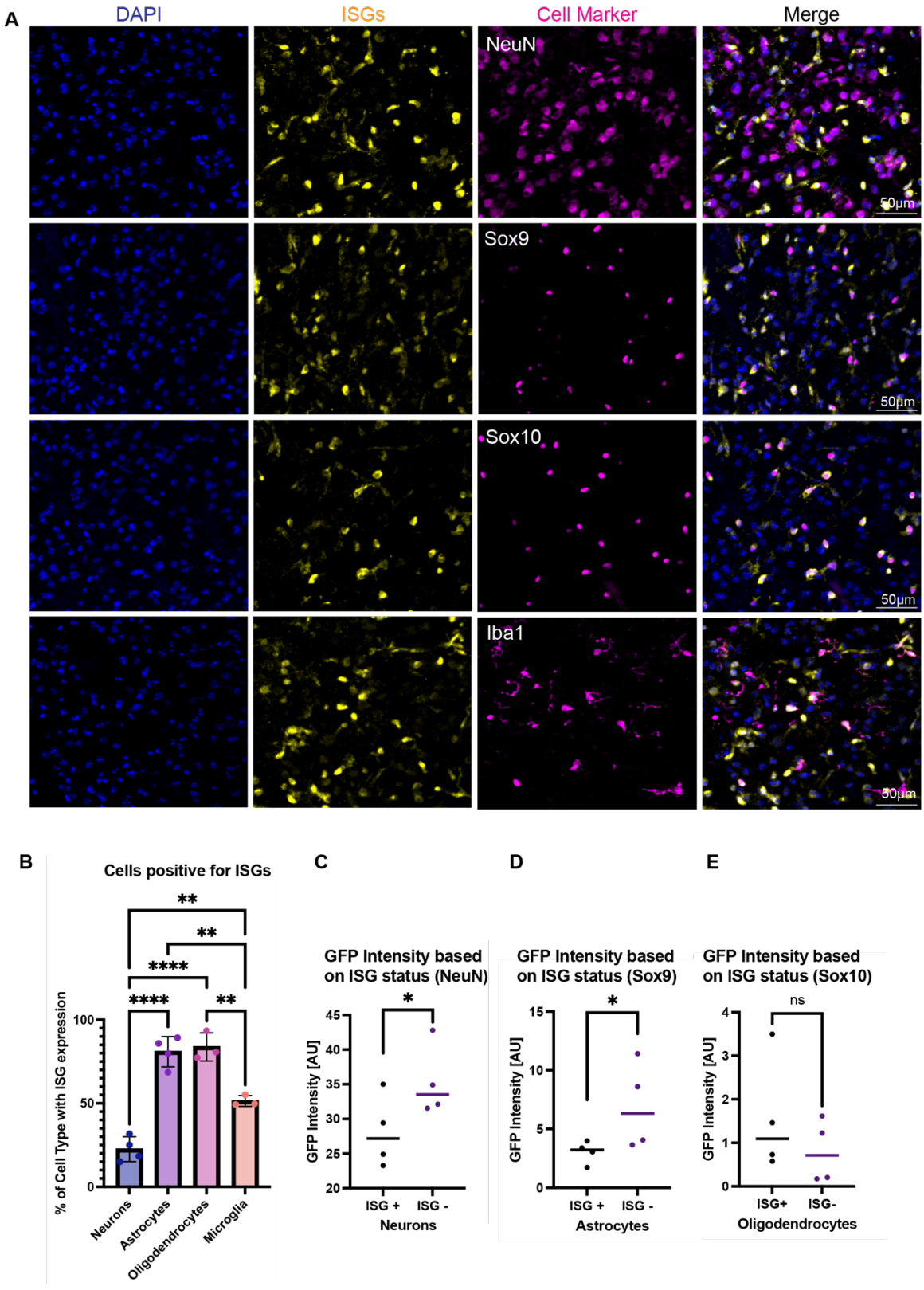

Figure 2.7 (continued)

2.4 Discussion

Here we describe a novel dual labeling viral system based on VSV to track differing states of infection and characterize CNS cell types by these infection states. This dual labeling VSV can differentiate between productive infection (GFP-positive), abortive infection (Cre recombination positive and no GFP), and uninfected (no infection markers). These markers correlate with VSV genome and transcripts where we observed a higher amount of both genome and transcript in GFP-positive cells, and conversely, we were able to detect low amounts of VSV genomes in abortively infected cells with limited to no viral transcripts. We find that the majority of neurons, and to a lesser extent, astrocytes, are productively infected, while oligodendrocytes are more likely to be abortively infected. Microglia were largely uninfected, with some exhibiting abortive infection at the time points assessed. The glial cells exhibited greater colocalization with ISGs than neurons, which could suggest a correlation to infection status. Further investigation of this abortive infection phenotype and its possible causes is warranted. Additional inquiry could better inform transsynaptic viral tool design and viral host dynamics in the CNS.

Dual labeling viral system

Previous approaches have taken advantage of the Cre/lox system and used it for permanent labeling of infected cells either in the case of fusion assays, viral tracing, or capturing abortive infection events [17, 54, 55]. We have expanded upon these strategies and paired the Cre recombinase readout with a typical fluorescent readout of viral

infection, H2B-eGFP. One could separately stain for other viral proteins, but utilizing GFP eliminates any technical limitations that might limit the detection and standardizes the output to make for easier comparison. Additionally, using a nuclear-localized signal for both infection markers makes for easier segmentation and automated quantification.

We showed from the *in vitro* experiments that Cre mediated recombination can be induced by primary transcription of VSV. Cells that were only labeled with Cre recombination marker do not necessarily indicate that viral replication was inhibited directly after primary transcription but rather there was not enough viral genome replication and subsequent secondary transcription for sufficient accumulation of GFP. In some cases, if the image contrast is enhanced, low levels of GFP can be detected in abortively infected cells but the signal is low enough that they are not detectable by eye (data not shown).

Curiously, despite using Cre recombination to permanently label virally infected cells, we observed cells that were GFP-positive only. In these circumstances, it could be simply due to the accessibility/efficiency of the Cre/lox system, but it also could be an additional indicator of virus/host dynamics. We utilized both the binary presence and level of GFP as a proxy for viral replication. Conversely, tdTomato expression (Cre recombination readout) could be an indicator of host transcription/translation. Despite GFP-only cells making up for ~5% of the infected region, these cells were overwhelmingly represented by neurons as compared to the glial cells (data not shown). Neurons were the cells that were the most productively infected, both by percentage of the population and by GFP intensity. Consequently, cells that demonstrate higher levels of viral replication might be more significantly impacted, leading to a concurrent decline

in their homeostatic functions. In support of this theory, many of the GFP-positive only cells also had the most number of viral transcripts, as detected by FISH (data not shown). It has been proposed that greater than 60% of the total polysome-associated mRNA in a VSV infected cell maps to the viral genes within 6hrs post infection when significant host cell translation shut-off is observed [56]. In our analysis, we treated all GFP-positive cells as functionally productively infected and did not distinguish between GFP-only and GFP + tdTomato-positive cells (double positive). Further investigation between these populations could yield further insight into viral/host dynamics.

Cre mRNA transfer

It has been shown that neurons and glial cells can communicate in the form of exosomes and other extracellular vesicles (EVs) [57, 58]. If this occurs in the form of Cre mRNA or protein, this could confound our findings and suggest that Cre recombination only cells might not have been abortively infected by a virus. Recently it has been reported that Cre mRNA itself can induce recombination in bystander cells *in vitro* 72hrs post-lentivirus transduction. These results have been extended further when it was observed that EVs containing Cre mRNA can emanate and spread *in vivo* upon lentivirus transduction (4-16wks post infection) [41]. In both scenarios, this Cre mRNA packaging occurred without any specific targeting to EVs, suggesting that simply overexpression led to this encapsulation and secretion.

Currently, we do not believe EVs containing Cre mRNA are behind our abortive infection readout. We first tested this under similar conditions *in vitro* with HEK293Ts

when we both transferred infected cells onto a monolayer of transfected Cre reporting cells and when we directly applied the cell extract of infected cells onto another set of cells transfected with a Cre reporter (Figure 2.2). In both scenarios, we did not observe any bystander (cells not infected by a virus) recombination within the 24hrs that we tested. However, HEK293Ts do not represent the potential EV effect that might be observed in the CNS. Therefore, to see if Cre recombination cells were in fact virally infected with performed FISH experiments to detect viral genomes directly. Although we did not quantify specifically how many abortively infected cells contained viral genomes, we were able to detect viral genomes in single cells of sparsely infected regions (Figure 2.4). In infected regions containing productive and abortive infections, we observed a significant number of viral genomes in general, suggesting that all of the cells in the infected region were indeed exposed to viruses.

Thus, with the present data, at the timepoints that we assessed, we believe that the abortive infection phenotype is solely attributable to viral infection. If we were to assay at later timepoints, then there is an increased risk that Cre mRNA or protein could be transferred, thus warranting greater prudence and additional controls.

Susceptibility of different cell types in the CNS to VSV infection

We posited a thought experiment that since VSV-G's cognate receptor, LDLR, is ubiquitously expressed, every cell should in fact be susceptible to infection. From the data presented in this chapter, we show that different cell types exhibit varying levels of susceptibility to viral infection and replication. We observe a gradient of infection

phenotypes that progress from productive infection to abortive infection and ending with uninfected. Of note, glial cells in general seem to be more resistant to viral infection than neurons, which are overwhelming productively infected. Astrocytes, while also predominately productively infected, also exhibited much less GFP intensity suggesting that viral replication is stunted even in productively infected cells. Most interestingly are the infection phenotypes presented by oligodendrocytes and microglia. Oligodendrocytes have historically been neglected in terms of viral replication dynamics as compared to the other glial cells. We see that Sox10 positive oligodendrocytes are mostly abortively infected. Even in the productively infected oligodendrocytes, we observe even less viral replication than that of astrocytes; by measuring GFP intensity. This would suggest that our dual labeling VSV is able to initiate early stages of infection (e.g., attachment, fusion, primary transcription) but is resistant to viral replication cycle progressing further. Conversely, microglia being mostly uninfected indicates that these cells are able to prevent VSV from initiating the early stages of the infection process. Most likely, in our system, VSV attached and endocytosed is unable to fuse with the endosomal membrane and deposit its genome in the cytosol of the microglia to initiate primary transcription with any great efficiency. Although we did not perform this experiment, we could confirm this hypothesis by detecting viral genomes directly and see if microglia with no infection markers contain any viral genomes.

Our findings that microglia are more resistant to viral replication are in line with some literature, where is has been found that microglia are difficult to infect [59]. Curiously though, it has been reported that microglia can be productively infected by VSV [24, 60]. The discrepancies are likely associated with the different experimental

setup. The modifications that we made to our dual reporting virus were the deletion of the glycoprotein from the genome and the double mutations made in the matrix protein (Figure 2.1). By removing the glycoprotein, we were better able to capture and interrogate primary infection dynamics of VSV due to its lack of the ability to spread. In so doing, we also reduced the propagation of infectious virions and thus lowered the effective MOI in the local region. If the infection outcome of cell is based on efficiency of viral replication, then having a greater amount of virus might overcome any host barriers to viral infection; in which case, we would observe more infected cells. Additionally, although the mutation in the matrix protein reduces the amount of cellular cytotoxicity, by removing the virus's ability to block host transcription and host mRNA transport, we are also diminishing the virus's ability to actively thwart the host cell's immunity [31-33]. Thus, we are effectively attenuating VSV with the modifications that we have made. This attenuated VSV as compared to wt-VSV is more susceptible to the host's antiviral immunity and therefore changes the replication dynamics/outcomes that we observe. Despite these differences, our virus still accurately captures primary infection dynamics of a neurosynaptic tracing version of VSV.

Potential causes of the differential infection phenotype

We observe varying infection outcomes depending on the cell type involved. Since all of the cells exhibit a percentage of abortive infection, this suggest that, to a certain extent, some properties that dictate abortive infection are shared among all of the cell types. Conversely, given the varying levels of the abortive infection and other infection outcomes, this indicates that each cell type harbor varying abilities of viral

resistance. Identifying pathways that are involved in the differential infection status outcomes is important for a better understand of virus/host dynamics in the CNS and informing neuronal tracing viral tool design.

Local MOI likely contributes to infection outcome. Neurons are productively infected but the small percentage that were either uninfected or abortively infected were typically found at the periphery of the infected region. We expect there to be a viral particle gradient disseminating from the infection tract where it goes from the highest number of particles to a decreasing number the further you are away from the infected foci region. This is corroborated by viral genome detection as well. The gradient presents with regions where there are few viral particles, and there is also an increase in the amount of uninfected and abortive infections. This is likely due to the fact that a certain number of viral infections would likely fail to replicate despite no pressure from the host cell. Similar to the concept of particle-PFU ratio, only a fraction of viral particles can complete an infectious cycle and this amount varies depending on the virus and the cell [61]. Therefore, a certain amount of uninfected cells and abortively infected cells are attributable to the local MOI. Despite this gradient, we still see abortively infected cells at the center of the infected region indicating MOI is not solely responsible for this phenotype.

One of the greatest factors dictating infection outcome early post-infection is that of innate immunity. Innate immunity is led by the response to viral infection by releasing of cytokines which can signal and induce antiviral factors in an autocrine and paracrine manner. VSV has been shown to be exceptionally sensitive to IFN and innate immune pathways, both affecting the amount of primary infection and spread/pathogenesis of the

virus [21, 24, 51]. In an effort to partially address this mechanism, we assessed the expression of interferon-stimulated genes (ISGs) across the cell types. There was a significant trend where more glial cells were expressing detectable levels of ISGs as compared to neurons. This roughly tracks with the infection outcomes, as well where we observed a negative correlation between ISG presence and productive infection in neurons. Additionally, there was an association of ISG expression and lower GFP intensity/expression in neurons and astrocytes. However, this trend of infection status does not perfectly correlate with ISGs. For example, a similar percentage of astrocytes and oligodendrocytes were expressing ISGs despite different ratios of infection outcomes. Moreover, microglia, which are typically known for their high amount of ISG expression, had a lower percentage that was positive for ISGs yet had the highest number of uninfected cells. One explanation is that the ISG transcripts (ISG15, IFIT3, and RSAD2) that we used as a proxy for general ISG expression might not best represent the most relevant ISGs in our system. The ISGs selected were based on previous RNA sequencing results showing that they were the most highly expressed, but perhaps specific ISGs are more associated with controlling the dual labeling VSV infection [14, 24]. Additionally, rather than a specific ISG dictating infection outcome, there could be a threshold effect of ISG expression. We only assessed the presence of ISG based on a minimal threshold, but that does not account for the varying levels of ISG expression that could be exhibited. Anecdotally, despite varying amounts of ISG positive oligodendrocytes and microglia, if these cell types were ISG positive, they had higher intensity of ISG expression than astrocytes or neurons.

Lastly, another possibility for the differential infection status of CNS cell types is that they may exhibit varying degrees of intrinsic immunity. The intrinsic immunity which we are referring to is independent of innate IFN signaling pathways yet could control primary viral infection. Intrinsic factors have not been extensively explored for VSV and were not assessed in this study. Further follow-up is warranted to address if intrinsic immunity could dictate VSV infection outcomes and if CNS cell types are known to exhibit differing amounts of intrinsic immunity.

2.5 Material and Methods

Virus cloning and production

The dual labeling VSV (rVSV-Cre-N-P-Md-H2B-eGFP-L) was generated from a VSVΔG backbone [62]. The Cre, H2B-eGFP and Md (double mutation in Matrix) were introduced into the backbone by Gibson assembly of gBlock fragments with a restriction digested linearized vector. Viruses were rescued as previously described [39]. The dual labeling VSV was expanded by first transfecting 293Ts in a 10cm dish at 70% with pCAG-VSV-G. 36hrs post transfection the cells were infected at an MOI of 0.01 with the rescued dual labeling virus. Viral supernatants were harvested 48hrs post infection and spun down to pellet cellular debris at 4000rpm for 15min at 4C. Supernatant was collected from spin and concentrated using a SW28 rotor at 20K rpm for 2hrs at 4C. Supernatant was discarded, and the viral pellet was resuspended in DMEM overnight at 4C. The resuspended virus was then overlayed on a 10% sucrose cushion (10ml) in tubes for spinning in a SW40 rotor for 2hrs at 4C. Supernatant was discarded, and the viral pellet was resuspended in 1xPBS and subsequently stored at -80C.

Primary transcription *in vitro* experiments

The virus lacking the VSV nucleocapsid (N), phosphoprotein (P), and glycoprotein (G); (rVSV-Cre-dN-dP-M-eGFP-L) to test this proof of concept was generous donated by Dr. Xiang Ma from the Cepko lab. 293Ts in a 6-well plate were transfected at 70% confluency using PEI with plasmids expressing N, P, L and Cre

reporter; N, P and L; or only Cre reporter plasmid. 36hrs post transfection, the cells were infected at an MOI of 3 with the VSV lacking N and P. Images were taken 24hrs post infection showing the GFP and tdTomato readouts (Cre recombination readout) separately.

In vitro Cre transfer experiment

The experimental setup was depicted in Figure 2.2, A. 293Ts in a chamber slide were all transfected using PEI with a Cre reporter plasmid. Concurrently, two sets of other 293Ts were infected at an MOI of 3. 36hrs post transfection of the chamber slide wells, one chamber of was infected with the dual reporting virus, another chamber was left uninfected, the 3rd chamber was not infected but rather infected cells from the other 293Ts were detached with Trypsin-EDTA and overlayed on top of the transfected 293Ts, the 4th condition was also not infected and instead previously infected 293Ts were lysed for 20min (lysis buffer: 150mM NaCl, 1% Triton X-100, 50mM Tris ph 8.0), spun down and the supernatant was added to transfected 293Ts in the chamber well. Images are depicted with separated channels showing tdTomato (Cre recombination readout) and GFP followed by a merge with DAPI.

Mouse strains

12-week old Ai75d mice (025106, The Jackson Laboratory) which contain a floxed nuclear reporter were used for all *in vivo* experiments. The experiment was

composed of 2 males and 2 females. The mice were breed under BSL-1 conditions within the Harvard Center for Comparative Medicine facilities.

Stereotaxic injections

All brain injections were performed under BSL-2 conditions in the Harvard Center for Comparative Medicine facilities. These experiments were performed with 12-week-old mice, 2 males and 2 females. The animals were injected using pulled capillary microdispensers (Drummond Scientific) using the following coordinates for the striatum; A/P 1.0 from bregma, L/M 1.8, D/V -2.5. We injected 200nl of dual labeling virus at a concentration of 1.3x10^9 PFU/ml (tittered on 293Ts).

Tissue processing

16hrs post infection the mice were perfused, and the brains were harvested and fixed in 4% paraformaldehyde (w/v in 1xPBS) overnight at 4C. The brains were then left in a 30% sucrose solution (w/vv 1xPBS) complemented with 1x RNase inhibitor (RNase OUT, Thermo Scientific) until the tissue was saturated and lost buoyancy (24-36hrs post infection). The brain tissue was the flash frozen in O.C.T (4583; VWR) using dry ice. Frozen tissue was stored at -80C until sectioned. Tissue sections were made at a thickness of 20µm using a Leica CM (3050S cryostat). Only the infected regions were sectioned and mounted on PDL coated (0.3mg/ml) Superfrost Plus microscope slides (22-037-446; Fisher Scientific)

VSV genome and transcript detection

Original experiments staining for VSV were performed using SABER-FISH but we migrated to utilizing HCR-FISH. The image of VSV genomes and transcripts detection along white matter vs grey matter regions were performed with SABER. Viral genome detection in single cells was performed using HCR-FISH. All incubations were performed on the microscopy slide with a hybridization coverslip (HybriSlip, Grace Bio-Labs) in a humidified chamber (23-769-522; Fisher Scientific). Any incubations at elevated temperatures were conducted within a hybridization oven.

SABER

SABER-FISH was performed as described previously [16]. Briefly, frozen tissue sections were rehydrated with 3 x 5min in 1X PBSTw (PBS + 0.1% Tween 20), washed with a wash-hybridization solution (40% formamide + 1% Tween 20 + 2X saline sodium citrate [SSC]) at 43C for 15min, followed by a 16hr incubation at 43C in a hybridization solution (40% formamide +10% dextran sulfate + 1% Tween 20 + 2X SSC) containing 8.33ug/ml of FISH probes. Afterwards, samples underwent 2 x 30min washes with the wash-hybridization solution at 43C followed by 2 x 5min washes in 1X SSCT at room temperature. Hybridization probes were then detected by incubating 0.2μM fluorescent oligonucleotides (from IDT) in 1X PBS + 0.2% Tween 20 for 30min at 37C. Samples were subsequently washed 2 x 5min with 1X PBSTw + DAPI at room temperature before being mounted in Fluoromount-G mounted medium (00-4958-02; Thermo Scientific) with a glass coverslip for imaging.

HCR-FISH

All probes and reagents were designed and ordered from Molecular Instruments. HCR-FISH was performed as described previously [63]. Briefly, slides were rehydrated with 2 x 5min 1X PBST washes. Afterwards 200ul of probe hybridization buffer was incubated with the tissue section on the slide for 10min at 37C. The sample was subsequently incubated in a hybridization solution containing 0.4 pmol of each probe set was mixed with 100ul of hybridization solution, incubated overnight at 37C in a humidified chamber in a hybridization oven. After the overnight incubation the tissue section was washed in series of serial solutions for 15min each (75% probe wash buffer / 25% 5X SSCT, 50%/50%, 25%/75%, 0%/100%. Amplification was conducted by apply 200ul of amplification buffer to section in a humidified chamber for 30min at room temperature. Snap cooled hairpins (6 pmol of hairpin h1 and 6 pmol of hairpin h2, heated separately at 95C for 90 seconds and cooled in a dark drawer for 30min) were mixed with 100ul amplification buffer and applied to tissue sections. The samples were incubated overnight at room temperature. The following day 2 x 30min washes of 5X SSCT was conducted at room temperature before a 10min incubation in 1X SSCT + DAPI followed by mounting in Fluoromount-G mounting media with a coverslip.

Immunofluorescence

All immunofluorescence was carried out after DNAse treatment of FISH experiments to ensure that no signal carryover occurred. Incubations were conducted in humidified slide boxes and included the use of hybridization coverslips (as stated in FISH

experiments above). Primary antibody incubation occurred at 4C, overnight with a 1:200 dilution of antibody in blocking/staining buffer (0.1% Triton X-100, 1% BSA, 3% Donkey Serum, in 1X PBS). Washes with 1X PBS occurred at an interval of 3 x 5min. Secondary antibody was diluted to 1:500 in the same blocking/staining solution as mentioned above for 2hrs at room temperature. Samples were washed 3 x 5min with 1X PBS before being mounted in Fluoromount-G with a coverslip.

The antibodies used were as followed: anti-NeuN (ABN91, Millipore), anti-Sox9 (AB5535, Millipore), anti-Sox10 (ab180862, Abcam), Iba1 (GTX100042, GeneTex), Donkey anti-Rabbit Alexa 647 (711-605-152, Jackson ImmunoResearch), and Donkey anti-Chicken Alexa 647 (703-605-155, Jackson ImmunoResearch).

Fluorescent microscopy

Sections were initially screened using a Nikon Eclipse E100 upright epifluorescent microscope to identify samples with the most amount of infection. These slides were subsequently used for staining, imaging and quantification. All imaging took place on a Nikon Ti2 inverted spinning disc microscope using the 20x objective unless stated otherwise. All images were taken using consistent laser power and excitation times within each channel.

Image processing and semi-automated quantification with CellProfiler

FIJI

All images were preprocessed using ImageJ/FIJI macros to streamline analysis. The macros briefly consisted of: 1) running a max intensity Z projection to compress Z stack for each image set, 2) split channel, 3) running the plugin "MultistackReg" for registering serial images when necessary (GFP channel was common among each imaging session and used as reference), "Rigid body" transformation setting was used unless poor registration in which case others transformations were tested, 4) performed background subtraction with a rolling ball radius of 50.0 pixels, 5) performed auto enhanced brightness and contrast at a saturation level of 0.35 (images used for fluorescent intensity comparison used same brightness/contrast parameters for each image), 6) channels merged when more than 4 channels present and pseudo colors used for LUTs for color differentiation.

CellProfiler

Channels from preprocessed images (mentioned above) were separated and imported into CellProfiler pipeline. The pipeline briefly consists of: 1) performing "IdentifyPrimaryObjects" for each channel. A set of thresholds based on size and intensity were used as a baseline for each fluorescent marker/stain but were manually checked. If threshold was not sufficient, the threshold was changed and noted. 2) identified infection marker objects were related and filtered based on colocalization to obtain distinct classifications (i.e. abortive infection [tdTomato-only], double positive [tdTomato + GFP], and GFP-only]). 3) new infection marker objects were masked on cell

markers and binned based on percentage overlap (e.g. 80% infection marker overlap with cell marker counted as infected cell). 4) overlays of infection markers and cell markers were made to ensure limited errors in automated analysis. 5) object intensity measurements for identified objects based on cell markers, genes of interests, and infection markers. 6) data counts and intensities were export to a CSV file and transferred to excel for subsequent calculations.

2.6 References

1. Beier, K. and C. Cepko, *Viral tracing of genetically defined neural circuitry.* J Vis Exp, 2012(68).

2. Beier, K.T., et al., *Transsynaptic tracing with vesicular stomatitis virus reveals novel retinal circuitry.* J Neurosci, 2013. **33**(1): p. 35-51.

3. Beier, K.T., et al., *Anterograde or retrograde transsynaptic labeling of CNS neurons with vesicular stomatitis virus vectors.* Proc Natl Acad Sci U S A, 2011. **108**(37): p. 15414-9.

4. Beier, K.T., et al., *Vesicular stomatitis virus with the rabies virus glycoprotein directs retrograde transsynaptic transport among neurons in vivo.* Front Neural Circuits, 2013. **7**: p. 11.

5. Finkelshtein, D., et al., *LDL receptor and its family members serve as the cellular receptors for vesicular stomatitis virus.* Proc Natl Acad Sci U S A, 2013. **110**(18): p. 7306-11.

6. Nikolic, J., et al., *Structural basis for the recognition of LDL-receptor family members by VSV glycoprotein.* Nat Commun, 2018. **9**(1): p. 1029.

7. Mundell, N.A., et al., *Vesicular stomatitis virus enables gene transfer and transsynaptic tracing in a wide range of organisms.* J Comp Neurol, 2015. **523**(11): p. 1639-63.

8. Gillies, S. and V. Stollar, *Generation of defective interfering particles of vesicular stomatitis virus in Aedes albopictus cells.* Virology, 1980. **107**(2): p. 497-508.

9. Mudd, J.A., et al., *Natural selection of mutants of vesicular stomatitis virus by cultured cells of Drosophila melanogaster.* J Gen Virol, 1973. **20**(3): p. 341-51.

10. Seganti, L., et al., *Study of receptors for vesicular stomatitis virus in vertebrate and invertebrate cells.* Microbiologica, 1986. **9**(3): p. 259-67.

11. Kandel, E.S., et al., *Applications of green fluorescent protein as a marker of retroviral vectors.* Somat Cell Mol Genet, 1997. **23**(5): p. 325-40.

12. Soboleski, M.R., J. Oaks, and W.P. Halford, *Green fluorescent protein is a quantitative reporter of gene expression in individual eukaryotic cells.* FASEB J, 2005. **19**(3): p. 440-2.

13. Combe, M., et al., *Single-Cell Analysis of RNA Virus Infection Identifies Multiple Genetically Diverse Viral Genomes within Single Infectious Units.* Cell Host Microbe, 2015. **18**(4): p. 424-32.

14. Huang, K.W. and B.L. Sabatini, *Single-Cell Analysis of Neuroinflammatory Responses Following Intracranial Injection of G-Deleted Rabies Viruses.* Front Cell Neurosci, 2020. **14**: p. 65.

15. Kotliar, D., et al., *Single-Cell Profiling of Ebola Virus Disease In Vivo Reveals Viral and Host Dynamics.* Cell, 2020. **183**(5): p. 1383-1401 e19.

16. Kishi, J.Y., et al., *SABER amplifies FISH: enhanced multiplexed imaging of RNA and DNA in cells and tissues.* Nat Methods, 2019. **16**(6): p. 533-544.

17. Pfefferkorn, C., et al., *Abortively Infected Astrocytes Appear To Represent the Main Source of Interferon Beta in the Virus-Infected Brain.* J Virol, 2016. **90**(4): p. 2031-8.

18. Trottier, M.D., Jr., B.M. Palian, and C.S. Reiss, *VSV replication in neurons is inhibited by type I IFN at multiple stages of infection.* Virology, 2005. **333**(2): p. 215-25.

19. Kreit, M., et al., *Inefficient type I interferon-mediated antiviral protection of primary mouse neurons is associated with the lack of apolipoprotein l9 expression.* J Virol, 2014. **88**(7): p. 3874-84.

20. Peferoen, L., et al., *Oligodendrocyte-microglia cross-talk in the central nervous system.* Immunology, 2014. **141**(3): p. 302-13.

21. Chhatbar, C., et al., *Type I Interferon Receptor Signaling of Neurons and Astrocytes Regulates Microglia Activation during Viral Encephalitis.* Cell Rep, 2018. **25**(1): p. 118-129 e4.

22. Hwang, M. and C.C. Bergmann, *Neuronal Ablation of Alpha/Beta Interferon (IFN-alpha/beta) Signaling Exacerbates Central Nervous System Viral Dissemination and Impairs IFN-gamma Responsiveness in Microglia/Macrophages.* J Virol, 2020. **94**(20).

23. Matejuk, A. and R.M. Ransohoff, *Crosstalk Between Astrocytes and Microglia: An Overview.* Front Immunol, 2020. **11**: p. 1416.

24. Drokhlyansky, E., et al., *The brain parenchyma has a type I interferon response that can limit virus spread.* Proc Natl Acad Sci U S A, 2017. **114**(1): p. E95-E104.

25. Kaspar, B.K., et al., *Adeno-associated virus effectively mediates conditional gene modification in the brain.* Proc Natl Acad Sci U S A, 2002. **99**(4): p. 2320-5.

26. Hadjantonakis, A.K. and V.E. Papaioannou, *Dynamic in vivo imaging and cell tracking using a histone fluorescent protein fusion in mice.* BMC Biotechnol, 2004. **4**: p. 33.

27. Kim, I.S., et al., *Mechanism of membrane fusion induced by vesicular stomatitis virus G protein.* Proc Natl Acad Sci U S A, 2017. **114**(1): p. E28-E36.

28. Hoffmann, M., et al., *Fusion-active glycoprotein G mediates the cytotoxicity of vesicular stomatitis virus M mutants lacking host shut-off activity.* J Gen Virol, 2010. **91**(Pt 11): p. 2782-93.

29. Janelle, V., et al., *Mutations in the glycoprotein of vesicular stomatitis virus affect cytopathogenicity: potential for oncolytic virotherapy.* J Virol, 2011. **85**(13): p. 6513-20.

30. Ferran, M.C. and J.M. Lucas-Lenard, *The vesicular stomatitis virus matrix protein inhibits transcription from the human beta interferon promoter.* J Virol, 1997. **71**(1): p. 371-7.

31. Ahmed, M., et al., *Ability of the matrix protein of vesicular stomatitis virus to suppress beta interferon gene expression is genetically correlated with the inhibition of host RNA and protein synthesis.* J Virol, 2003. **77**(8): p. 4646-57.

32. Petersen, J.M., et al., *The matrix protein of vesicular stomatitis virus inhibits nucleocytoplasmic transport when it is in the nucleus and associated with nuclear pore complexes.* Mol Cell Biol, 2000. **20**(22): p. 8590-601.

33. von Kobbe, C., et al., *Vesicular stomatitis virus matrix protein inhibits host cell gene expression by targeting the nucleoporin Nup98.* Mol Cell, 2000. **6**(5): p. 1243-52.

34. Perrault, J., G.M. Clinton, and M.A. McClure, *RNP template of vesicular stomatitis virus regulates transcription and replication functions.* Cell, 1983. **35**(1): p. 175-85.

35. Whelan, S.P. and G.W. Wertz, *Transcription and replication initiate at separate sites on the vesicular stomatitis virus genome.* Proc Natl Acad Sci U S A, 2002. **99**(14): p. 9178-83.

36. Flamand, A. and D.H. Bishop, *Primary in vivo transcription of vesicular stomatitis virus and temperature-sensitive mutants of five vesicular stomatitis virus complementation groups.* J Virol, 1973. **12**(6): p. 1238-52.

37. Dutia, B.M., et al., *A novel Cre recombinase imaging system for tracking lymphotropic virus infection in vivo.* PLoS One, 2009. **4**(8): p. e6492.

38. Madisen, L., et al., *A robust and high-throughput Cre reporting and characterization system for the whole mouse brain.* Nat Neurosci, 2010. **13**(1): p. 133-40.

39. Whelan, S.P., et al., *Efficient recovery of infectious vesicular stomatitis virus entirely from cDNA clones.* Proc Natl Acad Sci U S A, 1995. **92**(18): p. 8388-92.

40. Ridder, K., et al., *Extracellular vesicle-mediated transfer of genetic information between the hematopoietic system and the brain in response to inflammation.* PLoS Biol, 2014. **12**(6): p. e1001874.

41. Rufino-Ramos, D., et al., *Extracellular communication between brain cells through functional transfer of Cre mRNA mediated by extracellular vesicles.* Mol Ther, 2023. **31**(7): p. 2220-2239.

42. Gusel'nikova, V.V. and D.E. Korzhevskiy, *NeuN As a Neuronal Nuclear Antigen and Neuron Differentiation Marker.* Acta Naturae, 2015. **7**(2): p. 42-7.

43. Sun, W., et al., *SOX9 Is an Astrocyte-Specific Nuclear Marker in the Adult Brain Outside the Neurogenic Regions.* J Neurosci, 2017. **37**(17): p. 4493-4507.

44. Liu, Z., et al., *Induction of oligodendrocyte differentiation by Olig2 and Sox10: evidence for reciprocal interactions and dosage-dependent mechanisms.* Dev Biol, 2007. **302**(2): p. 683-93.

45. Pozniak, C.D., et al., *Sox10 directs neural stem cells toward the oligodendrocyte lineage by decreasing Suppressor of Fused expression.* Proc Natl Acad Sci U S A, 2010. **107**(50): p. 21795-800.

46. Takada, N., S. Kucenas, and B. Appel, *Sox10 is necessary for oligodendrocyte survival following axon wrapping.* Glia, 2010. **58**(8): p. 996-1006.

47. Jurga, A.M., M. Paleczna, and K.Z. Kuter, *Overview of General and Discriminating Markers of Differential Microglia Phenotypes.* Front Cell Neurosci, 2020. **14**: p. 198.

48. Wittekindt, M., et al., *Different Methods for Evaluating Microglial Activation Using Anti-Ionized Calcium-Binding Adaptor Protein-1 Immunohistochemistry in the Cuprizone Model.* Cells, 2022. **11**(11).

49. Schneider, W.M., M.D. Chevillotte, and C.M. Rice, *Interferon-stimulated genes: a complex web of host defenses.* Annu Rev Immunol, 2014. **32**: p. 513-45.

50. Schoggins, J.W. and C.M. Rice, *Interferon-stimulated genes and their antiviral effector functions.* Curr Opin Virol, 2011. **1**(6): p. 519-25.

51. Detje, C.N., et al., *Local type I IFN receptor signaling protects against virus spread within the central nervous system.* J Immunol, 2009. **182**(4): p. 2297-304.

52. van den Pol, A.N., S. Ding, and M.D. Robek, *Long-distance interferon signaling within the brain blocks virus spread.* J Virol, 2014. **88**(7): p. 3695-704.

53. Lang, R., et al., *Expression and mechanisms of interferon-stimulated genes in viral infection of the central nervous system (CNS) and neurological diseases.* Front Immunol, 2022. **13**: p. 1008072.

54. Pan, R., et al., *Oligodendrocytes that survive acute coronavirus infection induce prolonged inflammatory responses in the CNS.* Proc Natl Acad Sci U S A, 2020. **117**(27): p. 15902-15910.

55. Esposito, A.M., et al., *A High-throughput Cre-Lox Activated Viral Membrane Fusion Assay to Identify Inhibitors of HIV-1 Viral Membrane Fusion.* J Vis Exp, 2018(138).

56. Neidermyer, W.J., Jr. and S.P.J. Whelan, *Global analysis of polysome-associated mRNA in vesicular stomatitis virus infected cells.* PLoS Pathog, 2019. **15**(6): p. e1007875.

57. Cano, A., et al., *Extracellular vesicles, the emerging mirrors of brain physiopathology.* Int J Biol Sci, 2023. **19**(3): p. 721-743.

58. Gassama, Y. and A. Favereaux, *Emerging Roles of Extracellular Vesicles in the Central Nervous System: Physiology, Pathology, and Therapeutic Perspectives.* Front Cell Neurosci, 2021. **15**: p. 626043.

59. Welsch, J.C., et al., *Type I Interferon Receptor Signaling Drives Selective Permissiveness of Astrocytes and Microglia to Measles Virus during Brain Infection.* J Virol, 2019. **93**(13).

60. Chauhan, V.S., et al., *Vesicular stomatitis virus infects resident cells of the central nervous system and induces replication-dependent inflammatory responses.* Virology, 2010. **400**(2): p. 187-96.

61. Bhat, T., A. Cao, and J. Yin, *Virus-like Particles: Measures and Biological Functions.* Viruses, 2022. **14**(2).

62. Chandran, K., et al., *Endosomal proteolysis of the Ebola virus glycoprotein is necessary for infection.* Science, 2005. **308**(5728): p. 1643-5.

63. Choi, H.M., V.A. Beck, and N.A. Pierce, *Next-generation in situ hybridization chain reaction: higher gain, lower cost, greater durability.* ACS Nano, 2014. **8**(5): p. 4284-94.

2.7 Acknowledgements

This work was made possible with the help of Dr. Xiang Ma who supplied reagents, training, and valuable insight for experimental design. Additionally, the work would not have progressed without the training and support offered by the MicRoN team including but not limited to Dr. Paula Montero Llopis and Dr. Praju Vikas Anekal.

Chapter III.

IFN Signaling Heterogeneity in the Brain and Influence of IFN Signaling on Primary Infection Outcome

3.1 Abstract

To better inform viral neuronal tracing tools and virus/host interactions in the CNS, we sought to characterize the earliest responses to viral infection in the brain and determine their influence on infection outcomes. One of the quickest and most robust responses of the host to viral infection is the activation and coordination of the innate immune system. Specifically, this involves the detection of viral infiltrates and the secretion of signaling molecules, such as interferon (IFN), which activate early antiviral pathways. IFN and these interferons-stimulated genes (ISGs) have been heavily implicated in dictating viral infection and pathogenesis. Upon viral infection, we observed distinct regional expression of IFNb and IFNl. This expression was an acute response, with IFN detectable 8hrs post-infection followed by a gradual decrease beginning at 24hrs post-infection. Most interestingly, there was a switch in which glial cells were primarily responsible for IFNb induction; microglia were the main producers early post-infection, while oligodendrocytes made up the majority of IFNb expressing cells later post-infection. Lastly, we tested whether IFN signaling affects the ratio of productive versus abortive primary infection and found that there was only a slight shift in some glial cells, indicating that other pathways are involved in primary infection outcomes.

3.2 Introduction

Upon early viral infection, it is well established that innate immunity plays a significant role in terms of viral pathogenesis and the recruitment/coordination of host immunity. Specifically, the IFNs induced by this innate immune response can prevent both the spread of infection with neurotropic viruses and the use of neurosynaptic tracing viruses as tools. VSV is particularly known to be quite sensitive to IFN-induced antiviral immunity [1-5]. Therefore, it is crucial to characterize identify which IFNs are induced, and which cells are coordinating this response.

It has been observed that depending on the virus and the route of administration, all IFN types (type I, type II, and type III) can be induced in the context of a viral infection of the CNS. Type I IFNs are historically considered the most important due to the potent antiviral activity they elicit through the induction of ISGs. However, throughout the course of certain viral diseases, both IFNγ (type II) and IFNλ (type III) can also be induced and contribute to the control of viral infection as well [6-12]. Our objective was to determine which IFNs are induced upon viral infection with our dual-labeling VSV.

In terms of which cells contribute to the IFN response, historical literature suggests that both astrocytes and microglia are the main producers of type I IFNs upon viral infection of the CNS [13]. However, there is a discrepancy regarding which of the two glial cells express IFNβ in the context of specific viral infections. Reports have shown RABV infection inducing IFNβ expression in microglia, while other report its induction in astrocytes [14, 15]. Similarly, astrocytes have been noted as the primary

IFNβ producers for VSV infection, though published data from our lab indicate that microglia were exclusively responsible for IFNb expression during VSV infection of the CNS [1, 2, 16]. These discrepancies could be due to variations in the virus (such as specific strains or mutations), the route of infection, the experimental setup/readout, or the timing of the assay. Overall, the key take away is that IFNb expression can originate from multiple sources, depending on the context of the viral infection.

Once we've identified the specific IFNs and the cells expressing them, we can investigate whether IFN signaling contributes to the primary infection outcome. The underlying hypothesis of this research is that we could enhance neurosynaptic tracing systems by pinpointing mechanisms that govern infection outcomes, such as whether cells are uninfected, productively infected, or abortively infected. Identifying such mechanisms may enable us to influence cells to transition from being uninfected or abortively infected to becoming productively infected.

Previous studies have demonstrated that IFN signaling can alter viral tropism in the CNS. For instance, there is a noted difference in neurovirulence between RABV street and lab strains due to attenuating mutations introduced to the lab strain [17-20]. It has been suggested that this attenuation reduces the lab strain's ability to disrupt innate immune pathways, making it more sensitive to host-mediated antiviral activity [18, 21-23]. Additionally, the differences between these strains affect the level of productive viral infection in astrocytes, with street strains infecting astrocytes more productively than lab-attenuated stains [20]. In other studies, these astrocytes were found to be abortively infected [14].

A shift in tropism due to a lack of type I IFN signaling has been demonstrated even more directly with measles virus and a tick-borne flavivirus. In both systems, IFNAR KO led to increased susceptibility of microglia to productive infection [24, 25]. When type I IFN signaling was intact, microglia were resistant to infection. This suggests that type I IFN signaling influences both viral tropism and the selective permissiveness of different cell types within the CNS.

The data presented in this chapter identify which IFN subtypes are induced upon infection with our dual-labeling VSV. After determining the IFN species, we tracked which cells were the primary producers over time. We also assessed whether IFN signaling influenced the primary infection outcome of the dual-labeling VSV. The findings of this section enhance our understanding of early viral-host responses and provide new directions for further advancing neurosynaptic tracing viral tools.

3.3 Results

IFN types detected in the brain post infection with dual labeling VSV

Previous studies have implicated several IFN subtypes as being highly upregulated during viral infection of the brain; IFNα, IFNβ, IFNλ, and IFNγ [5, 12]. We investigated whether these subtypes were also activated upon our dual labeling VSV infection in the brain parenchyma. Specifically, we employed HCR-FISH to detect *IFNa4, IFNb1*, *IFNl2, IFNg* (labeled IFNa, IFNb, IFNl, and IFNg in Figure 3.1) in tissue sections from infected brains. At 16hrs post-infection, we detected IFNb in the white matter, grey matter, ependyma/subventricular zone (SVZ), and the rostral migratory stream (RMS) (Figure 3.1). IFNb signals from the ependyma, SVZ, and RMS were regionally localized, suggesting that cells specific to these regions are involved in the upregulation of IFNb (Figure 3.1 D, E, F). Additionally, we detected IFNl in the SVZ and the RMS, with a lesser amount observed in the ependymal layer further away from the SVZ (Figure 3.1 A, D, E, F). At no point were any of the IFN subtypes detectable outside the infected region, indicating that IFN induction was dependent on viral infection. IFNb and IFNl signals were mutually exclusive, suggesting that the cell populations expressing these subtypes of IFN are distinct (Figure 3.1 D, E, F). We did not detect IFNa or IFNg in these regions or at this timepoint.

Figure 3.1| IFN subtypes detected upon dual labeling VSV infection in the brain

A) Table depicting detection of IFN subtypes *IFNa4, IFNb1*, *IFNl2, IFNg* (labeled IFNa, IFNb, IFNl, and IFNg) upon VSV infection 16hrs post infection. **B)** IFNb detection in grey matter (striatum). **C)** IFNb detection in grey matter (striatum - left side of image) and white matter (corpus callosum - right side of image). Detection of IFNb and IFNl in **D)** subventricular zone (SVZ), **E)** ependymal layer, **D)** rostral migratory stream (RMS). Images show GFP and tdTomato (Cre recombination readout) combined and IFNb and IFNl labeled separately along with a merge panel including all images.

A

	Grey Matter	White Matter	SVZ / Ependyma	RMS
IFNa	-	-	-	-
IFNb	+	+	+	+
IFNl	-	-	+	+
IFNg	-	-	-	-

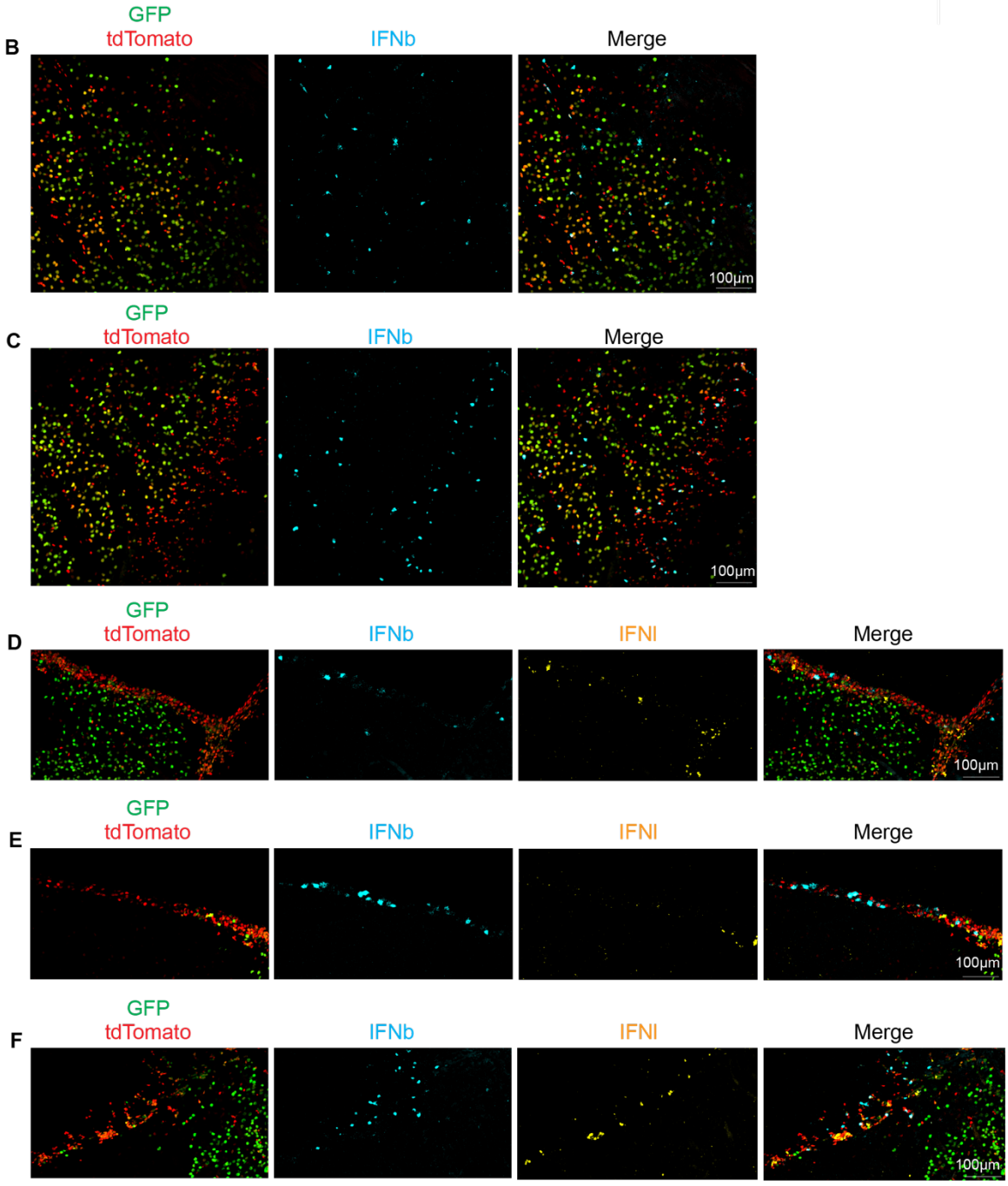

Figure 3.1 (Continued)

IFNb time course: shifting contributions by glial cells

Now that we know which IFN subtypes are expressed upon dual labeling VSV infection, we wanted to determine how quickly this response is initiated and which cells might be involved in the IFN induction. For the remainder of the experiments, we focused specifically on the striatum, to maintain consistency with our neuronal tracing studies, and did not extensively investigate the origins of the IFNb and IFNl in the ependyma, SVZ, or RMS.

IFN induction is known to be an acute response; therefore, we harvested mouse brains at specific time points early post-infection (4hrs, 8hrs, 16hrs, and 24hrs post-infection) to determine when IFN is specifically expressed and which cells are involved. Although in some cases the IFNb signal could be detected as early as 4hrs post-infection, the accumulation of the signal was first apparent at 8hrs post-infection, where we observed an average of one IFNb expressing cell per 15,000um^2 area (Figure 3.2). At 16hrs post-infection, IFNb expressing cells were slightly more evident, reaching upwards of one IFNb positive cell per 10,000um^2 in some cases. Although not statistically significant, there was a trend at 24hrs post-infection where we began to see a decrease in IFNb signal and IFNb positive cells, indicating that the response IFN induction had peaked and was beginning to dissipate (Figure 3.2). This trend was evident due to the lack of accumulation of the IFNb signal and the decreased number of cells that met the minimum threshold for being considered IFNb positive.

Figure 3.2| IFNb induction time course post dual labeling VSV infection

Dual labeling VSV was injected into the striatum of Ai75d mice and the brains were harvested a specific intervals post infection to determine onset of IFNb induction. **A)** representative images showing DAPI staining along with HCR-FISH signal for *IFNb1* (labeled IFNb) in an uninfected brain or brains harvested 4hrs, 8hrs, 16hrs, or 24hrs post infection. **B)** quantification of IFNb induction time course. Nested One-way ANOVA was performed with Tukey's multiple comparison test for statistical analysis. $* \leq 0.0332$, $** \leq 0.0021$, $*** \leq 0.0002$, $**** \leq 0.0001$. 8hrs, 16hrs and 24hrs post infection were significantly ($p < 0.03$) different from "Uninfected" and "4hrs post infection" but were not significantly different between themselves.

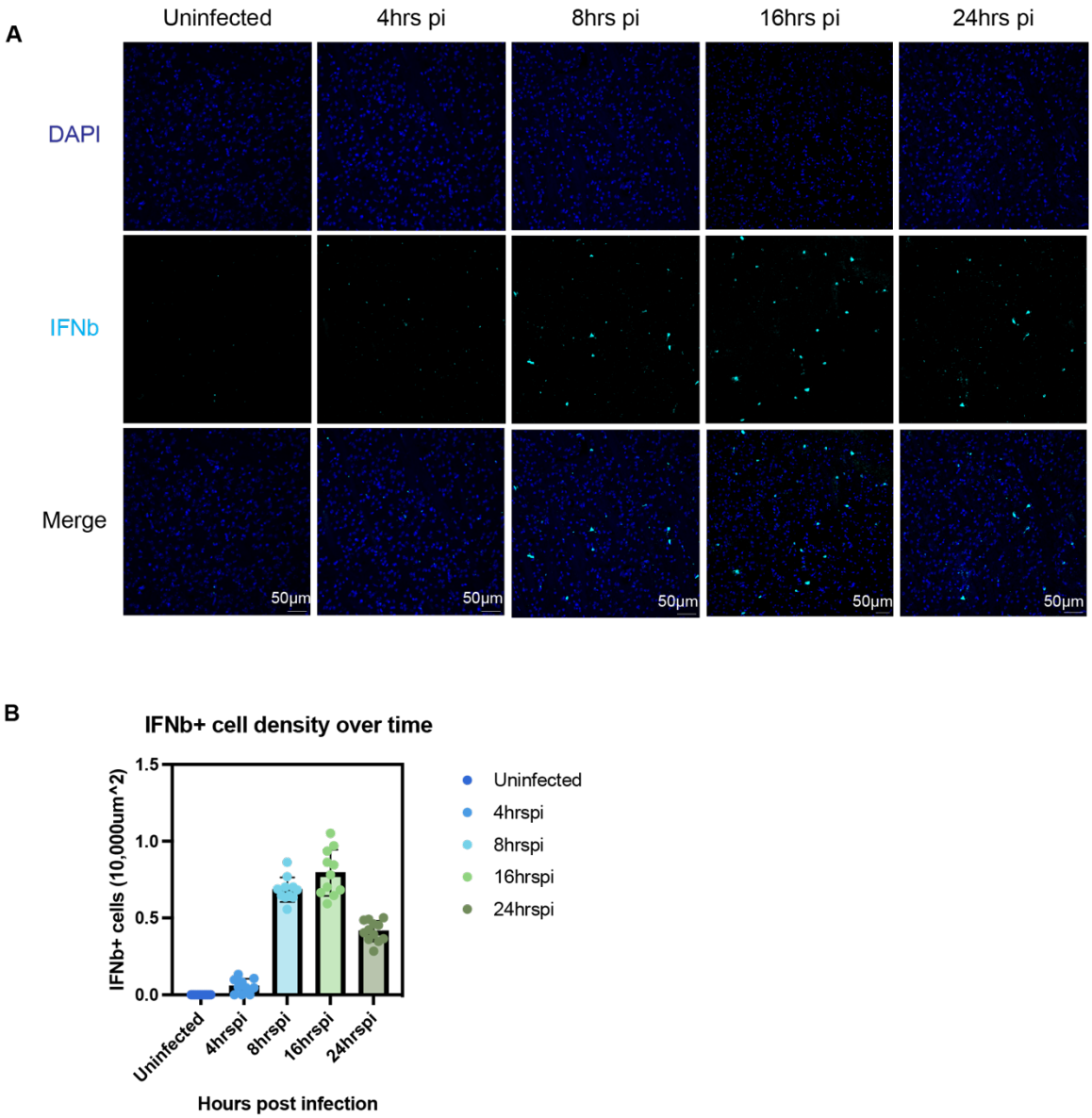

Figure 3.2 (continued)

Next, we investigated which cell type was responsible for IFNb production at the time points where we could actively detect IFNb (8hrs, 16hrs, and 24hrs post-infection). Previous literature suggests that microglia or astrocytes would likely be expressing IFNb upon VSV infection, but we wanted to verify if this was the case with our dual labeling VSV [1, 2]. We did this by measuring the percentage of IFNb signal that could be attributed to each cell type, using the same cell markers as before, at each time point when IFNb was detectable.

At 8hrs post-infection observed a significant association (more than 80%) of IFNb expression with Iba1 positive microglia (Figure 3.2 A, B). To a much lesser extent, the rest of the IFNb signal could be accounted for by mostly Sox10 positive oligodendrocytes, while Sox9 positive astrocytes and NeuN positive neurons did not represent any significant IFNb expression. We initially thought this trend might persist, with microglia representing the source of IFNb in the context of dual labeling VSV infection across all time points, but this assumption was proved to be incorrect.

At 16hrs post-infection microglia were no longer the predominant IFNb producing cells. Instead, oligodendrocytes constituted the majority of IFNb production (> 60%) (Figure 3.3. C, D). This shift was followed by microglia and astrocytes, which colocalized with the remainder of the IFNb signal and contributed similar amounts (< 40% together). This trend continued at 24hrs post-infection; despite a decrease in the amount of IFNb positive cells, oligodendrocytes still accounted for the majority (~60%) of the IFNb signal association (Figure 3.3 E, F). The rest of the IFNb expression was attributed to the other glial cells (astrocytes and microglia).

Figure 3.3| IFNb time course with cell type specific origin

HCR-FISH used to detect IFNb for a time course post dual labeling VSV infection. Cell markers used are the following; NeuN = neurons, Sox9 = astrocytes, Sox10 = oligodendrocytes, Iba1 = microglia. Images and corresponding quantification are: **A)** and **B)** 8hrs post infection, **C)** and **D)** are 16hrs post infection, **E)** and **F)** are 24hrs post infection. **G)** is a summary line graph containing all timepoint and percent of IFNb positive cells that can be accounted for by each cell type. Graph display means for each metric. Each point is a separate animal with an average of 2-4 images per animal. One-way ANOVA was performed with Tukey's multiple comparison test for statistical analysis. $* \leq 0.0332$, $** \leq 0.0021$, $*** \leq 0.0002$, $**** \leq 0.0001$

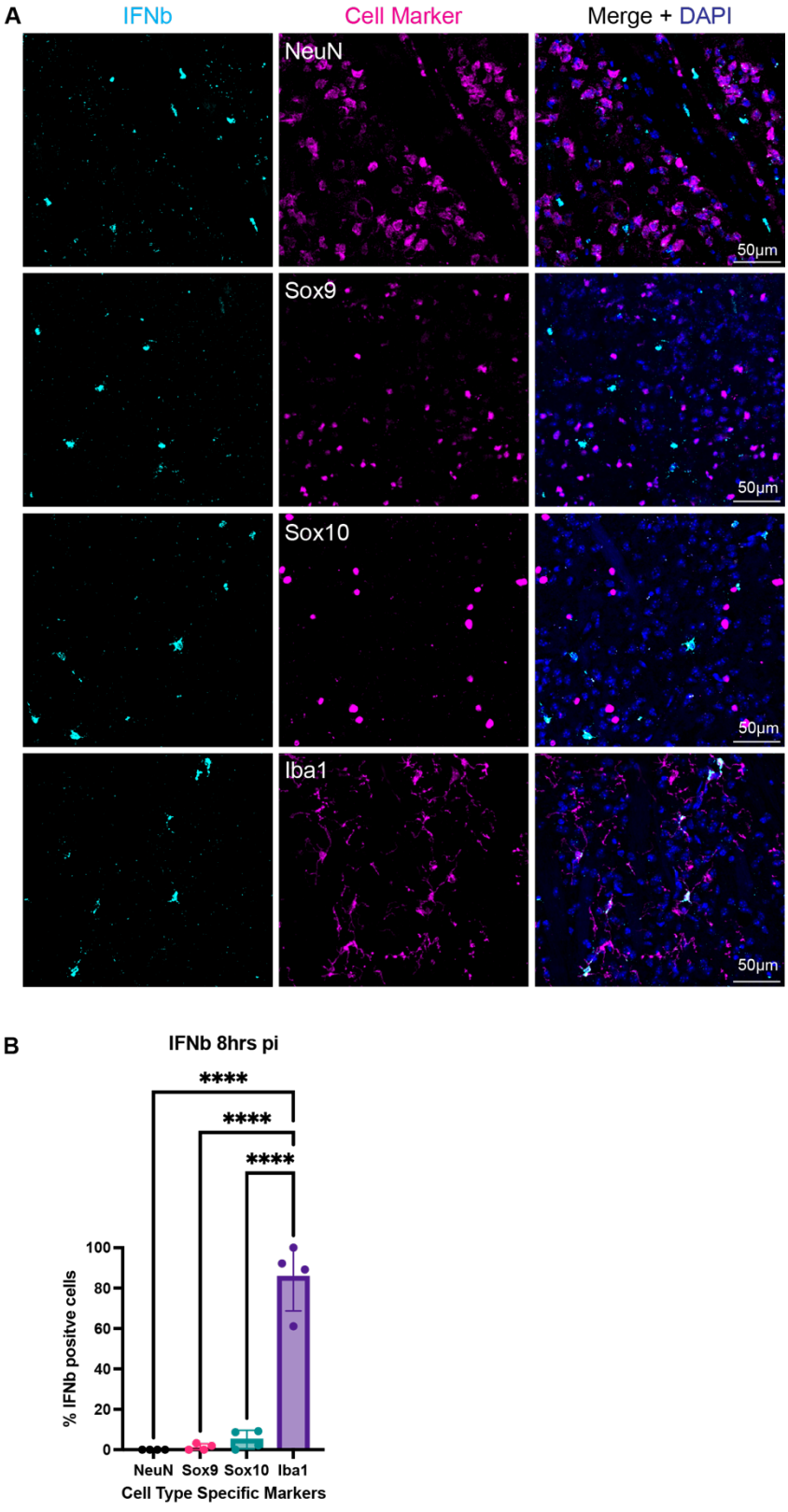

Figure 3.3 (Continued)

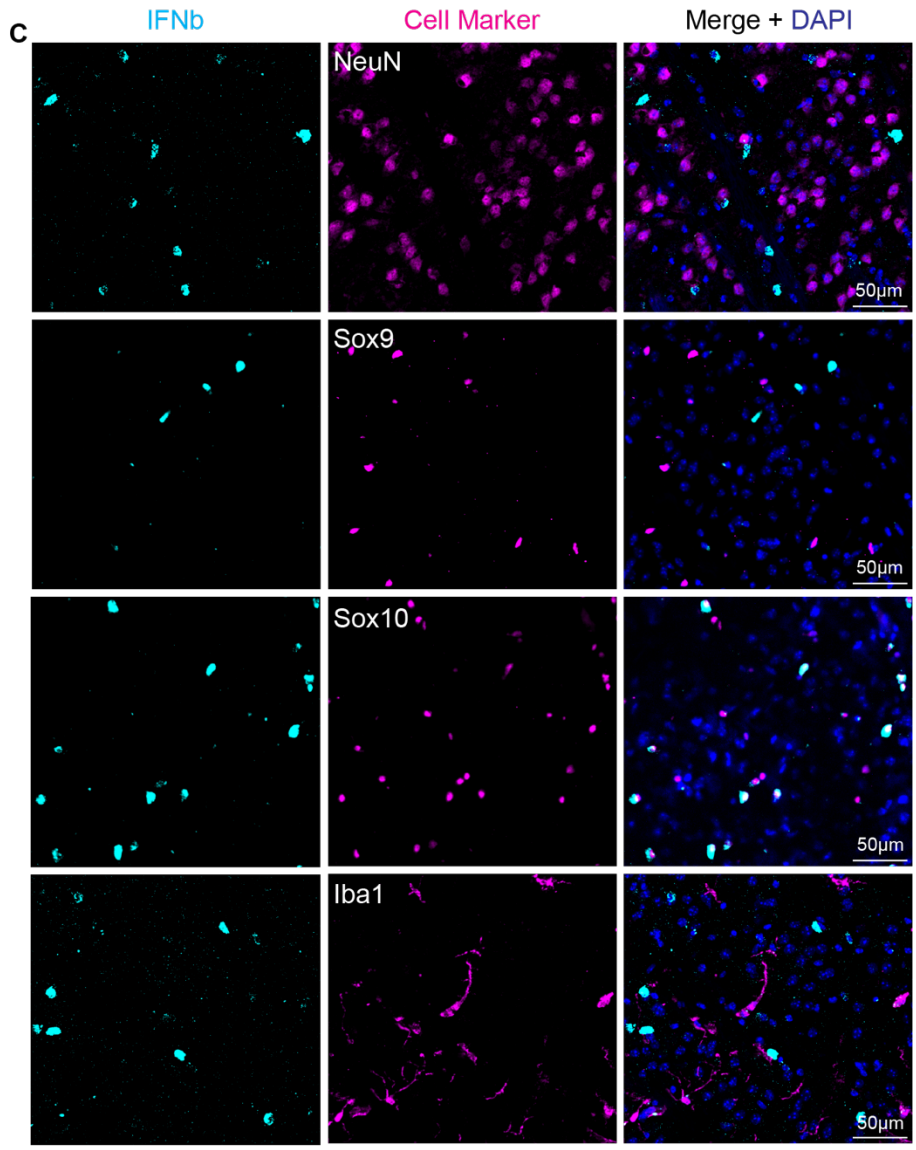

Figure 3.3 (Continued)

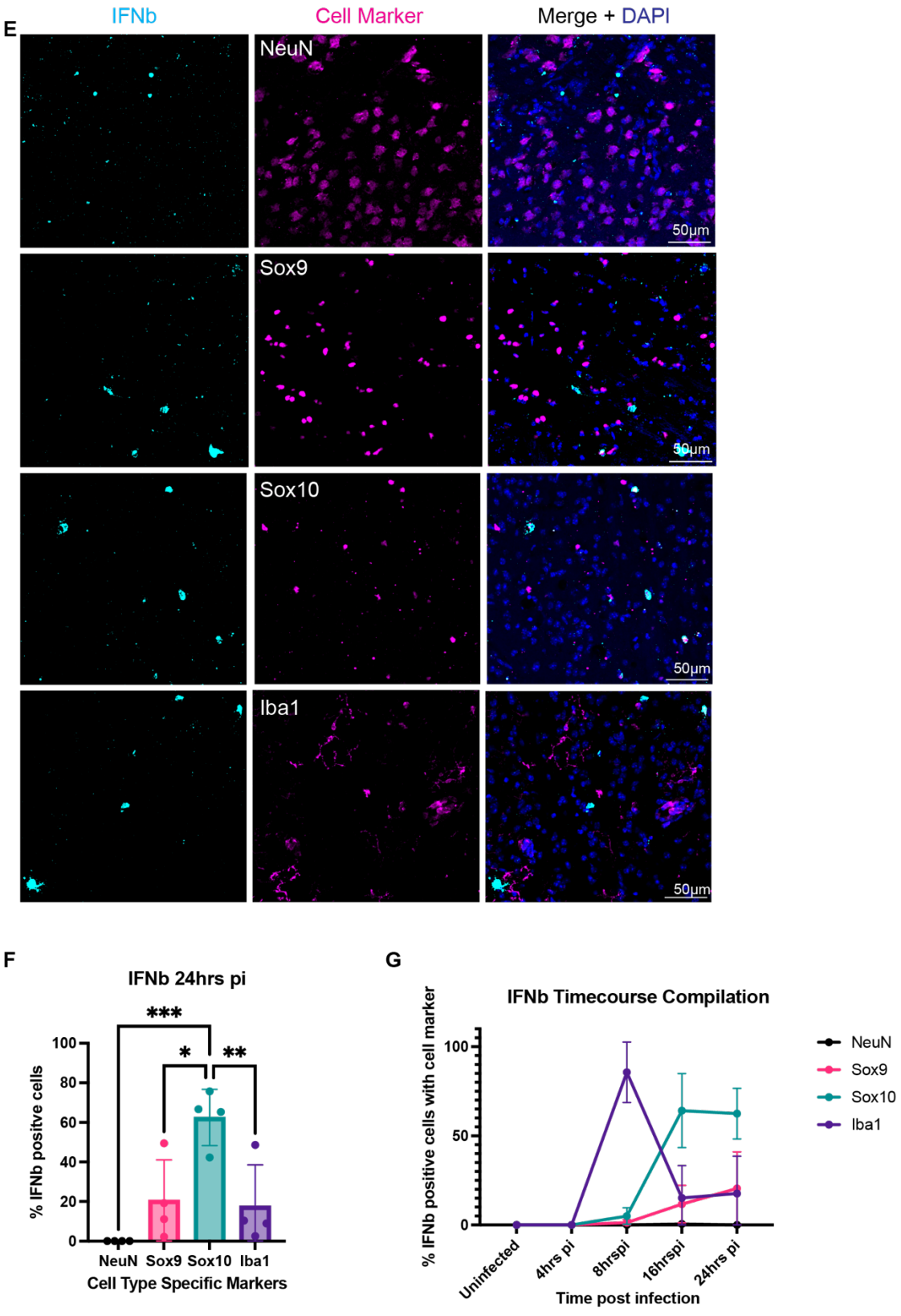

Figure 3.3 (Continued)

At no time point did we detect neurons expressing IFNb. Overall, a shift in IFNb was observed: expression where microglia were the initial responders soon after infection and as time progressed, oligodendrocytes began to express the majority of IFNb (Figure 3.3, G). Further investigation is needed to understand the changes occurring in microglia and oligodendrocytes between 8 and 16hrs post-infection.

Next, we aimed to determine the infection status of the IFNb producing cells. For this purpose, we quantified the association of the infection markers GFP and tdTomato (Cre recombination readout) with the HCR-FISH detection of IFNb and immunofluorescence of the cell markers. We found that the majority of IFNb expressing cells, across all cell types, were abortively infected (Figure 3.4, B, C, D). Notably 70-80% of the IFNb expressing cells from oligodendrocytes and microglia were abortively infected, while the astrocytes were more heterogeneous, given the small number of them expressing IFNb. However, over 25% of the IFNb expressing oligodendrocytes were productively infected, and ~15% of the IFNb expressing microglia did not contain any detectable infection markers, indicating that IFNb is not solely expressed by abortively infected cells. The Cre recombination readout conveniently allowed us to account for a greater number of infected IFNb producing cells than if we had used the viral readout of infection, GFP, alone.

The quantification of infection status of IFNb producing cells was only presented at 16hrs post-infection. At 8hrs post-infection there was insufficient accumulation of GFP and tdTomato infection markers to define cells by their infection status. The trends observed at 24hrs post infection were similar to those at 16hrs, with abortively infected cells constituting the majority of IFNb positive cells (data not shown).

Figure 3.4| Infection status of IFNb expressing cells

A) Representative image of infection markers, GFP and tdTomato, along with HCR - FISH signal for IFNb (cyan), and IF for Sox10 (magenta) 16hrs post infection with dual labeling VSV. The graphs depict infection status quantification of IFNb positive cells of each cell population: **B)** oligodendrocytes, **C)** microglia, **D)** astrocytes. Quantifications are taken from 16hrs post infection timepoint. Graph display means for each metric. Each point is a separate animal with an average of 2-4 images per animal. One-way ANOVA was performed with Tukey's multiple comparison test for statistical analysis. $* \leq 0.0332$, $** \leq 0.0021$, $*** \leq 0.0002$, $**** \leq 0.0001$

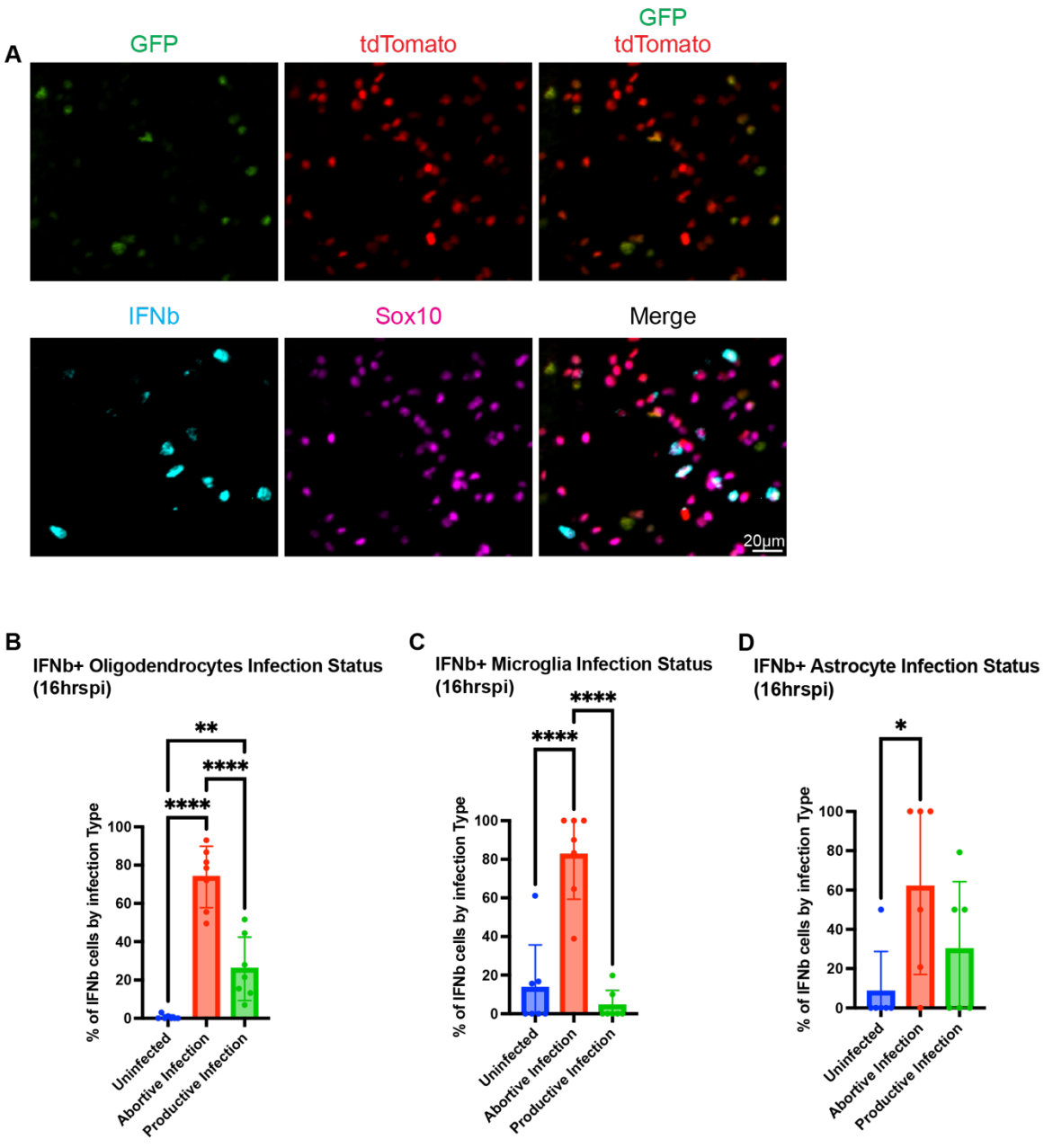

Figure 3.4 (Continued)

Microglia observations: number and morphology changes

The switch in IFNb production between microglia and oligodendrocytes was both interesting and unexpected. We have not delved deeply into the changes occurring within these microglia at various time points; however, we have noted some concurrent observations that may pave the way for new lines of investigation. The 16hrs post-infection was chosen as the standard time point for most experiments because it is when we observed the highest level of IFNb expression and sufficient accumulation of infection markers to quantify colocalization. Additionally, this time points yields a clearer microglia signal in the infected region compared to later time points. For instance, the later post-infection we stain for microglia, using Iba1, the less signal is evident in the infected region. Closer to the initial infection foci, we detect fewer microglia, and they are no longer evenly distributed as seen in uninfected tissue (Figure 3.4 A). In line with prior studies, we also observe distinct morphological changes to the microglia within infected regions (Figure 3.4 A, C) [26]. Specifically, near to infected cells/regions, microglia appear more ameboid, while towards the periphery of the infected area, the microglia exhibit fewer processes and enlarged somas, indicative of an activated state. Just outside the infected region, we detect microglia exhibiting characteristics more typical of a resting or surveillance state.

Figure 3.5| Microglia detection in infected region; unique observation and insights

A) Iba1 staining (magenta) comparison in an uninfected brain tissue section and a tissue section from a brain 24hrs post infection. **B)** magnified image of microglia (Iba1), HCR-FISH for IFNb, and an enhanced brightness/contrast image of GFP infection marker 8hrs post infection. **C)** Iba1 staining with infection markers along the ependymal layer.

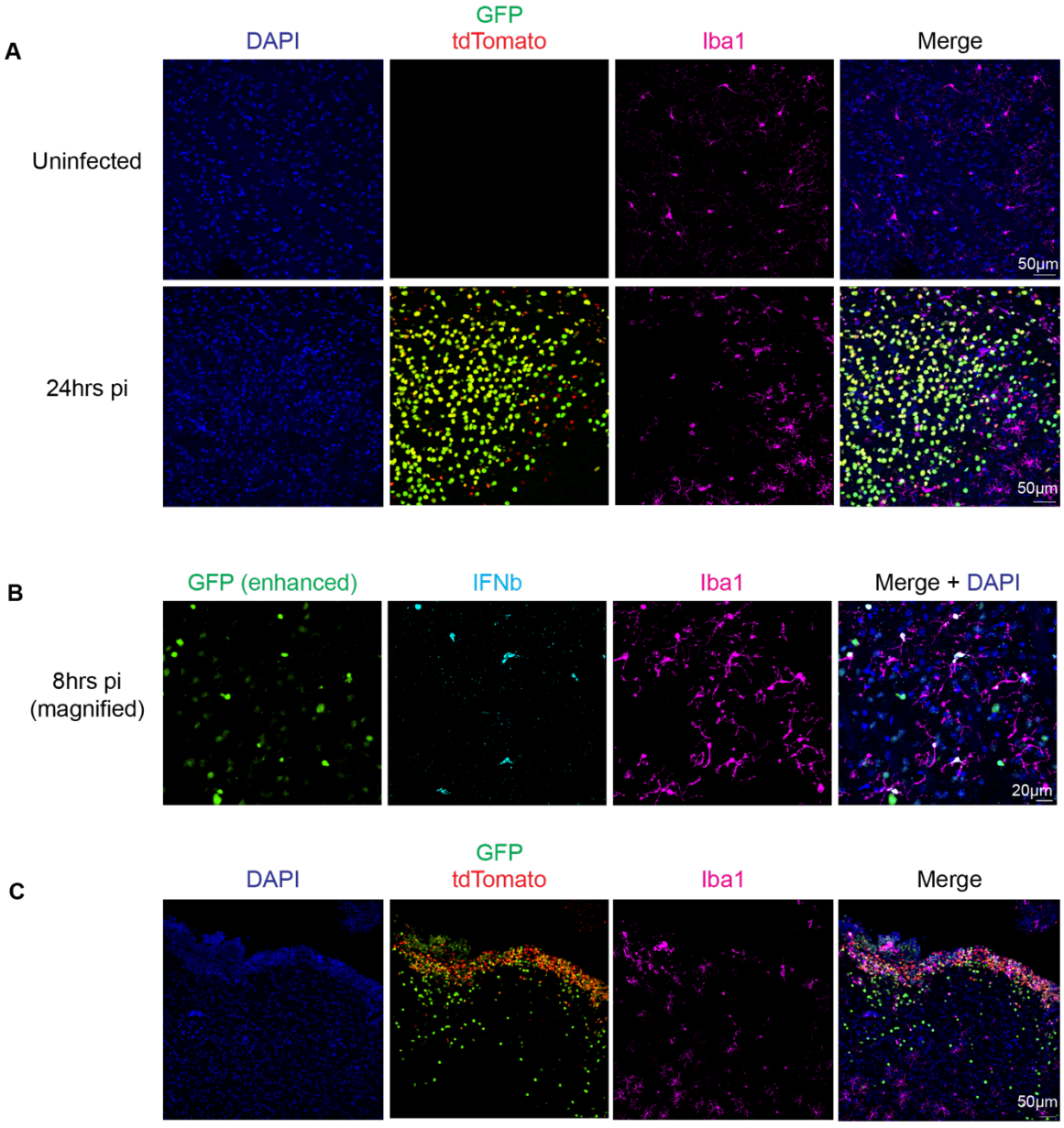

Figure 3.5 (Continued)

Another observation we made was that, if we look early post-infection (8hrs pi), when infection markers haven't accumulated sufficiently, we can enhance the GFP brightness/contrast to detect productively infected microglia that are expressing IFNb (Figure 3.4 B). This contrasts with later timepoints when we rarely detect any GFP-positive microglia. Additionally, similar to the morphological activation characteristics observed earlier, we can also detect ameboid-like microglia within the ependymal layer that encircles infected cells and may be in the process of phagocytosing them (Figure 3.5 C).

IFN signaling influence on primary infection outcomes

Knowing that IFNs are induced upon dual labeling VSV infection and that various glial cells contribute to this response at different times post-infection, we were curious if IFN signaling and the downstream upregulation of antiviral interferons stimulated genes (ISGs) influence the type of infection occurring in each cell type. To investigate this, we utilized several IFN receptor KO strains of mice crossed with our Ai75d mice. This generated mice lacking specific IFN signaling pathways, which could manifest our Cre recombination phenotype that we have previously monitored to identify abortive infections (Figure 3.6 A). Specifically, we used mice that lack the IFNa receptor (IFNAR KO), mice lacking the IFNg receptor (IFNGR KO) and a mouse line that lacked both receptors, IFN(A/G)R KO, labeled as IFNDR KO (double receptor KO). Although we did not detect IFNg upon our viral infections, we have previously observed that the spread of VSV in the brain is more pronounced in the double IFN receptor KO compared to IFNAR KO alone, indicating IFNGR KO does contribute to VSV pathogenesis (data not shown).

Figure 3.6| Experimental setup of IFN receptor KO data with ISG expression phenotypes

A) Experimental setup for addressing IFN receptor signaling in dual labeling VSV primary infection. IFNARKO, IFNGRKO, and IFN(A/G)R aka IFNDRKO (lacking both IFNAR and IFNGR) were crossed with the Cre recombination reporting mice (Ai75d). Mice brains were harvested 16hrs post infection followed by serial HCR-FISH and IF. **B)** HCR-FISH of ISGs (*ISG15, IFIT3, RSAD2)* (yellow) from infected brains in the separate IFN receptor KO mouse lines. Last panel row shows enhanced brightness/contrast of ISG channel.

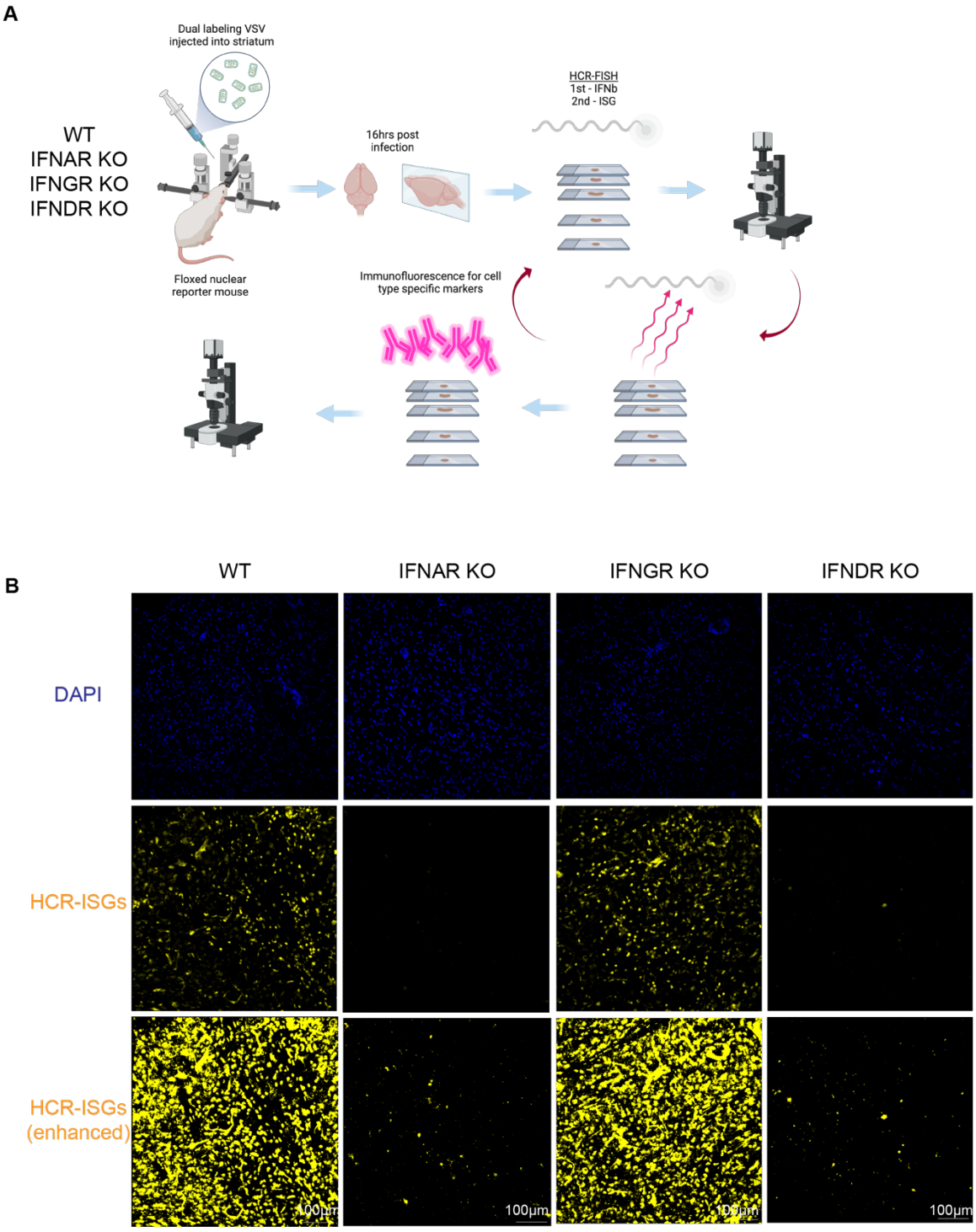

Figure 3.6 (Continued)

Additionally, although we did not detect IFNa upon dual labeling VSV infection, all Type I IFNs, including IFNb, signal through IFNAR. Therefore, by utilizing IFNAR KO mice, we disrupt all signaling in this pathway [27]. Our lab and others have previously shown that IFNAR KO enhances VSV spread and pathogenesis in the brain [1, 5].

To ascertain how IFN receptor KO might affect ISG expression and potential antiviral activity, we employed HCR-FISH to detect our pooled ISGs (*ISG15, IFIT3, RSAD2)* in tissue sections from brains infected with the dual labeling VSV. We noted a significant decrease in ISG expression in both the IFNAR KO and the IFNDRKO (Figure 3.6, B). In contrast, ISG expression of our pooled ISGs was not substantially affected in the IFNGR KO. This suggests that the diminished ISG signal observed in the IFNDR KO mice was primarily due to the IFNAR KO. Despite the decreased ISG signal in the IFNAR KO and IFNDR KO, ISG expression was still present, as indicated in the enhanced contrast images showing low ISG expression.

To determine whether IFN receptor KO can affects the primary infection of our dual-labeling VSV, we monitored the infection status of each cell type across all the KO backgrounds. In both neurons and astrocytes, we did not observe any significant differences between infection outcomes (i.e., uninfected, abortive, productive) in any of the IFN receptor KOs compared to the wildtype controls (Figure 3.7 A, B). However, we did see a slight decrease in abortive infection in oligodendrocytes in the IFNDR KO mice compared to wildtype (Figure 3.7 C). Although there was a corresponding trend toward an increased percentage of productive infection of oligodendrocytes in the IFNDR KO and IFNAR KO, it was not statistically significant. By taking the ratio of abortive

infection to total infection (abortive + productive) in oligodendrocytes, we could discern a slight, but significant, shift toward productive infection in the IFNDR KO mice (Figure 3.7 D). This shift was also significant compared to IFNGR KO, indicating that IFNAR KO might play a larger role in the phenotype. However, the IFNAR KO itself was not statistically significantly different compared to wildtype.

Microglia exhibited an even greater change in infection outcomes due to the lack of IFN signaling. Previously, at 16hrs post-infection, we barely detected any productively infected microglia in wildtype mice. Now, in both the IFNDR KO and IFNAR KO, there was an increase in productive infection with a corresponding decrease in uninfected cells (Figure 3.7 E). Although these differences were significant, the majority (~60%) of microglia remained uninfected. This shift toward productive infection was significantly different from the IFNGR KO condition, indicating that the IFNAR KO background contributed to this phenotype. When comparing the ratio of infection types, the shift toward productive infection was evident in the IFNDR KO and IFNAR KO conditions (Figure 3.7 F). Interestingly, although the ratio shift toward productive infection was not apparent in the IFNGR KO, the disparate data points could suggest sex differences, since the two lowest points showing the greatest shift were the male mice (Figure 3.7 F).

Lastly, we once again used GFP expression (fluorescent intensity) as a proxy for viral replication. When comparing GFP intensity between wildtype and IFNDKO conditions, we observed an increase in GFP expression in productively infected Sox9 positive astrocytes and Sox10 positive oligodendrocytes, while there was no difference in neurons (Figure3.7 G, H, I), suggesting viral replication was more efficient in conditions with less ISG expression.

Figure 3.7| IFN receptor KO effects on infection dynamics across cell types

IFNAR KO, IFNGR KO or IFNDR KO mice with floxed fluorescent reporter were infected with dual labeling VSV and the brains were harvested 16hrs post infection. Infection status of all cell types was compared across IFN receptor KO conditions. **A)** NeuN+ neurons, **B)** Sox9+ astrocytes, **C)** Sox10+ oligodendrocytes, **E)** Iba1+ microglia. Infection ratio of abortive infection: total infection (abortive + productive) were taken for **D)** oligodendrocytes and **F)** microglia. Integrated intensity of GFP was compared between wildtype and IFNDR KO (labeled DKO) for **G)** neurons, **H)** astrocytes, **I)** oligodendrocytes. Graph display means for each metric. Each point is a separate animal, 2 males and 2 females, with an average of 2-4 images per animal for all timepoints except 16hrs post infection (4 males and 4 females for wildtype). Nested One-way ANOVA was performed with Tukey's multiple comparison test for statistical analysis. $* \leq 0.0332$, $** \leq 0.0021$, $*** \leq 0.0002$, $**** \leq 0.0001$

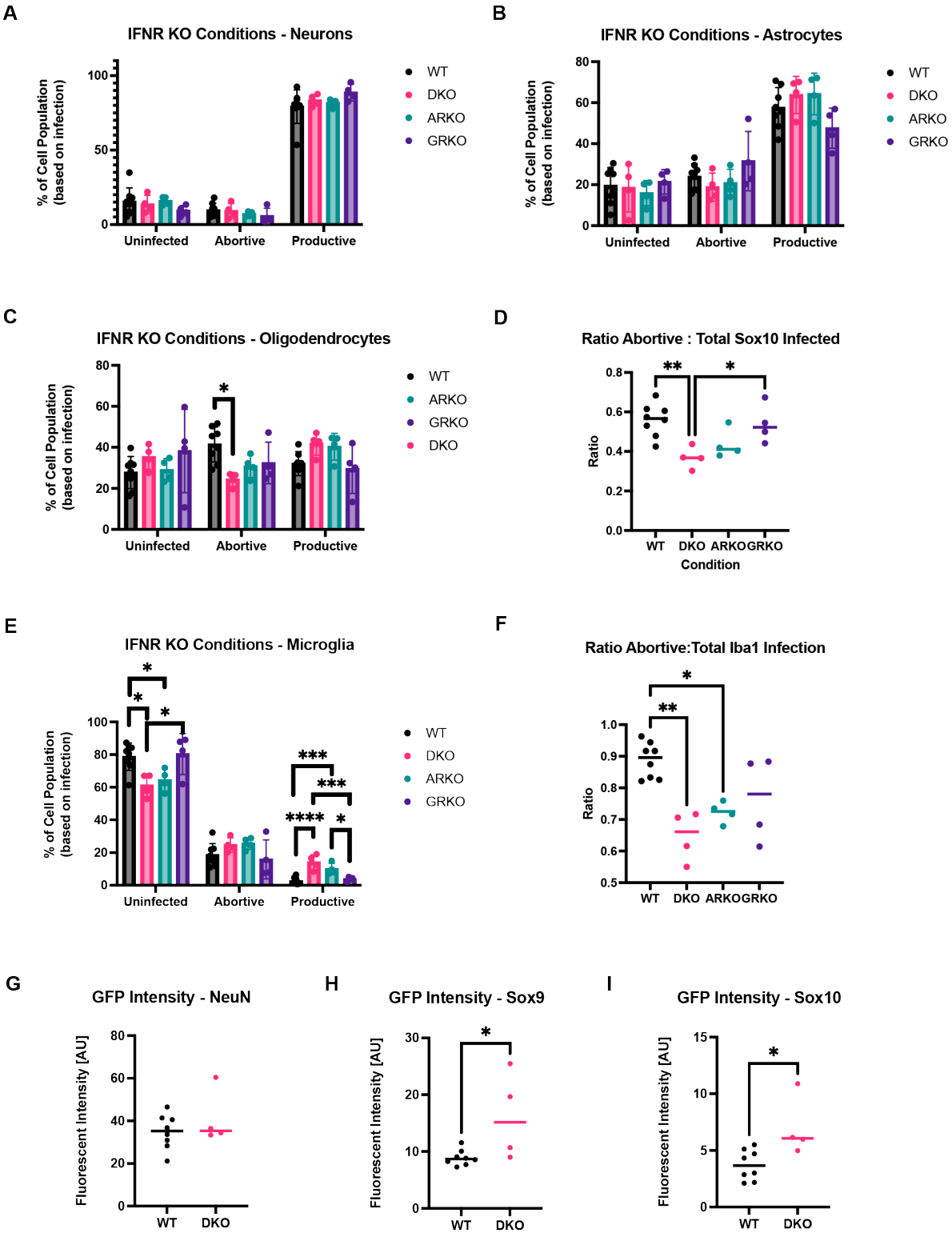

Figure 3.7 (continued)

3.4 Discussion

Here, we describe the IFN response induced by dual-labeling VSV infection of the murine brain and the interesting dynamics we encountered. In our system, we were able to detect IFNb and IFNl upon viral infection. IFNb was detectable in white and gray matter, as well as in distinct regions of the brain, including the SVZ, ependyma, and RMS. IFNl, on the other hand, was found exclusively in the SVZ, ependyma, and RMS. We tracked the acute response of IFNb expression and found that it was detectable by 8rs post-infection with a slight peak around 16hrs post-infection. This was followed by a decrease in IFNb positive cells and IFNb intensity, starting at 24hrs post-infection. Most interestingly, when we profiled which cells were expressing IFNb, it switched depending on how long the infection persisted. Early post infection (8hrs), microglia comprised the majority of IFNb producing cells. However, by 16hrs-post infection only a fraction of the IFNb expression was coming from microglia, and instead, it was oligodendrocytes that were more associated with the IFNb signal. Oligodendrocytes remained the major IFNb expressing cell at 24hrs post-infection.

This was quite surprising and leads to many areas of inquiry regarding what is occurring in microglia early on and why there is this switch. In pursuit of these questions, we also made some additional observations about microglia that could clue us on potential hypotheses. Notably, at later timepoints, we observed a lack of Iba1 positive microglia in the infected region. Additionally, areas of infected exhibited activated microglia with some taking on morphologies consistent with microglia phagocytosis.

Another curious observation is that at 8hrs post-infection low expression of GFP could be detected in microglia that were producing IFNb.

In an effort to follow up with potential mechanisms dictating primary infection outcomes (i.e., uninfected, abortive infection, and productive infection), we tested if IFN signaling plays a role. We did not observe any differences in infection population dynamics in neurons or astrocytes among the IFN receptor signaling KO conditions (IFNAR KO, IFNGR KO, IFNDR KO). Oligodendrocytes exhibited a slight shift from abortive to productive infection in the IFNDR KO condition, while we observed a larger shift toward productive infection of microglia in both IFNDR KO and IFNAR KO. However, these differences do not change the underlying fact that primary infection outcomes remained largely consistent across IFN receptor KO conditions, indicating that IFN signaling does not contribute significantly.

IFN subtype detection

The IFN subtypes that were detected remained largely consistent with what has been previously reported in the literature regarding VSV infection in the brain [5]. In different experimental setups, the IFNl was likely derived from an alternative source due to the intranasal route of administration, highlighting that epithelial cells and other cells bordering the brain can be a source of IFNl expression [5]. We did not detect IFNg in our system, despite literature suggesting that it is involved in cellular activation in the brain with other viruses [8, 28, 29]. This does not necessarily mean that IFNg isn't expressed but rather that the likely source of IFNg, such as infiltrating CD4 and/or CD8 T cells, is not present within the infection region at this particular time point. In later stages of

infection, IFNg may contribute to VSV infection, suggested by some unpublished IFNDR KO experiments from lab our that examined at transsynaptic spread (data not shown).

IFNl and IFNb in SVZ, ependyma, RMS

We did not rigorously explore the cellular origins of IFNl or IFNb in the SVZ, ependyma, or RMS, but we conducted several assays that could begin to shed light on these. Through colocalization studies using Iba1 and Sox9 staining, we identified potential sources of IFNb in these regions, although this data is not shown. The colocalization of these markers indicates that at least microglia nad ependymal cells (inferred from location) are two sources of IFNb. While we used Sox9 to label astrocytes, it is also known to mark neural progenitor cells and ependymal cells in neurogenic regions [30]. Therefore, we cannot rule out the possibility of astrocytes or neural progenitor cells expressing IFNb. However, based on their ventricular location, ependymal cells are likely candidates. We observed no significant colocalization of any markers with IFNl, and the signals for the IFNl and IFNb signals did not overlap, suggesting distinct sources for each. Further research in to the induction of IFN subtypes in these areas is justified due to the significant roles the ventricles may play in viral pathogenesis and dissemination.

Microglia to oligodendrocyte switch of IFNb expression

The most intriguing observation we encountered was the switch in IFNb production. We initially anticipated either microglia or astrocytes to be the probable sources of IFNb. This finding raises two questions: 1) Why aren't microglia expressing

IFNb at later stages post-infection? 2) Why are oligodendrocytes expressing IFNb when others aren't? Given that the relative number of IFNb expressing cells remains consistent between 8 and 16hrs post-infection, the issue isn't just a steady number of IFNb expressing microglia at the two timepoints. Instead, it appears that fewer microglia are expressing IFNb later.

Several reasons could explain why microglia are not expressing IFNb at later times. Observing IFNb production by microglia shortly after infection indicates they are initially active in the innate immune response. Moreover, the observed activation (ameboid morphology) and potential phagocytosis by microglia suggests the are being recruited and altered in response to viral infection. However, we also noted decreased Iba1 staining in the infection area at later points, suggesting a few possibilities: the microglia might have undergone cell death, they could be in a post-activation refractory state coinciding with the resolution of viral infection in the tissue, or they could be in a refractory state triggered by tissue or cellular damage.

Inducing cell death in cells heavily associated in immune activation seems counterintuitive. Yet, we observed GFP-positive microglia at 8hrs post-infection that we were not able to detect as time progressed. These cells could become abortively infected. However, the H2B-eGFP is less transient than cytosolic GFP, therefore we would expect the H2B-eGFP to remain detectable if the infected microglia were still present later post-infection. This scenario suggests that cell death could be a defense strategy to stunt viral spread by eliminating susceptible cells that could otherwise serve as replication hubs for the virus.

Another consideration is the possibility that microglia enter a refractory or exhausted stage later post-infection. As our dual-labeling virus does not spread, the later stages post-infection represents a phase where active infection is subsiding. In this resolution phase, perhaps the microglia have done their part and are no longer stimulated to maintain activation. Iba1 should be more present in activated microglia, so when we observe less Iba1 staining in the infected region, it could mean that the microglia are no longer there, or that Iba1 staining has decreased. Staining with other markers of activated and resting microglia could help elucidate these scenarios [31].

Regarding oligodendrocytes expressing IFNb, there could be a number of explanations. It could be related to the timing of when we are looking at infections compared to previous literature, or it could also be due to the modifications of the virus when we made it more attenuated and added a Cre recombinase.

Timing could be related to why we are observing IFNb expressing oligodendrocytes since many of the previous examples of microglia expressing IFNb with VSV infection are made with viruses that contained the glycoprotein of VSV and could therefore continue spreading [1, 16]. In this scenario, if one were to assay for IFNb producing cells, they would constantly be capturing new infection events and could theoretically keep observing microglia producing IFNb, which are active early post-infection. Conversely, with a virus that is only able to mediate a primary infection event, at later timepoints we are not witnessing new infections but rather the resolution of viral replication/infection. If other studies take multiple timepoints, they too might be able to capture the window at which infection has resolved and might find the involvement of other cell types.

Similarly, in addition to removing the glycoprotein, we also utilized a mutated matrix protein which lacks the ability to inhibit host cell transcription and block mRNA transport from the nucleus [32-34]. In other iterations, involving infection with wildtype viruses, these viruses typically harbor proteins that can antagonize the host antiviral response [35, 36]. If these viruses are capable of inhibiting the antiviral activity of cells, perhaps they do so more effectively in oligodendrocytes. In which case, one of the reasons we observe IFNb expression in oligodendrocytes could be due to our use of an attenuated VSV.

Lastly, we must consider the possibility that Cre recombination itself is eliciting IFNb production. Since Cre recombination induces DNA damage, this could theoretically lead to the activation of pathogen recognition receptors. It has been reported, *in vitro,* that Cre recombination can activate the cGAS-STING innate immune response due to the sensing of cytosolic DNA [37]. STING is an upstream regulator of inflammation and can induce the expression of type I IFNs [38]. This observation has not been extensively reported in the literature when using the Cre/lox system, which might be due to the acute timing of this response. However, if Cre was inducing IFNb production via STING, then we would have expected IFNb expression to be occurring in more cells and to be less dependent on a specific cell type. It raises the question of what would predispose oligodendrocytes to be more sensitive to this Cre-mediated STING activation compared to other glial cells, namely microglia, which are known to express STING and other IFN effectors.

IFN signaling and infection status outcomes

In an effort to identify mechanisms dictating primary infection outcomes, we tested whether IFN signaling could contribute. It has been previously reported that disrupting the innate immune signaling pathways, via viral proteins or through KO of IFN receptors, can change viral tropism [20, 24, 25]. From these observations, we thought that by manipulating these pathways, we could push viral infection from abortive to productive. However, when we tested this, we observed only a small shift in the ratio of productive infection in oligodendrocytes and microglia. In the case of oligodendrocytes, there was a decrease in the amount of abortive infection, as expected, but only a slight shift toward more productive infection. For microglia, there was a significant increase in productive infection, though the majority of cells remained uninfected. Concurrently with the increase in productive infection in the IFNDR KO and IFNAR KO we observed a decrease in uninfected cells. This might suggest that the cells becoming productively infected were previously uninfected, or that a pool of uninfected cells became abortively infected while some abortively infected cells transitioned to productive infection. Due to our system design, we would not be able to distinguish between these two scenarios.

One reason why we might have seen only a shift toward productive infection when the IFN receptors were KO is because of the timing of the IFN response. We were only able to detect IFNb 8hrs post-infection. This would leave only another 8hrs before the tissue was harvested, potentially making IFN signaling too late to induce antiviral ISG expression. However, after 8hrs, we would expect that most cells exposed to the

virus would be infected, indicating that IFN signaling and subsequent ISG expression would occur too late to impact the primary infection outcome. However, IFN signaling could affect monosynaptic infection outcomes depending on the replication dynamics of the cell. This would mean that although IFN signaling might be too late to affect the primary infection outcome in the initially infected cells, it could interfere with replication dynamics in the downstream projections [1, 5].

Correspondence with another researcher studying abortive HSV infection has revealed a similar finding: IFN signaling does not contribute to the dichotomy of abortive versus productive primary infection in their *in vitro* system. Additionally, a recent study on human cytomegalovirus (HCMV) infection outcomes was determined to be based on cell-intrinsic, rather than induced, host cell ISG expression [39]. Thus, our results collectively suggest that IFN signaling does not significantly infleunce primary infection outcomes; instead, other intrinsic factors are likely responsible for these differential infection dynamics.

3.5 Materials and Methods

Virus cloning and production

The dual labeling VSV (rVSV-Cre-N-P-Md-H2B-eGFP-L) was generated from a VSVΔG backbone [40].The Cre, H2B-eGFP and Md (double mutation in Matrix) were introduced into the backbone by Gibson assembly of gBlock fragments with a restriction digested linearized vector. Virus were rescued as previously described [41]. The dual labeling VSV was expanded by first transfecting 293Ts in a 10cm dish at 70% with pCAG-VSV-G. 36hrs post transfection the cells were infected at an MOI of 0.01 with the rescued dual labeling virus. Viral supernatants were harvested 48hrs post infection and spun down to pellet cellular debris at 4000rpm for 15min at 4C. Supernatant was collected from spin and concentrated using a SW28 rotor at 20K rpm for 2hrs at 4C. Supernatant was discarded, and the viral pellet was resuspended in DMEM overnight at 4C. The resuspended virus was then overlayed on a 10% sucrose cushion (10ml) in tubes for spinning in a SW40 rotor for 2hrs at 4C. Supernatant was discarded, and the viral pellet was resuspended in 1xPBS and subsequently stored at -80C.

Mouse strains

12-week old Ai75d mice (025106, The Jackson Laboratory) which contain a floxed nuclear reporter were used for all time course experiments and wildtype comparisons in the IFN receptor KO experiments. The IFNb time course experiment was composed of 2 males and 2 females for each timepoint (uninfected, 4hrs pi, 8hrs pi, 16hrs

pi, 24hrs pi). For the IFN receptor KO experiments, the Ai75d mice were crossed with IFNAR KO (028288, The Jackson Laboratory), IFNGR KO (003288, The Jackson Laboratory), or IFN(A/G)RKO aka IFNDRKO (029098, The Jackson Laboratory) to create a mouse line that contained a floxed fluorescent reporter and lacked the IFNa/b receptor, IFNg receptor, or both, respectively. Mice used for the KO experiments were 12-16 weeks old and consisted of 2 males and 2 females per each condition. Mice were breed under BSL-1 conditions within the Harvard Center for Comparative Medicine facilities.

Stereotaxic injections

All brain injections were performed under BSL-2 conditions in the Harvard Center for Comparative Medicine facilities. These experiments were performed with 12-16week-old mice, 2 males and 2 females. The animals were injected using pulled capillary microdispensers (Drummond Scientific) using the following coordinates for the striatum; A/P 1.0 from bregma, L/M 1.8, D/V -2.5. We injected 200nl of dual labeling virus at a concentration of 1.3x10^9 PFU/ml (tittered on 293Ts).

Tissue processing

For the IFNb time course experiments mice were collected 4hrs post infection, 8hrs pi, 16hrs pi, or 24hrs pi and perfused, and the brains were harvested and fixed in 4% paraformaldehyde (w/v in 1xPBS) overnight at 4C. The brains were then left in a 30% sucrose solution (w/vv 1xPBS) complemented with 1x RNase inhibitor (RNase OUT,

Thermo Scientific) until the tissue was saturated and lost buoyancy (24-36hrs post infection). The brain tissue was the flash frozen in O.C.T (4583; VWR) using dry ice. Frozen tissue was stored at -80C until sectioned. Tissue sections were made at a thickness of 20µm using a Leica CM (3050S cryostat). Only the infected regions were sectioned and mounted on PDL coated (0.3mg/ml) Superfrost Plus microscope slides (22-037-446; Fisher Scientific).

For the IFN receptor KO experiments, the same steps were taken as above except all brains were harvested 16hrs post infection. The rest of the protocol remained the same.

HCR-FISH for IFNs and ISGs

All incubations were performed on the microscopy slide with a hybridization coverslip (HybriSlip, Grace Bio-Labs) in a humidified chamber (23-769-522; Fisher Scientific). Any incubations at elevated temperatures were conducted within a hybridization oven.

All probes and reagents were designed and ordered from Molecular Instruments. HCR-FISH was performed as described previously [42]. Briefly, slides were rehydrated with 2 x 5min 1X PBST washes. Afterwards 200ul of probe hybridization buffer was incubated with the tissue section on the slide for 10min at 37C. The sample was subsequently incubated in a hybridization solution containing 0.4 pmol of each probe set was mixed with 100ul of hybridization solution, incubated overnight at 37C in a humidified chamber in a hybridization oven. After the overnight incubation the tissue

section was washed in series of serial solutions for 15min each (75% probe wash buffer / 25% 5X SSCT, 50%/50%, 25%/75%, 0%/100%. Amplification was conducted by apply 200ul of amplification buffer to section in a humidified chamber for 30min at room temperature. Snap cooled hairpins (6 pmol of hairpin h1 and 6 pmol of hairpin h2, heated separately at 95C for 90 seconds and cooled in a dark drawer for 30min) were mixed with 100ul amplification buffer and applied to tissue sections. The samples were incubated overnight at room temperature. The following day 2 x 30min washes of 5X SSCT was conducted at room temperature before a 10min incubation in 1X SSCT + DAPI followed by mounting in Fluoromount-G mounting medium with a coverslip.

For multiplexed imagining with more than one FISH signal the protocol continues with a 1X PBST wash to remove mounting medium followed 2 x 5min 5X SSCT washes at room temperature.

For removing IFNb signal (or another low signal), you can use dissociation strands (specialty made from MolecularInstruments) to displace the amplifier. After the washes, apply 10x concentration of dissociation strands matching the amplifier (60 pmol) in 5X SSCT for 3-4hrs at room temperature (the longer the better). Wash samples 5 x 5min in 5X SSCT. Check under the microscope to ensure signal is gone. Proceed to the next round of amplification.

For removing ISGs (or another high signal) then DNAse treatment is used. After washes, incubate samples in a 1:50 DNAse solution (18047019, Invitrogen) at 37C for 1hr. Follow initial DNAse treatment with another 1:50 DNAse incubation overnight at 37C. Wash with 65% formamide in 2X SSC for 1hr at room temperature. Wash

formamide solution away with 2 x 5min washes with 5X SSCT. Check under the microscope to ensure signal is gone. Proceed to the next round of imaging.

Immunofluorescence

All immunofluorescence was carried out after DNAse treatment of FISH experiments to ensure that no signal carryover occurred. Incubations were conducted in humidified slide boxes and included the use of hybridization coverslips (as stated in FISH experiments above). Primary antibody incubation occurred at 4C, overnight with a 1:200 dilution of antibody in blocking/staining buffer (0.1% Triton X-100, 1% BSA, 3% Donkey Serum, in 1X PBS). Washes with 1X PBS occurred at an interval of 3 x 5min. Secondary antibody was diluted to 1:500 in the same blocking/staining solution as mentioned above for 2hrs at room temperature. Samples were washed 3 x 5min with 1X PBS before being mounted in Fluoromount-G with a coverslip.

The antibodies used were as followed: anti-NeuN (ABN91, Millipore), anti-Sox9 (AB5535, Millipore), anti-Sox10 (ab180862, Abcam), Iba1 (GTX100042, GeneTex), Donkey anti-Rabbit Alexa 647 (711-605-152, Jackson ImmunoResearch), and Donkey anti-Chicken Alexa 647 (703-605-155, Jackson ImmunoResearch).

Fluorescent microscopy

Sections were initially screened using a Nikon Eclipse E100 upright epifluorescent microscope to identify samples with the most amount of infection. These

slides were subsequently used for staining, imaging and quantification. All imaging took place on a Nikon Ti2 inverted spinning disc microscope using the 20x objective unless stated otherwise. All images were taken using consistent laser power and excitation times within each channel.

Image processing and semi-automated quantification with CellProfiler

FIJI

All images were preprocessed using ImageJ/FIJI macros to streamline analysis. The macros briefly consisted of: 1) running a max intensity Z projection to compress Z stack for each image set, 2) split channel, 3) running the plugin "MultistackReg" for registering serial images when necessary (GFP channel was common among each imaging session and used as reference), "Rigid body" transformation setting was used unless poor registration in which case others transformations were tested, 4) performed background subtraction with a rolling ball radius of 50.0 pixels, 5) performed auto enhanced brightness and contrast at a saturation level of 0.35 (images used for fluorescent intensity comparison used same brightness/contrast parameters for each image), 6) channels merged when more than 4 channels present and pseudo colors used for LUTs for color differentiation.

Quantification

IFNb counting was done by hand, marking the number of IFNb positive cells and colocalization with cell or infection markers. The infection counts and ratios for IFN receptor KO data was performed automatically in CellProfiler.

CellProfiler

Channels from preprocessed images (mentioned above) were separated and imported into CellProfiler pipeline. The pipeline briefly consists of: 1) performing "IdentifyPrimaryObjects" for each channel. A set of thresholds based on size and intensity were used as a baseline for each fluorescent marker/stain but were manually checked. If threshold was not sufficient, the threshold was changed and noted. 2) identified infection marker objects were related and filtered based on colocalization to obtain distinct classifications (i.e. abortive infection [tdTomato-only], double positive [tdTomato + GFP], and GFP-only]). 3) new infection marker objects were masked on cell markers and binned based on percentage overlap (e.g. 80% infection marker overlap with cell marker counted as infected cell). 4) overlays of infection markers and cell markers were made to ensure limited errors in automated analysis. 5) object intensity measurements for identified objects based on cell markers, genes of interests, and infection markers. 6) data counts and intensities were export to a CSV file and transferred to excel for subsequent calculations.

3.6 References

1. Drokhlyansky, E., et al., *The brain parenchyma has a type I interferon response that can limit virus spread.* Proc Natl Acad Sci U S A, 2017. **114**(1): p. E95-E104.

2. Detje, C.N., et al., *Upon intranasal vesicular stomatitis virus infection, astrocytes in the olfactory bulb are important interferon Beta producers that protect from lethal encephalitis.* J Virol, 2015. **89**(5): p. 2731-8.

3. Detje, C.N., et al., *Local type I IFN receptor signaling protects against virus spread within the central nervous system.* J Immunol, 2009. **182**(4): p. 2297-304.

4. Trottier, M.D., Jr., B.M. Palian, and C.S. Reiss, *VSV replication in neurons is inhibited by type I IFN at multiple stages of infection.* Virology, 2005. **333**(2): p. 215-25.

5. van den Pol, A.N., S. Ding, and M.D. Robek, *Long-distance interferon signaling within the brain blocks virus spread.* J Virol, 2014. **88**(7): p. 3695-704.

6. Hwang, M. and C.C. Bergmann, *Alpha/Beta Interferon (IFN-alpha/beta) Signaling in Astrocytes Mediates Protection against Viral Encephalomyelitis and Regulates IFN-gamma-Dependent Responses.* J Virol, 2018. **92**(10).

7. Zhou, J.H., et al., *Type III Interferons in Viral Infection and Antiviral Immunity.* Cell Physiol Biochem, 2018. **51**(1): p. 173-185.

8. Chesler, D.A., et al., *Interferon-gamma-induced inhibition of neuronal vesicular stomatitis virus infection is STAT1 dependent.* J Neurovirol, 2004. **10**(1): p. 57-63.

9. Chesler, D.A. and C.S. Reiss, *The role of IFN-gamma in immune responses to viral infections of the central nervous system.* Cytokine Growth Factor Rev, 2002. **13**(6): p. 441-54.

10. Lazear, H.M., et al., *Interferon-lambda restricts West Nile virus neuroinvasion by tightening the blood-brain barrier.* Sci Transl Med, 2015. **7**(284): p. 284ra59.

11. Kawai, T. and S. Akira, *Innate immune recognition of viral infection.* Nat Immunol, 2006. **7**(2): p. 131-7.

12. Singh, H., J. Koury, and M. Kaul, *Innate Immune Sensing of Viruses and Its Consequences for the Central Nervous System.* Viruses, 2021. **13**(2).

13. McNab, F., et al., *Type I interferons in infectious disease.* Nat Rev Immunol, 2015. **15**(2): p. 87-103.

14. Pfefferkorn, C., et al., *Abortively Infected Astrocytes Appear To Represent the Main Source of Interferon Beta in the Virus-Infected Brain.* J Virol, 2016. **90**(4): p. 2031-8.

15. Huang, K.W. and B.L. Sabatini, *Single-Cell Analysis of Neuroinflammatory Responses Following Intracranial Injection of G-Deleted Rabies Viruses.* Front Cell Neurosci, 2020. **14**: p. 65.

16. Chauhan, V.S., et al., *Vesicular stomatitis virus infects resident cells of the central nervous system and induces replication-dependent inflammatory responses.* Virology, 2010. **400**(2): p. 187-96.

17. Feige, L., et al., *Susceptibilities of CNS Cells towards Rabies Virus Infection Is Linked to Cellular Innate Immune Responses.* Viruses, 2022. **15**(1).

18. Ito, N., et al., *Role of interferon antagonist activity of rabies virus phosphoprotein in viral pathogenicity.* J Virol, 2010. **84**(13): p. 6699-710.

19. Liu, S.Q., et al., *Rabies viruses of different virulence regulates inflammatory responses both in vivo and in vitro via MAPK and NF-kappaB pathway.* Mol Immunol, 2020. **125**: p. 70-82.

20. Potratz, M., et al., *Astrocyte Infection during Rabies Encephalitis Depends on the Virus Strain and Infection Route as Demonstrated by Novel Quantitative 3D Analysis of Cell Tropism.* Cells, 2020. **9**(2).

21. Vidy, A., M. Chelbi-Alix, and D. Blondel, *Rabies virus P protein interacts with STAT1 and inhibits interferon signal transduction pathways.* J Virol, 2005. **79**(22): p. 14411-20.

22. Vidy, A., et al., *The nucleocytoplasmic rabies virus P protein counteracts interferon signaling by inhibiting both nuclear accumulation and DNA binding of STAT1.* J Virol, 2007. **81**(8): p. 4255-63.

23. Yamaoka, S., et al., *Involvement of the rabies virus phosphoprotein gene in neuroinvasiveness.* J Virol, 2013. **87**(22): p. 12327-38.

24. Fares, M., et al., *Pathological modeling of TBEV infection reveals differential innate immune responses in human neurons and astrocytes that correlate with their susceptibility to infection.* J Neuroinflammation, 2020. **17**(1): p. 76.

25. Welsch, J.C., et al., *Type I Interferon Receptor Signaling Drives Selective Permissiveness of Astrocytes and Microglia to Measles Virus during Brain Infection.* J Virol, 2019. **93**(13).

26. Vidal-Itriago, A., et al., *Microglia morphophysiological diversity and its implications for the CNS.* Front Immunol, 2022. **13**: p. 997786.

27. Wong, G. and X.G. Qiu, *Type I interferon receptor knockout mice as models for infection of highly pathogenic viruses with outbreak potential.* Zool Res, 2018. **39**(1): p. 3-14.

28. Cantin, E., B. Tanamachi, and H. Openshaw, *Role for gamma interferon in control of herpes simplex virus type 1 reactivation.* J Virol, 1999. **73**(4): p. 3418-23.

29. Parra, G.I., et al., *Gamma interferon signaling in oligodendrocytes is critical for protection from neurotropic coronavirus infection.* J Virol, 2010. **84**(6): p. 3111-5.

30. Sun, W., et al., *SOX9 Is an Astrocyte-Specific Nuclear Marker in the Adult Brain Outside the Neurogenic Regions.* J Neurosci, 2017. **37**(17): p. 4493-4507.

31. Jurga, A.M., M. Paleczna, and K.Z. Kuter, *Overview of General and Discriminating Markers of Differential Microglia Phenotypes.* Front Cell Neurosci, 2020. **14**: p. 198.

32. Ahmed, M., et al., *Ability of the matrix protein of vesicular stomatitis virus to suppress beta interferon gene expression is genetically correlated with the inhibition of host RNA and protein synthesis.* J Virol, 2003. **77**(8): p. 4646-57.

33. Newcomb, W.W. and J.C. Brown, *Role of the vesicular stomatitis virus matrix protein in maintaining the viral nucleocapsid in the condensed form found in native virions.* J Virol, 1981. **39**(1): p. 295-9.

34. von Kobbe, C., et al., *Vesicular stomatitis virus matrix protein inhibits host cell gene expression by targeting the nucleoporin Nup98.* Mol Cell, 2000. **6**(5): p. 1243-52.

35. Beachboard, D.C. and S.M. Horner, *Innate immune evasion strategies of DNA and RNA viruses.* Curr Opin Microbiol, 2016. **32**: p. 113-119.

36. Scott, T.P. and L.H. Nel, *Subversion of the Immune Response by Rabies Virus.* Viruses, 2016. **8**(8).

37. Pepin, G., et al., *Cre-dependent DNA recombination activates a STING-dependent innate immune response.* Nucleic Acids Res, 2016. **44**(11): p. 5356-64.

38. Webb, L.G. and A. Fernandez-Sesma, *RNA viruses and the cGAS-STING pathway: reframing our understanding of innate immune sensing.* Curr Opin Virol, 2022. **53**: p. 101206.

39. Schwartz, M., et al., *Molecular characterization of human cytomegalovirus infection with single-cell transcriptomics.* Nat Microbiol, 2023. **8**(3): p. 455-468.

40. Chandran, K., et al., *Endosomal proteolysis of the Ebola virus glycoprotein is necessary for infection.* Science, 2005. **308**(5728): p. 1643-5.

41. Whelan, S.P., et al., *Efficient recovery of infectious vesicular stomatitis virus entirely from cDNA clones.* Proc Natl Acad Sci U S A, 1995. **92**(18): p. 8388-92.

42. Choi, H.M., V.A. Beck, and N.A. Pierce, *Next-generation in situ hybridization chain reaction: higher gain, lower cost, greater durability.* ACS Nano, 2014. **8**(5): p. 4284-94.

3.7 Acknowledgments

This work was made possible with the help of Dr. Xiang Ma who supplied reagents, training, and valuable insight for experimental design. Additionally, the work would not have progressed without the training and support offered by the MicRoN team including but not limited to Dr. Paula Montero Llopis and Dr. Praju Vikas Anekal.

Chapter IV.

Discussion and Future Directions

The previous chapters presented data characterizing a novel dual reporting VSV to track infection dynamics in the CNS. We further investigated the host response early post-infection and tested how this might impact primary infection outcome. The discussion sections of these previous chapters contextualized and summarized the nuances of our findings. This final discussion chapter will focus on the broader implications of our results with an emphasis on future directions to pursue.

4.1 Dual labeling viruses to track viral/host dynamics

We designed a viral system that had both a host readout of infection and a viral readout of infection. By comparing the two readouts and monitoring their presence or absence, we were able to discern the susceptibility and permissiveness of cell types within the CNS. Our specific observations regarding the infection outcomes of each cell type are likely unique to the VSV that we utilized. The dual labeling strategy can be adopted by other viruses to discern viral host dynamics in their own respective systems.

Cell type primary infection outcomes

Using our dual labeling VSV system, we broadly observed that glial cells were more resistant to viral infection than neurons. Furthermore, within the glial population, we demonstrated heterogeneity in the infection outcomes. Specifically, astrocytes were more productively infected, oligodendrocytes were more abortively infected, and microglia were mostly uninfected. The mechanisms of these differential infections likely differ. Uninfected microglia were likely due to the virus never escaping the endosome due to fusion or attachment inhibition, while abortive infection events in the

oligodendrocytes are mediated by post-entry events. However, our lab and others have previously recognized that microglia can be productively infected [1, 2]. Therefore, the modifications that we made to our VSV likely contribute to the specific infection dynamics that we observed.

Future directions

Given that previous literature has shown that microglia can be productively infected, despite us not observing this phenomenon in wildtype conditions, it is reasonable to test which modifications changed these attributes. Notably, we removed the G protein (to prevent spread) and utilized a mutated M which lacks the ability to shut off host transcription/translation [3-5]. We can test the contributions of these two modifications and track infection outcomes across the cell types. We did generate a replication competent (encoding G in the genome) version of our dual-labeling virus but never tested infection across the cell types due to the difficulty in distinguishing primary infection from secondary infection. Additionally, we did not test wt M with our dual labeling virus due to concerns that we might lose the host readout of infection. However, there might be a sufficient window for Cre-recombination readout accumulation since it has been reported that inhibition of host transcription and translation is 80-90% complete 4-6hrs post-infection. Immunofluorescence staining of the Cre recombination readout, tdTomato, could compensate for the lack of accumulation.

Another utilization of the current dual-labeling VSV is to track cell survival post-infection. We focus on using the dual readout of infection for capturing abortive infection events however, since the Cre-recombination permanently labels cells, one can also track

infection dynamics and viral clearance. One suggested modification would be to use a cytosolic GFP rather than H2B-eGFP. H2B-eGFP is extremely stable, and we found it present in dead/dying cells. Cytosolic GFPs are more transient and can be used to track the loss of viral products in cells. If the Cre recombination readout is also utilized, then assaying surviving cells at later timepoints could reveal long-term consequences of acute viral infection. This strategy has been utilized to identify resolved infections in MHV infected oligodendrocytes; these surviving oligodendrocytes exhibited greater chronic neuroinflammation compared to uninfected oligodendrocytes [6].

Applicability to other viruses

As indicated above, this dual labeling strategy can be adopted by other viruses as well. Virologist have utilized Cre-recombination for stable labeling of infected cells, but it hasn't been commonly combined with an active viral readout of infection. We utilized the system to track abortive infections, but as mentioned above, it can also track infection resolution dynamics. Additionally, although our dual labeling virus was based on infection readouts, dual labeling strategies in general can distinguish between viral replication stages. HSV and other viruses that are known to have both early and late gene transcription can also benefit from a dual reporting system. A dual reporting approach with these viruses might be able to identify mechanisms conferring abortive or latent infection.

Future directions

Although a dual reporting approach can be adopted by many viruses, one of the easiest ones for us to test would be that of RABV. Specifically, the variety of street

versus lab strains of RABV could benefit from this dual labeling approach since productive infection has been compared between the strains, but abortive infection has often been neglected [7]. Additionally, there is great interest in improving AAV for gene therapy. One of the main approaches that is being utilized is capsid design strategies to improve the tropism of transduction. However, we and others have recognized that certain cell types, such as microglia, are readily transduced (with the genome detectable in the cell) yet do not express the transgene. The AAV might never have uncoated or reached the nucleus in these circumstances, but in some cases, it could be related to the episomal maintenance of the transgene. If this is the case, then utilizing a Cre-recombination readout of infection could identify transduced cells versus cells where the episomal genome was not maintained.

4.2 IFN production upon viral infection of CNS

IFN production upon viral infection of the CNS is well recognized as one of the early antiviral pathways that are induced upon sensing a foreign pathogen. When characterizing the type of IFN response and the cells mediating this response, we observed significant heterogeneity depending on how long the infection has persisted and where the infection occurred. This indicates to us that the CNS is capable of a wide and varied IFN response depending on viral pathogenesis.

Oligodendrocytes expressing IFNb

One of the most unique observations that we encountered was IFNb being expressed by oligodendrocytes. In the literature, oligodendrocytes have been described to

do this only once during a MHV infection *in vitro* [8]. Given the extent that microglia and astrocytes have historically contributed to this response, the IFNb producing oligodendrocytes might be a more unique feature of our dual labeling VSV system. Even MHV infections exhibited IFNb induction in microglia under different conditions [9]. The modifications that we made attenuated VSV to the point that perhaps cells that normally wouldn't participate in the type I response are now able to do so because the virus lacks the ability to shut off host antiviral pathways. Conversely, the Cre recombinase from the virus might induce a DNA damage response that triggers IFNb. If this is the case, the DNA sensing PRR that would activate this pathway should also be present the other glial cells; in which case there isn't an obvious reason why oligodendrocytes would be more predisposed to Cre mediated IFNb induction. Nonetheless, this is something that we should test. Independently of these circumstances, one main takeaway is that oligodendrocytes are capable of mounting a type I IFN response *in vivo.*

Future directions

Several modifications we made to the dual labeling VSV differ from our wt rVSV-eGFP we have used previously. To test if the Cre recombinase is inducing IFNb production in oligodendrocytes, we can create a VSV without the Cre recombinase but still sharing the other features; deletion of the G protein and use of a mutated M protein that are present in the dual labeling VSV. Using this virus, we can infect and look at similar timepoints to determine if we observe oligodendrocytes expressing IFNb when the Cre-recombinase is absent from the system.

We used Sox10 to label oligodendrocyte lineage cells, but we did not differentiate between mature oligodendrocytes and oligodendrocyte progenitors (OPCs). We began to test this theory by using transcriptional markers unique to the two cell populations *Plp1* (which is more abundant in mature oligodendrocytes) and *Pdgfra* (unique to OPCs) [10]. However, upon infection, we did not see a significant HCR-FISH signal from the *Pdgfra* probes, which were detectable in uninfected cells. We did, however, detect an association of *Plp1* with IFNb and concluded that at least mature oligodendrocytes produce IFNb but couldn't verify the extent of IFNb production from OPCs. Therefore, performing the same experiment but with protein markers specific to OPCs (such as PDGFRa), which might be more persistent, can be used to determine if one of the two cell types has a more predominant IFNb expression. This is an immediate and obtainable goal.

Temporal progression of IFNb production

Most experimental assays look at a specific timepoint. The chosen timepoint serves as a snapshot of what is occurring during viral infection but might not capture the acute response dynamics that occur earlier or later. We observed that upon infection with a virus that does not spread, we were able to capture primary infection along with the resulting host response changes. Specifically, we were able to detect IFNb producing microglia earlier post-infection and IFNb producing oligodendrocytes later. It is as curious that oligodendrocytes are producing IFNb as it is surprising that microglia stop doing so after a certain amount of time has elapsed. We observed active and potentially phagocytic microglia earlier post-infection and less Iba1 staining in the infected region later post-infection. This might suggest that microglia are either becoming inactive or are no longer present. Nevertheless, the field needs to begin considering the temporal

dynamics during infection events. This could partially explain the discrepancy between which glial cells are producing IFNb following viral infection.

Future directions

Between 8 and 16hrs post-infection, something unique is occurring with the microglia. Monitoring the changes with additional microglia, cell death, and senescence markers might provide further insight into wha is happening in the microglia as time progresses post-infection. Using markers such as CD40 and CD68 (both upregulated in activated microglia), along with TMEM119 (downregulated in reactive microglia), will help determine whether the lack of Iba1 staining at later timepoints is due to the absence of the microglia or downregulation of Iba1 [11]. If the absence of microglia is confirmed, cell death pathways will need to be explored.

Given the sequential contribution of IFNb from microglia and then oligodendrocytes, it is intriguing that the oligodendrocytes do not express IFNb earlier. This delay could be due to the slower responsiveness of the oligodendrocytes, or it might be that activating signals from microglia or other cells are necessary for oligodendrocytes to express IFNb. It has been previously shown that the combination of ISGs from neurons and astrocytes is necessary for the recruitment and activation of microglia upon VSV infection of nasal epithelia [12]. In a similar vein, microglia might be responsible for inducing oligodendrocyte activation. We can test this theory by depleting microglia with CSF1R inhibitors (such as PLX5622) [13]. Following microglia depletion, we can assess whether oligodendrocytes are still capable of expressing IFNb upon dual labeling VSV infection.

Regional heterogeneous IFN response

Another confounding variable leading to the differential observation in which glial cells are contributing to IFN production could be related to regional differences of cell populations within certain areas of the brain. We primarily focused on the type I IFN response from oligodendrocytes and microglia in the white and grey matter (striatum and corpus callosum, respectively), but we also observed IFNb and IFNl from the SVZ, ependyma, and RMS. Preliminary experiments suggest that microglia and ependymal cells contribute to IFNb expression at least partially, but this needs further verification. Additionally, it is unclear which cells might be expressing IFNl in these regions.

Unique IFN signatures from these regions are intriguing due to their importance in neurodevelopment and brain homeostasis. I am particularly curious about the role ependymal cells play in controlling viral infection. Our experiments showed high ISG expression in the ependyma, which correlated with abortive infection (data not shown). Although the ependyma has not been extensively studied in viral pathogenesis, at least one recent publication showed that type I IFN signaling was necessary to prevent tick-borne flavivirus infection of the brain parenchyma from the ventricles [14]. Specifically, when type I IFN signaling was intact, infection was restricted to the meninges and the choroid plexus. Only in the IFNAR KO mice was viral dissemination beyond the border of the brain evident. Since ependymal cells line the choroid plexus, it is reasonable to assume that they are controlling viral spread and preventing further dissemination of the virus.

Future directions

Studying cell type responses via imaging in the RMS and SVZ is challenging due to the extreme cell density and overlapping markers. Further along the ventricles, the ependymal barrier is more distinct and recognizable. We can use markers such as Foxj1 to differentiate between ependymal cells and other cells in the region [15]. A convenient experiment using our replication-competent dual labeling VSV would be to infect one ventricle and observe whether the ependymal cell layer in the contralateral ventricles can control infection and prevent viral spread. Comparing IFNAR KO with wildtype mice can help us determine if the spread dynamics change and whether there is more abortive infection in the wildtype conditions (using the IFNAR KO mice with a floxed reporter).

4.3 Mechanisms dictating primary infection outcome

Despite early indications from other viruses, we did not observe a significant change in the primary infection outcome when IFN signaling was disrupted. There was only a slight shift in oligodendrocytes and microglia, but the predominate infection status remained the same for each cell type. The most likely explanation for this is that IFN signaling does not occur quickly enough to impact primary infection. Instead, intrinsic immunity likely plays a more significant role in determining the success of viral infection and replication from primary infections.

Innate immunity

As previously mentioned, the 8hr timepoint at which we detected IFNb likely represented a response too slow to affect the primary infection, which occurred earlier. This is illustrated in measles virus (MV) infection, where IFNAR KO organoids showed increased permissiveness of infection in microglia and astrocytes only at later stages [16]. Initially, MV could infect both astrocytes and microglia; IFN signaling only altered the infection outcome at later timepoints. A similar effect might be observed with replication-competent viruses, where we can monitor spread dynamics. IFN is known to mediate long-distance signaling and can increase ISG expression in regions distant from the initial site of infection [1, 17]. Therefore, IFN signaling may impact secondary infections, potentially leading to differences in abortive versus productive infections under these conditions.

Future directions

Initially, we can compare the infection outcomes from replication-competent dual-labeling VSV in IFNARKO, IFNGR KO, and IFNDR KO at later timepoints post-infection. With a replication-competent virus and additional time for spread, the presence or absence of IFN signaling could influence infection outcomes and spread beyond the primary infection. If differences are detected, we could apply these findings to our monosynaptic VSV models. Currently, there is insufficient anterograde monosynaptic spread with VSV. We've tested whether IFN receptor KOs affect primary infection with VSV, but if we use a monosynaptic VSV tracing system we can monitor secondary infection outcomes in downstream synaptic partners. We hypothesize that there would be

more abortive infection in the transsynaptic partners because IFN signaling from the primary infection has time to induce ISG expression in the distal connections. We can investigate whether there are more abortive or productive infections in the monosynaptic connections in the IFN receptor KOs.

Intrinsic immunity

Our results demonstrate that IFN signaling does not significantly change the primary infection outcome, likely due to a lagging IFN response compared to when primary infection first occurred. The next most plausible explanation for the differential infection outcomes across the cell types is due to intrinsic immunity. Recently, intrinsic immunity was shown to be one of the main contributing factors dictating non-productive versus productive HCMV infection in monocytes compared to macrophages, respectively [18]. Due to this relationship, determining whether intrinsic immunity is linked to abortive infection in our dual labeling VSV system is the next stage of this project.

Future directions

Our dual labeling VSV system was designed to facilitate the easy application of snRNA-seq. Using snRNA, we can determine cell intrinsic-immunity prior to infection and early post-infection (before IFN signaling). Cells can be sorted by their infection markers and sequenced to determine factors that might differentiate infection outcomes both between and within cell types. From the sequencing data, we can generate a candidate list of genes that may contribute to the abortive infection phenotype across

cells. Manipulating these genes/pathways could then potentially improve neurosynaptic tracing viruses and neurotropic virus infection outcomes.

4.4 References

1. Drokhlyansky, E., et al., *The brain parenchyma has a type I interferon response that can limit virus spread.* Proc Natl Acad Sci U S A, 2017. **114**(1): p. E95-E104.

2. Chauhan, V.S., et al., *Vesicular stomatitis virus infects resident cells of the central nervous system and induces replication-dependent inflammatory responses.* Virology, 2010. **400**(2): p. 187-96.

3. Ahmed, M., et al., *Ability of the matrix protein of vesicular stomatitis virus to suppress beta interferon gene expression is genetically correlated with the inhibition of host RNA and protein synthesis.* J Virol, 2003. **77**(8): p. 4646-57.

4. Ferran, M.C. and J.M. Lucas-Lenard, *The vesicular stomatitis virus matrix protein inhibits transcription from the human beta interferon promoter.* J Virol, 1997. **71**(1): p. 371-7.

5. Petersen, J.M., et al., *The matrix protein of vesicular stomatitis virus inhibits nucleocytoplasmic transport when it is in the nucleus and associated with nuclear pore complexes.* Mol Cell Biol, 2000. **20**(22): p. 8590-601.

6. Pan, R., et al., *Oligodendrocytes that survive acute coronavirus infection induce prolonged inflammatory responses in the CNS.* Proc Natl Acad Sci U S A, 2020. **117**(27): p. 15902-15910.

7. Potratz, M., et al., *Astrocyte Infection during Rabies Encephalitis Depends on the Virus Strain and Infection Route as Demonstrated by Novel Quantitative 3D Analysis of Cell Tropism.* Cells, 2020. **9**(2).

8. Li, J., Y. Liu, and X. Zhang, *Murine coronavirus induces type I interferon in oligodendrocytes through recognition by RIG-I and MDA5.* J Virol, 2010. **84**(13): p. 6472-82.

9. Roth-Cross, J.K., S.J. Bender, and S.R. Weiss, *Murine coronavirus mouse hepatitis virus is recognized by MDA5 and induces type I interferon in brain macrophages/microglia.* J Virol, 2008. **82**(20): p. 9829-38.

10. Saunders, A., et al., *Molecular Diversity and Specializations among the Cells of the Adult Mouse Brain.* Cell, 2018. **174**(4): p. 1015-1030 e16.

11. Jurga, A.M., M. Paleczna, and K.Z. Kuter, *Overview of General and Discriminating Markers of Differential Microglia Phenotypes.* Front Cell Neurosci, 2020. **14**: p. 198.

12. Chhatbar, C., et al., *Type I Interferon Receptor Signaling of Neurons and Astrocytes Regulates Microglia Activation during Viral Encephalitis.* Cell Rep, 2018. **25**(1): p. 118-129 e4.

13. Spiteri, A.G. and N.J.C. King, *Putting PLX5622 into perspective: microglia in central nervous system viral infection.* Neural Regen Res, 2023. **18**(6): p. 1269-1270.

14. Fares, M., et al., *Pathological modeling of TBEV infection reveals differential innate immune responses in human neurons and astrocytes that correlate with their susceptibility to infection.* J Neuroinflammation, 2020. **17**(1): p. 76.

15. Jacquet, B.V., et al., *FoxJ1-dependent gene expression is required for differentiation of radial glia into ependymal cells and a subset of astrocytes in the postnatal brain.* Development, 2009. **136**(23): p. 4021-31.

16. Welsch, J.C., et al., *Type I Interferon Receptor Signaling Drives Selective Permissiveness of Astrocytes and Microglia to Measles Virus during Brain Infection.* J Virol, 2019. **93**(13).

17. van den Pol, A.N., S. Ding, and M.D. Robek, *Long-distance interferon signaling within the brain blocks virus spread.* J Virol, 2014. **88**(7): p. 3695-704.

18. Schwartz, M., et al., *Molecular characterization of human cytomegalovirus infection with single-cell transcriptomics.* Nat Microbiol, 2023. **8**(3): p. 455-468.

Page intentionally left blank